A MECHANISTIC EXPLANATION OF THE PHYSICAL PROPERTIES OF UNDISTURBED LOESS

by

Harrison Kane
Associate Professor of Civil Engineering
University of Iowa

Research Project HR-126
Iowa State Highway Commission

DEPARTMENT OF CIVIL ENGINEERING
UNIVERSITY OF IOWA
IOWA CITY, IOWA 52240

February, 1968

A MECHANISTIC EXPLANATION OF THE PHYSICAL PROPERTIES OF UNDISTURBED LOESS

by

Harrison Kane
Associate Professor of Civil Engineering
University of Iowa

Research Project HR-126
Iowa State Highway Commission

DEPARTMENT OF CIVIL ENGINEERING
UNIVERSITY OF IOWA
IOWA CITY, IOWA 52240

February, 1968

FOREWORD

This is the final report on the research performed in the Department of Civil Engineering at the University of Iowa for the Iowa State Highway Commission under Research Project HR-126. The principal investigator was assisted by Mr. Bruce Bailey, Graduate Research Assistant, and Mr. Richard W. Long, an undergraduate student assistant.

ABSTRACT

The relation between the properties and the water content of an undisturbed loess were investigated to provide insight into the mechanical behavior of the natural soil. Hand-carved samples from a single deposit, at their natural water contents, and at water contents modified in the laboratory to provide a range from 8% to 32%, were subjected to unconsolidated-undrained triaxial compression tests, consolidation tests, and initial negative pore water pressure tests. In addition, the clay-size fraction was separated from the remainder of the loess for a separate series of tests to establish its properties. The natural water content of the deposit in the field was measured at regular intervals for one year to provide an example of the range in properties that would be encountered at this site.

The test results are presented and their interpretation leads to conclusions regarding the volumetric relations that exist as the water content varies. The significance of the water content in relation to the properties of the natural soil is explored and the concept of a critical water content for loess is introduced.

CONTENTS

LIST OF TABLES

LIST OF FIGURES

CHAPTER 1

INTRODUCTION

1.1 General Aspects of the Problem

Large areas of the midwestern United States, including over half of Iowa and Nebraska, are covered with deposits of loess, a wind-deposited sediment of predominately silt-sized material. Loess also covers large portions of the central areas of all other continents. While there is great variety in the physical properties of loess, the general characteristics and associated problems are consistent on an international scale (Terzaghi, 1951).[1]

The physical properties of the natural, undisturbed loess are of great interest to engineers who are concerned with the design and performance of foundations, excavations, slopes, and other engineering works associated with the in-situ soil. However, the engineer can approach many of these problems with only limited confidence because the properties of loess and the variations in these properties are not completely understood. The results of this uncertainty may be troublesome structures, uneconomical designs, or both.

As an example, the procedures for the design of spread footings on loess may be cited. Authorities in the field of foundation engineering

---

[1] References are listed alphabetically in Appendix I.- References.

recommend that the footing design be based on field load tests supplemented by a study of the effect of seasonal and other moisture changes on the test results (Terzaghi and Peck, 1967). The interpretation of the tests must be empirical and follow precedents in the area because there is no theory to relate the test results to the physical properties of the loess and the test conditions.

This study has been undertaken to develop a mechanistic explanation of the physical properties of loess. An understanding of this mechanical behavior should support the development of realistic theories for bearing capacity and other phenomena of interest to the soils engineer. In the next section, the general character of loess is described to provide background for the more detailed description of the scope of this study which follows.

1.2 Physical Properties of Loess

There is general agreement among investigators that loess is a wind-deposited sediment transported from the flood plains of glacial and other rivers. The engineering properties are derived from its composition and structure. Studies of the composition of loess deposits in Kansas and Nebraska (Gibbs and Holland, 1960) and in Iowa (Lyon, Handy, and Davidson, 1954; Handy, Lyon, and Davidson, 1955) show a clay content of 10% to 30% with the balance being composed of silt and fine sand. The clay occurs as particles, aggregates, or coatings on the silt particles and is montmorillonite with possibly small amounts of illite.

The behavior of loess, as distinguished from that of other soils with the same constituents, depends on its undisturbed structure. When its undisturbed structure is destroyed, loess loses its unique character. It has been observed (Larionov, 1965; Gibbs and Holland, 1960) that the silt-sized particles do not contact each other but are separated by the clay coatings or the clay aggregates. As a result, the strength and compressibility of loess are determined primarily by the properties of the clay fraction.

The undisturbed structure has a high porosity but the voids are not uniformly distributed throughout the aggregate. Larionov (1965) classifies these voids as ultramicroscopic pores (clay-size), occupying to 10% of the total volume, interparticle pores (silt-size to 0.5 mm diameter), occupying from 13% to 36% of the volume, and macropores which are channels with consolidated or calcified walls.

Under natural conditions, the clay-size voids are always saturated (Larionov, 1965) and water may occupy parts of the other voids as well. For loess deposits in Iowa, Davidson and Sheeler (1952) report natural water contents from 5% for soils with a 10% clay content to 30% for soils with 30% clay. The natural water content is also related to the average annual rainfall (Peck and Ireland, 1958) and it may vary considerably with the seasons as well (Terzaghi, 1951).

The liquid limit and plasticity index range from 25 to 45 and 5 to 25 respectively. The lower values are representative of sandy loess while

the higher values are for clayey loess (Davidson and Sheeler, 1952; Clevenger, 1958). The natural state of loess is normally very loose as a result of its open structure and natural unit weights normally range from 70 pcf to 90 pcf. Densities have also been noted to increase slightly with depth (Lyon, Handy, and Davidson, 1954).

The significance of the open, loose structure of natural loess is exhibited in its compressibility and strength characteristics. The structure is maintained by the bond strength provided by the clay binder. If applied stresses exceed the binder strength, or if there is a loss in strength, the structure can collapse and large compressive deformations can occur. The primary cause for a loss in strength is the wetting and consequent swelling and softening of the clay binder (Holtz and Gibbs, 1951). There are numerous cases reported in the literature where the wetting of a loessial foundation soil contributed to unusual settlements of an otherwise stable foundation (e.g. Clevenger, 1958; Peck and Ireland, 1958).

The shear strength is influenced similarly. For a given density and clay content, an increase in water content can cause a marked decrease in the cohesive strength contributed by the binder. Gibbs and Holland (1960) report that with low water contents the cohesive strength of loess may be as high as 15 psi with a result that nearly vertical slopes, 50ft to 80 ft high, are stable. When the loess is wetted, its cohesion may drop to less than 1 psi. In addition, high pore pressures develop when

the wetted loess is loaded. These pore pressures cause a reduced frictional resistance until they are dissipated by drainage.

1.3 Scope of This Study

The physical properties described above make it clear that the water content of the loess and the related water content of the clay binder are key factors determining these properties. Based on these considerations, several questions, which are the substance of this research, can be formulated:

1. What seasonal variations in natural water content may occur in a loess deposit?

2. How is the water content of the whole soil related to the water content of the clay binder?

3. How are the compressibility and strength characteristics of the undisturbed loess related to these water contents?

4. Can the negative pore water pressure in the undisturbed loess, if measured, provide a means for determining the water content of the clay binder?

This research has been directed primarily at answering these questions through field and laboratory studies of the natural soil. The study has been limited to a single deposit so that the clay content, structure, and minerology of all samples would be as uniform as possible. The criteria used in selecting the site, and the soil index properties are presented in Chapter 2.

The field studies were designed to indicate the range in natural conditions to which the deposit was subjected. The results of these studies are included in Chapter 3, where the site installation and the field procedures used to obtain undisturbed samples are also described.

To investigate the variations in behavior of the loess, one-dimensional consolidation tests, unconsolidated-undrained triaxial compression tests, and initial negative pore water pressure tests were run on the loess in its natural state and with its water content varied to provide a range which might be encountered naturally. Consolidation and negative pore water pressure tests were also run on the clay fraction to study its properties. The conditions for these tests and the results are presented in Chapter 4.

In Chapter 5, the test results are discussed and the interrelationship among the variables is analysed. A volumetric explanation of the observed behavior follows from this interpretation. In the final chapter, the work is summarized and the conclusions are presented.

CHAPTER 2

SITE SELECTION AND SOIL INDEX PROPERTIES

2.1 Selection of Site

The laboratory and field testing program required a deposit of undisturbed loess, accessible throughout the year, and available for the construction of a test pit and periodic sampling for water content determinations. Seven sites in the vicinity of Iowa City were considered and all but two were eliminated for failing to meet one or more of the above criteria. Preliminary soil classification tests were run on samples from the two acceptable sites and the decision was made to use the deposit with the greater clay content for this study. Work on the site with the smaller clay content was deferred to a future time.

The site selected for this work is located about two miles west of Iowa City on the north side of the IWV county road, opposite the Johnson County School Number 2 and south of the Hawkeye Apartments. The loess deposit at this site will be identified as Hawkeye Loess or Loess H throughout the remainder of this report. The test pit was developed on top of a gently rolling hill where the loess was 15 ft thick and underlain by sand. In a boring located about 1000 ft to the south, the loess was underlain by a sandy clay glacial till.

2.2 Index Properties of Loess H

The loess in east-central Iowa which includes this site has been identified as a Wisconsin-age, or Peorian, loess. The index properties

of the loess at the test site as determined from tests on samples taken from a depth of six ft, are summarized in Table 2.1 and the grain-size distribution curves are shown in Fig. 2.1. The liquid and plastic limits, specific gravity, and grain-size analyses were determined according to ASTM designations D 423, D 424, D 854, and D 422 respectively (ASTM, 1964). The ranges and average values for the natural dry density and water content of the specimens trimmed for triaxial and consolidation testing are also listed in the table. The methods used in determining these values are described in Chapter 4. The activity (Skempton, 1953) has been calculated using the modified definition proposed by Seed, Woodward, and Lundgren (1964):

$$A = \frac{\text{Change in plasticity index}}{\text{Corresponding change in clay content}}$$

in which A denotes the activity of the clay and the clay content is the per cent finer than 0.002 mm. The plasticity index and clay content for Loess H and the corresponding values for the fractionated clay described in section 2.3 below were used in this calculation.

A comparison of the plasticity properties of Loess H with other loessial soils is shown in Fig. 2.2. Loess H plots in the "silty loess" zone which includes most of the Missouri River Basin loessial soil (Clevenger, 1958). The plasticity index is slightly lower than the average curve determined by Sheeler and Davidson (1957) for this east-central portion of Iowa.

2.3 Properties of the Clay Fraction

Samples of the clay fraction with a particle size less than 0.002 mm were separated from the whole soil by decantation. In this process, the loess was first soaked in distilled water for at least 24 hours. Approximately 200 gm of the wet soil were then agitated for two minutes in a dispersion cup, the procedure being similar to that used in a hydrometer analysis except that no chemical deflocculating agent was added. The dispersed soil was then placed in a 1000 ml cylinder of distilled water, mixed, and permitted to settle for a specified period of time. The suspended solids and water were then decanted. The same procedure was repeated two more times using the decantate to ensure the separation of the clay- and silt-size particles. The clay and water was then placed in a shallow pan and the water was permitted to evaporate. When the consistency of the clay was that of a slurry, it was placed in a metal cylinder and consolidated under a pressure of about 20 psi to a water content of 100% to 110%. The samples were then stored in a moist chamber until required for testing.

The Atterberg limits and specific gravity of the finer than 0.002 mm clay fraction are listed in Table 2.1. The shrinkage limit was determined according to ASTM designation D 427 (ASTM, 1964) and the other tests were the same as those described above.

CHAPTER 3

FIELD STUDIES AND SAMPLING PROCEDURES

3.1 Description of Site and Test Pit

A section through the test site showing the test pit and the observation well installations is shown in Fig. 3.1. The ground surface slopes gently away from the test pit on all sides except at the road cut on the south. The test pit was dug initially to a depth of 6 ft below the reference datum and was 3.5 ft square in plan. After all the sampling work was completed, the pit was 7 ft deep and about 6 ft square. A plywood cover and plastic tarpaulin were used to keep the test pit clean and dry.

Two observation wells consisting of 6-in.-diameter uncased auger borings were used to observe the level of the ground water. These became unusable after about 6 months of operation and they were replaced by piezometers installed nearby as shown in Fig. 3.1. The piezometers were 1-1/2 in.-diameter by 2 ft-long porous tubes with 1/2 in.-outside diameter polyethylene tubing extending to the ground surface. These elements were installed in 3-in. auger borings backfilled with sand. An electric water level indicator was used to locate the depth of the water surface in the polyethylene tube.

3.2 Field Water Content Measurements and Weather Data

To measure the natural variation in water content at the site, auger borings were made periodically and water content samples were taken

at depths from 2 ft to 12 ft below the ground surface. The borings were all located within 15 ft of a line extending from the reference post to the observation well No. 2 (Fig. 3.1). In all, forty-one borings were made in the area with a minimum spacing of 4 ft between adjacent holes. After the samples were taken, the holes were backfilled to eliminate any possible influence on subsequent water content measurements. The water content measurements and ground water levels from October 1966 through September 1967 are shown in Figs. 3.2 to 3.7. Since the ground surface slopes about 3 ft in the area in which the borings were made, and since the ground water surface was also observed to slope approximately parallel to the ground surface, the water content profiles are referenced by depth below the ground surface rather than by elevation. On the other hand, the water levels in the observation wells and piezometers are more conveniently tied to the reference datum.

The precipitation and temperature records for the same period are also shown in Figs. 3.2 to 3.7. These records were obtained from the Iowa City Cooperative Observers Weather Station. The precipitation at the site was also measured with a rain gage located on the reference post. The available records from this gage and the monthly records from the Weather Station are given in Table 3.1 for comparison. The agreement indicates that the Iowa City measurements are valid for the field site. Table 3.1 also lists the 10-year and 70-year averages of the monthly precipitation. The year from October 1966 to September 1967

is seen to be about average except for a somewhat wetter June and dryer May and July.

The variation of natural water content with depth below ground surface is shown in Figs. 3.8 to 3.11 for representative days, and the range in natural water contents for the period October 1966 to September 1967 is shown in Fig. 3.12. Below a 6 ft depth the spread in natural water contents was from 26% to 33%. This corresponds to a range in degree of saturation of about 75% to 90%.

3.3 Sampling Procedures

Blocks of soil were removed from the test pit to provide undisturbed specimens for the laboratory tests. This work was done between October 25 and December 12, 1966. The procedure was to hand-carve the blocks from the lower corners of the test pit. The blocks measured about 8 in. by 10 in. by 12 in. The plan-locations and depths of the blocks were recorded and three water content samples were taken from each block. The variation in these water contents from a single block was found to be from 1% to 3%.

After a block was removed, it was covered with a plastic bag, wrapped with moist rags, and finally covered with another plastic bag. The block was then placed in a cardboard carton and transported to the laboratory by car. Upon arrival at the laboratory, the blocks were divided into smaller samples or, when necessary, stored in a moist room for a maximum of two days before subdividing.

The blocks were subdivided by scoring them with an ice pick. The subdivided portions were then trimmed to the nominal dimensions of 3 in. by 3 in. by 6 in. for the triaxial test specimens, and 2 in. thick by 4 in. in diameter for the consolidation test specimens. At this time, water content samples were again taken for a final check before the samples were sealed for storage.

Since the laboratory testing program extended for about 8 months the samples had to be prepared for storage with great care. They were first wrapped in aluminum foil and then dipped several times into molten paraffin. Finally they were placed in a plastic bag and the weight of the entire package was recorded to permit a check on moisture loss if desired. Each packaged sample was identified so that its original location in the test pit could be determined.

The samples were stored in a moist room until needed for testing. The weights of the wrapped samples were measured just prior to testing and on the basis of these measurements and the earlier water content determinations it was found that the total loss in water content between carving the block at the test pit and removing the sample from storage was less than 1%.

CHAPTER 4

LABORATORY TESTS

4.1 Introduction

The purpose of the laboratory testing program was two-fold. First it was essential to define the strength and compressibility properties of the loess with its natural structure intact and with water contents throughout a range which might exist naturally over some period of time. To this end, the water contents of the structually undisturbed specimens were altered, as described in the following section, and nominal water contents of 8%, 14%, 20%, 26%, and 32% were achieved. The natural water content was about 26% and the loess became saturated at a water content of 35%. One-dimensional consolidation tests, undrained hydrostatic compression tests, and undrained triaxial compression tests were run and the equipment, conditions, and results of these tests are presented later in this chapter.

The second purpose was to measure other properties of the soil that would provide a basis for understanding the behavior mechanism. Thus the initial negative pore pressure was selected and measured for the undisturbed specimens with the water content again varied from 8% to 32%. In addition, the remolded clay fraction of the loess, separated by the procedure described in Chapter 2, was subjected to one-dimensional and hydrostatic consolidation tests. The negative pore water pressure in the remolded clay was also measured at various water contents. The final

sections of this chapter present the negative pore pressure test results and the results of the tests on the clay fraction.

4.2 Preparation of Test Specimens

The undisturbed samples at their natural water contents were stored in a moist-room as described in Chapter 3 until required by the testing program. For the tests on the soil at the nominal water content of 26%, the test specimens were carved directly from the samples at their natural water contents. For all other tests it was necessary to either reduce or increase the water content of the sample before trimming to test specimen size.

The alteration of the water content was accomplished in the following manner. To achieve a water content of 32%, the sample as stored at its natural water content was unwrapped and wetted by spraying the surface with a measured quantity of water. The sample was then rewrapped and placed in the moist room for several days to permit the dispersal of the water throughout the soil. This process was repeated until the water content of the sample, estimated from the sample's wet weight and its original weight and water content, was the desired 32%. The sample was then trimmed to triaxial specimen-size or into the consolidation ring for testing. The water contents of the specimen and the trimmings were compared to check the uniformity of water distribution in the sample and in all cases the differences were less than 1%.

Water contents below the natural water content were achieved by

permitting the surface of the sample to air-dry for several hours, during which time the sample was weighed periodically to determine the weight of water evaporated. The sample was then stored in the moist room to permit the remaining soil moisture to redistribute itself. This process was repeated until the desired water content was reached. It was found that air-drying the samples too rapidly produced cracks which required discarding the sample.

The modified water contents were in general within 2% of the desired nominal water content. The maximum deviation of the natural water contents from the nominal value of 26% was about the same.

The dry densities of the consolidation and triaxial test specimens were calculated from their initial dimensions and oven-dry weights. These densities are plotted against the initial water contents in Fig. 4.1 to illustrate the effect of varying the water content on the density of the loess. No significant change in density resulted from the increase in water content to 32% or the reduction to 20%. However, drying to water contents of 14% and 8% caused some shrinkage and an increase in density of 2 pcf to 4 pcf. Fig. 4.1 also shows that the initial degrees of saturation of the specimens range from about 90% for the wet specimens to 25% for the dry specimens. At the natural water content the degree of saturation varies from 70% to 80%.

4.3 One-Dimensional Consolidation Tests

Equipment. A bench model consolidation test machine[1], having dead-weight leading at a lever ratio of 10 to 1, was used to load the specimens in the one-dimensional consolidation tests. The consolidometer[1] was the fixed ring type, 2.5 in. in diameter and 0.75 in. in height with a cutting edge to permit the specimen to be trimmed directly into the ring. A dial indicator reading 0.0001 in. was used to measure the compression of the specimen.

Test Conditions. The soil specimen at the desired water content was trimmed directly into the consolidometer ring and weighed for the initial water content determination. Moistened filter paper circles were then placed on the top and bottom faces, and the specimen and the ring were placed in the consolidometer. The lower consolidometer stone and the loading cap stone were also moistened before being placed in contact with the filter paper. Drying of the sample during the test was prevented by enclosing the top of the consolidometer with a polyethylene cover, sealed to the sides and around the loading cap. Moist sponges inside the consolidometer maintained a high humidity.

The test specimen was loaded initially with a small seating load after which the load was increased in increments from 0.25 tsf to 32 tsf. The

---

[1] Manufactured by Wykeham Farrance Engineering Ltd.

conventional geometric progression of load increments was used. Each load increment was maintained for two hours after which the following increment was applied. The two-hour duration was determined to be adequate on the basis of tests with longer durations. These tests showed that the plot of compression dial reading vs. log of time flattened after one hour to a constant slope of 0.0025 in. or less for a ten-fold increase in time. This deformation corresponds to a change in void ratio equal to about 0.006 and does not have a significant effect on the pressure-void ratio relationship. The use of such durations shorter than the conventional 24-hour duration has been investigated by Leonards and Ramiah (1960) among others with the conclusion that the load increment duration has an insignificant effect on the pressure-void ratio relationship provided the duration is sufficiently long to permit most of the primary consolidation to occur.

Unloading was accomplished by removing load increments equal to three-fourths of the previous load until the pressure of 0.5 tsf was attained, whereupon all weights were removed. The specimen was then weighed and dried for the final water content determination.

Test Results

Typical void ratio-log pressure relationships for each nominal water content are shown in Fig. 4.2 and the results of all the consolidation tests are summarized in Table 4.1. The notation used in Table 4.1 is as follows:

Column (1) Specimen No.

(2) w_i = initial water content, %

(3) e_i = initial void ratio

(4) S_{ri} = initial degree of saturation, %

(5) p_o' = the pressure at the intersection on the void ratio - log pressure diagrams of the steepest slope of the consolidation curve and e_i, tsf.

(6) C_c' = the slope $\Delta e/\log (\frac{p + \Delta p}{p})$ of the steepest portion of the consolidation curve.

The definitions of p_o' and C_c' are illustrated in Fig. 4.3.

The consolidation curves for specimen Nos. 1 and 2, at the nominal water content of 8%, did not develop a steep slope in the manner of the wetter and more compressible samples. Fig. 4.2 shows the curve for specimen No. 2 which illustrates this point. If the test had been continued above the 32 tsf level of pressure, it is probable that the curve would appear similar to the others. Because the steep portion was not reached for these two specimens, no C_c' -values are listed in Table 4.1 and the values given for p_o' are probable lower and upper limits.

The variations of p_o' and C_c' with initial water content are shown in Figs. 4.4 and 4.5 repectively. The value of p_o' is essentially constant for water contents above 20% but increases sharply as the soil becomes drier than 20%. One the other hand, C_c' generally increases with decreasing water content. Fig. 4.5 shows a considerable scatter in C_c' -values.

A part, but not all, of this scatter is due to differences in initial void ratio; that is, at a given water content, the specimens with higher void ratios have higher C_c' -values in most cases. It is interesting to note that, while decreasing the water content increases p_o', C_c' also increases and thus the dry specimens are more compressible than the wet ones at pressures above p_o'.

4.4 Triaxial Compression Tests

Equipment. The equipment used for the triaxial compression tests included the following major elements[1]:

a. 5-ton capacity gear driven compression test machine.

b. Self-compensating constant pressure apparatus for applying cell pressures to 140 psi.

c. Cell volume change measuring apparatus.

d. Triaxial cells for 1-1/2 in. diameter specimens with working pressure of 150 psi.

e. Load rings for axial load measurement, of high strength steel with capacities of 500 and 1000 lbs.

Test Conditions and Procedures. The triaxial compression tests on the loess were unconsolidated-undrained tests; that is, the specimens were sealed so that water and air could neither enter nor leave the specimen during the application of both the cell pressure and the axial load. A series of tests with cell pressures ranging from zero to 140 psi was

[1] Manufactured by Wykeham Farrance Engineering Ltd.

run on specimens of the loess at each nominal water content. The specimens were trimmed in a humid room from the soil samples previously prepared and cured at the desired water content (Section 4.2). The trimmed specimens were 1.5 in. in diameter and 3.4 in. in height. Immediately after trimming, the specimens were weighed, placed in the triaxial cell, and enclosed in a rubber membrane which was sealed to a lucite base disc and loading cap.

The triaxial cell was then assembled, filled with water, and the cell pressure applied. The volume change in the specimen which occurred during the application of the cell pressure was measured by use of the volume change apparatus. In this apparatus, volume changes under pressure are indicated by the displacement of a liquid paraffin-water interface in a burette with 0.1 cc divisions. A zero reading is taken with the specimen in place and the cell filled with water. When the cell pressure is applied, water flows into the cell due to expansion of the cell and compression of the specimen. The cell expansion was determined for various cell pressures by calibration tests run in an identical manner but without a soil specimen. Thus the volume change of the specimen may be determined by subtracting the cell volume change from the measured volume change. The specimen volume change is accurate to $\pm$ 0.2 cc which, for the volumes, densities, and water contents in these tests, corresponds to a computed increase in degree of saturation currect to within $\pm$ 0.5%. The presence of air trapped in the cell and between the specimen

and the membrane would cause the computed increase in degree of saturation to be too great. Care was taken to avoid trapping any significant quantity of air but some air bubbles could be observed. With the effect of trapped air taken into account, the maximum error in the degree of saturation is estimated to be + 2%.

The compression of the soil under the cell pressure was not instantaneous and fixed durations of pressure were used to assure uniform compression. The duration was 10 min. for the 20 psi cell pressure; this was increased by 5 min. for each additional 20 psi to 40 min. for 140 psi. The volume changes due to the cell pressure were essentially complete by the end of these periods.

After compression under the cell pressure, the axial stress was increased using a strain rate of 0.6% per minute. The test was continued until the axial stress decreased or 20% strain was reached. After testing, the specimen was removed from the cell, weighed, and oven dried for the water content determination.

Test Results. The stress-strain curves for all tests, grouped according to nominal water content, are shown in Figs. 4.6 to 4.10 and the test results and pertinent data are summarized in Table 4.2. The notation used in the table is as follows:

Column (1) Specimen No.

(2) w = water content, %

(3) e_i = initial void ratio

(4) S_{ri} = initial degree of saturation, %

(5) σ_3 = cell pressure, psi

(6) S_{rc} = degree of saturation after compression due to cell pressure, %

(7) $(\sigma_1 - \sigma_3)_f/2$ = half the stress difference $(\sigma_1 - \sigma_3)$ at failure, psi

(8) ϵ_f = the axial strain at failure, %

(9) ϵ_s = the axial strain at half the failure stress, %

(11) E_s = the secant modulus at helf the failure stress, psi

(12) E_i = the initial tangent modulus, psi

In order that the results given in Table 4.2 may be readily interpreted, the influence of the water content and the confining pressure on various quantities in and derived from the table are discussed in the following paragraphs.

The relative increase in degree of saturation, as a result of undrained hydrostatic compression, defined here as the ratio of the actual to the potential increase in saturation $(S_{rc}-S_{ri}) / (100-S_{ri})$, is plotted against the confining pressure for each nominal water content in Fig. 4.11. The wettest specimens experienced the greatest relative increase in degree of saturation whereas the driest specimens experienced the least. Since the wettest specimens were also the weakest, this result would of course be expected. However, by the comparison of columns (4) and (6) in

Table 4.2, it is seen that the greatest absolute as contrasted to relative increase in the degree of saturation occurs for the specimens with nominal water contents of 20% and 26%. At these water contents the effects of a low strength and a relatively high potential volume change combine to produce this result. The drier specimens, having nominal water contents of 8% and 14%, have a greater strength and their structure does not collapse at the test pressure levels. The wettest specimens with a nominal water content of 32% have high degrees of saturation initially and therefore can compress only a small amount under undrained hydrostatic compression.

Separate plots of $(\sigma_1 - \sigma_3)_f/2$ versus water content, columns (7) and (2) respectively of Table 4.2, have been made for each value of confining pressure in order that the strengths at the nominal water contents could be interpolated. These plots are shown in Figs. 4.12 to 4.19. The difference between the strength at the nominal water content and at the actual water content is small in most cases because the actual and nominal water contents were not greatly different.

The adjusted values of $(\sigma_1 - \sigma_3)_f/2$ and the corresponding values of $(\sigma_1 + \sigma_3)_f/2$ are plotted for each nominal water content in Figs. 4.20 to 4.24. These plots are known as modified Mohr-Coulomb diagrams and, in each figure, a straight line has been fit to the plotted points using a least square analysis. The intercept $\underline{a}$ and slope ψ of this line are related directly to the cohesion intercept c_u and slope ϕ_u of the conventional Mohr-Coulomb failure envelope. In each figure the values of $\underline{a}$

and ψ obtained from the plot and the computed values of c_u and ϕ_u are listed.

The total stress failure envelope for unconsolidated-undrained tests on unsaturated soil is actually curved because the slope depends on the degree of saturation. As the confining pressure increases, pore air dissolves in the pore water and the degree of saturation increases. Thus the envelope flattens and approaches the horizontal when complete saturation is reached. The amount of curvature for a given pressure range depends on the magnitude of the change in degree of saturation. On the diagrams in Figs. 4.20 to 4.24, this curvature is small enough to be obscured by differences due to other causes, eg., differences in density and natural structure of the undisturbed specimens. Therefore the values of ϕ_u and c_u listed in the figures have been accepted as good approximations for the full pressure range under consideration and the corresponding Mohr-Coulomb failure envelopes for each water content are plotted in Fig. 4.25.

A final presentation of the strength data is given in Figs. 4.26 and 4.27 where the accepted values of ϕ_u and c_u are plotted against water content. The value of ϕ_u, Fig. 4.26, decreases rapidly as the water content increases from 14% to 26%. This behavior is the direct result of the dependence of ϕ_u on the degree of saturation S_r. At water contents of 14% and smaller, S_r is less than 40% (Fig. 4.1) and the relative increase in S_r as a result of undrained compression is small (Fig. 4.11). On the

other hand, at w = 26% the value of S_r is almost 80%, the relative increase in S_r is large, and the soil is nearly saturated. Since the value of ϕ_u becomes zero upon saturation, it is evident that the marked decrease in ϕ_u should occur in the range w = 14% to w = 26% as observed.

On the other hand, the value of the intercept c_u (Fig. 4.27) decreases sharply between w = 8% and w = 14%. The intercept c_u represents the undrained shear strength of the soil under a total normal stress of zero. This in turn depends on the attractive forces between the clay particles and the pore pressures which exist during shear, that is, on the undrained strength of the clay binder. Thus the observed reduction in c_u indicates that the undrained strength of the clay binder diminishes to a near minimum value as the water content increases to 14%.

The initial tangent modulus and the secant modulus are plotted against confining pressure for each water content in Fig. 4.28. Both moduli are greatest by a significant amount at the 8% water content. The greatest reductions in moduli occur in the increment of water content between 8% and 14%; this parallels the similar behavior of the apparent cohesion observed above. It is notable that the secant modulus at high confining pressures increases as the water content increases from 14% to 32%. This reversal in behavior may be explained by the greater volume reductions experienced by the drier specimens during the undrained application of the confining pressure. This compression altered the structure so that failure occurred at strains significantly greater than the failure

strains for specimens whose volume decreased only slightly, that is, those with low confining pressures or high water contents.

4.5 Initial Negative Pore Water Pressure Tests

Equipment. The initial negative pore water pressures were measured using the exposed end-plate procedure developed by the U. S. Bureau of Reclamation (Gibbs and Coffey, 1963).

This method makes use of a saturated fine-pore ceramic stone which is mounted so that the top is exposed to air and the bottom is connected to a closed system in which the pore water pressure can be adjusted and measured. Negative pressures in the stone are maintained by the menisci formed at the air-water interface on the exposed face of the stone. A partly saturated soil specimen is placed on the stone so that the water phase in the soil is continuous with the pore water in the stone. The negative pore water pressure in the stone is then adjusted so that there is no flow of water in either direction between the soil and the stone. Under these conditions, the pore pressure in the stone is equal to that in the soil. There are several technical problems which must be overcome. First, the water in the stone will cavitate when the negative pressure exceeds about 1 atmosphere. Should this occur, the pressure can no longer be measured or maintained. This condition is avoided by increasing the air pressure above the stone and the pore water pressure in the stone simultaneously. No change in the shapes of the menisci will occur since they depend only on the difference in pressure across the air-water interface.

In effect, the pressure datum is shifted sufficiently to keep the pore pressure in the stone at a level where there is no danger of cavitation. This technique is known as the "transfer of origin" method (Gibbs, et al, 1960) or the "axis translation technique" (Olsen & Langfelder, 1965).

The ceramic stone and plate must also be sufficiently fine so that the air entry value, i.e. the air pressure that will cause an air bubble to enter the stone, exceeds the negative pore pressure in the soil. If this precaution is not taken, air will enter the stone and the water in the stone will cavitate. Three stones were used in these tests having air entry values of approximately 40 psi, 80 psi, and 210 psi.

The major elements of the apparatus for measuring the negative pore pressures are shown schematically in Fig. 4.29. A standard triaxial cell was modified so that a 1-7/8 in. - diameter ceramic stone with the desired air entry value could be mounted on the base. The outlet from the stone was connected to a mercury U-tube null indicator through a length of 1/8 in. OD copper tubing. The null indicator was balanced by adjusting the pressure in a mercury U-tube manometer by means of a screw control. The outlet from the stone also led through a valve to a water-filled burette. A regulated air pressure supply was connected to the cell and measured with a Bourdon gage. The maximum pressure available was 80 psi.

Test Conditions and Procedures. The successful measurement of negative pore pressures requires that the apparatus between the stone

and the null indicator be completely deaired. To ensure this condition, the ceramic end plate was boiled under a vacuum and deaired water was forced through the remaining parts of the system prior to assembly. The triaxial cell base was then submerged in a deep basin of water and the end plate mounted under water. The cell base was removed from the basin and a positive pressure was maintained under the end plate by opening the valve to the burette.

The specimens used in the initial negative pore pressure tests were with few exceptions subsequently used for the triaxial tests. The specimens were thus 1-1/2 in. in diameter and 3.4 in. long. The test was started by first wiping the end plate with a moist cloth, seating the specimen firmly on the end plate, closing the valve to the burette, and assembling the top of the cell to the base. This procedure was accomplished very quickly and as soon as the burette valve was closed, the mercury in the null indicator started to move upwards indicating a flow of water into the soil specimen. This movement was neutralized by reducing the pressure in the manometer. When the pressure in the manometer was reduced to -5 psi, the cell pressure was increased by an increment of 5 psi, the manometer returned to zero pressure, and the burette valve opened and closed instantaneously to prevent a further build-up in negative pressure and possible cavitation. The process of adjusting the manometer pressure and increasing the cell pressure was repeated until equilibrium was indicated by no further tendency for flow into or out of the soil. At this point, the negative pore pressure

in the soil is taken to be the algebraic difference between the manometer pressure and the cell pressure. Thus a manometer pressure of - 3.0 psi and a cell pressure of 15.0 psi indicate an initial negative pore pressure of - 18.0 psi.

One of the major difficulties encountered in these tests was the need for the continuous adjustment of the pressure to maintain balance in the null indicator. For tests requiring one or two hours for equilibrium to be reached, it was possible to make the necessary adjustments. However, some of the tests, in particular the tests with high negative pore pressures and the finest stone, did not reach equilibrium until 10 to 20 hours after starting. In these cases it was necessary to shut the test down overnight and resume the following day. This was accomplished by closing the outlet valve on the cell thus ensuring that no water could be drawn into the system. The cell pressure was then increased to a level that would ensure that the pore pressure in the stone would not fall below - 5 psi before the next reading was to be taken. The next pressure reading could not be taken, however, without first placing the null indicator back in the system. In doing this, an effort was made to predict the negative pressure in the stone and to place the null indicator under this pressure before the outlet valve on the cell was opened. If the predicted pressure was correct, no flow would occur upon opening the valve. If the predicted pressure was not precisely correct, which was generally the case, an immediate flow would occur due to the overshoot or undershoot. Rapid

pressure adjustments were necessary to balance the null indicator and a tendency to over-correct existed. As a result the readings immediately after opening the outlet valve on the cell showed fluctuations in pressure as great as 2 psi. The fluctuations diminished with time and the system returned to its original rate of adjustment toward equilibrium.

Examples of the time lags in reaching equilibrium are shown in Figs. 4.30 and 4.31. In Fig. 4.30 the results of Test No. 15, in which the 80-psi stone was used, demonstrate a smooth approach to equilibrium which is attained at about 15 min. after the start of the test. A more irregular curve is shown in Fig. 4.31 for Test No. 1. The 210-psi stone was used for this test and the specimen was drier than that in Test No. 15. Equilibrium was not attained until about 22 hours after the start of the test. The time required for these long-duration tests put an unfortunate limitation on the number of tests that could be run.

Test Results. The results of the initial negative pore pressure tests are given in Table 4.3. In the tests in which a triaxial specimen was tested, the triaxial specimen number is also given and additional data on these specimens may be obtained in Table 4.2. For each negative pore pressure test, Table 4.3 gives the water content of the specimen, the degree of saturation, if available, the measured pore water pressure u, the time lag for equilibrium as illustrated in Figs. 4.30 and 4.31, and the air entry value of the stone used in the test. No test results are given for the specimens with nominal water contents of 8% because their negative

pore pressures were lower than the -80-psi capacity of the equipment. Test Nos. 6A and 6B were run on opposite ends of the same specimen and the difference in measured pore pressure is about 13% of the larger value. This may have been due to differences in the ends of the specimen, or due to errors caused by the test procedure. Based on these differences, on the fluctuations in the measurements that occurred in some of the longer tests (eg. Fig. 4.31), and on the scatter in the values at a given water content, the negative pressures are believed to be within ± 10% of the measured values.

The negative pore pressures are plotted against water content in Fig. 4.32. A different symbol is used for each end plate and the demonstrated agreement among the results with the different end plates supports the validity of the test procedure.

A curve has been fit to the plotted points to provide an empirical equation relating the water content to the negative pore pressure. The curve has the equation

$$u\,(\text{psi}) = -\left(\frac{32.5}{w\%}\right)^{5} \qquad 4.5.1$$

The good fit illustrated is, of course, empirical and other types of curves could be fit to the data with similar success.

The relation between negative pore pressure and degree of saturation is shown in Fig. 4.33. This relationship is similar to the negative pore pressure-water content relationship in Fig. 4.32 but there is somewhat greater scatter in the data points.

4.6 Tests on Clay Fraction

Consolidation Tests. A one-dimensional consolidation test and a triaxial consolidation test were run on the clay fraction which had been separated from the whole loess soil as described in Chapter 2. The specimens for both tests were saturated and had an initial water content slightly greater than 100%. The resulting void ratio-log pressure curves are shown in Fig. 4.34 and it is evident that the relationships are essentially the same for both tests.

Initial Negative Pore Pressure Tests. Specimens of the clay fraction at water contents ranging from 112.2% to 35.0% were prepared by permitting the clay to air-dry to the approximate water content desired, removing any crust from the surface, remolding to assure a uniform distribution of water, and finally curing for at least one day in a moist chamber. The specimens were then tested using the equipment and procedures described above in Section 4.5.

The results of the negative pore pressure tests are presented in Table 4.4 and the relationship between the water content and the negative pore pressure is shown in Fig. 4.35. An empirical curve which has been fit to the data having the equation

$$u(\text{psi}) = -\left(\frac{100}{w_c\%}\right)^5 \qquad 4.6.1$$

is also shown in the figure.

CHAPTER 5

INTERPRETATION OF RESULTS

5.1 Volumetric Relations

The physical properties of loess would be more readily understood if the structure and arrangement of the silt- and clay-size fractions were known. While the test results do not allow a definitive description to be made, several limiting conditions may be inferred. Additional results may permit the narrowing of these limits.

A diagram illustrating the volumetric relations is shown in Fig. 5.1. For convenience, the volume of solids V_s is taken to be 100 cc. As given in Table 2.1, the percentage of clay-size particles finer than 0.002 mm is 19% and the specific gravities of the silt and clay components are nearly equal. Therefore the total volume of solids in this example is composed of 19 cc of clay-size particles and 81 cc of silt-size particles. These volumes are denoted by the symbols V_{sc} and V_{sm} respectively. The undisturbed void ratio varies with water content from about 0.97 at w = 32% to 0.88 at w = 8% (Table 4.2). The void ratio of the loess when completely dry was found to be 0.85. Thus the total volume of the loess is shown in Fig. 5.1 to vary from 185 cc for w = 0% to 198 cc when saturated at w = 36% (line AB). The volume of water V_w increases linearly from 0 to 98 cc at w = 36% (line CB).

The voids V_v may be classed according to size as were the solids. Thus some of the voids exist between clay-size particles while the remaining

voids are larger in size and exist between the silt-size particles and aggregates of particles. The former are referred to as clay-voids V_{vc} and the latter macro-voids V_{vm} in the following discussion.

With the above notation, the void ratio e is:

$$e = \frac{V_v}{V_s} = \frac{V_{vm} + V_{vc}}{V_{sm} + V_{sc}}$$

It is convenient to define two additional ratios, the macro-void ratio, e_m:

$$e_m = \frac{V_{vm}}{V_{sm} + V_{sc} + V_{vc}}$$

and the clay-void ratio e_c:

$$e_c = \frac{V_{vc}}{V_{sc}}$$

The smallest volume of clay-voids must be greater than that corresponding to the shrinkage limit of the remolded clay fraction (Table 2.1). This clay-void ratio is 0.41 and therefore the lower limit for V_{vc} is 8 cc (line DEF). Since the finest voids will be the last to be dried, it is evident that the clay-voids will be saturated and that, if V_{vc} = 8 cc, there will also be water in the macro-voids for all values of w greater than about 3%. Thus the clay, if it were at the shrinkage limit initially, would be free to swell in accordance with the void ratio-pressure relationship for rebounding from the shrinkage limit. An estimate of the void ratio after swelling may be obtained from Fig. 4.34 by extending the compression curve to e = 0.41, and then returning to a pressure of 0.1 tsf along a path

parallel to the rebound curves. This procedure indicates a final void ratio of about 1.25 after swelling. This volume increase is shown by line EG, Fig. 5.1, and the clay volume with free water in the macro-voids is line GH.

If the clay particle arrangement is flocculent, the clay-void volume will be represented by a higher line, such as JKLM, instead of DEGH which was based on remolded clay and therefore a dispersed particle arrangement. The location of JKLM is not known but may be deduced indirectly. Thus a significant change in the properties of the loess would be expected when the clay is compressed by desiccation as the water content decreases from L to K. On the other hand, for water contents between L and M, where the clay volume is stable, the properties of the loess should be relatively constant. Point L in Fig. 5.1 has been set in a water content range where the properties of the loess were found vary significantly; however, the location within the range was arbitarily chosen to correspond with a clay-void ratio twice that of line GH, ie. with $e_c = 2.5$.

It is of interest to consider the implications of the location of line JKLM with regard to the structure and particle arrangement of the loess as a whole. If it is assumed that the clay occurs as a coating on the surface of the silt particles and if the resulting clay-silt particle is considered as an individual grain, then the structural arrangement and packing of these grains is reflected in the value of the macro-void ratio in the same manner that the packing of a sand is reflected in the value of its void ratio. For line JKLM in Fig. 5.1, the macro-void ratio is from 0.33 to 0.42,

whereas for line DEGH it is from 0.59 to 0.74. The former values are representative of a dense single grain packing and the latter a medium to loose packing. If JKLM is accepted as the most likely clay-void line, the structure of the loess would be described as a dense packing of low-density grains, that is,of grains which are composed of silt particles coated with a porous clay binder.

5.2 Strength and Compressibility as a Function of Water Content

The volumetric relations in Fig. 5.1 may be used to explain the influence of the water content on the strength and compressibility of loess. The variation with water content of the strength, as described by the undrained failure parameters ϕ_u and c_u, and of the compressibility, described by the parameters p_o' and C_c' was shown in Figs. 4.26, 4.27, 4.4, and 4.5 respectively. The relationships between these parameters and the volumetric relations are considered in the following paragraphs.

The value of ϕ_u, as discussed in section 4.4, depends on the degree of saturation S_r and approaches zero as S_r approaches 100%. The observed reduction in ϕ_u as the water content increases from 14% to 26% is the result of the increase in saturation which occurs in this interval under confining pressures to 140 psi. Thus ϕ_u depends not only on the water content, but also on the confining pressure and compressibility of the soil structure, all of which influence the degree of saturation. As a result of these considerations, it is evident that the volumetric relations

in Fig. 5.1 can not in themselves explain the behavior of ϕ_u.

On the other hand, the value of c_u depends on the undrained strength of the clay binder because it represents the shear strength with zero confining pressure. The cohesion vs. water content plot in Fig. 4.27 shows a marked change in behavior at a water content of 14%. As the water content increases to 14%, there is a sharp reduction in c_u whereas above 14% water content there is only a slight reduction. Reference to Fig. 5.1 indicates that 14% water content is between points K and L, that is, within the range where the clay binder is swelling and thus softening and losing strength.

The slope C_c' of the steep portion of the void ratio-log pressure diagram decreases with increasing water content (Fig. 4.5), but the total reduction is small. It should be noted that C_c' could not be obtained for water contents below 14% because the void ratio-log pressure curves did not extend to a sufficiently high pressure. The observed decrease in C_c' may reflect a more gradual compression as the clay binder softens, but no conclusive explanation based on the volumetric relations is evident.

The pressure p_o', which is a quasi-preload, decreases as the water content increases to 20%, and thereafter remains essentially constant (Fig. 4.4). This parameter depends on the strength of the binder before compression, and therefore on the water content, because only a small decrease in volume occurred under pressures lower than p_o'. A further

illustration of the compressibility-water content relations is given in Fig. 5.2 where the total change in void ratio for each of four pressure increments in the one-dimensional consolidation tests is plotted against water content. The distinct break in the curves for the increments from 2 to 4 tsf and from 4 to 8 tsf occurs between water contents of 16% to 20%. For the load increment from 8 to 32 tsf there is a peak in the curve at a water content of 16%. This results from the fact that the steepest portion of the void ratio-log pressure curves occurs wholly within the increment for specimens at this water content. The figure clearly illustrates that there is little or no difference in behavior for water contents above 20%. Fig. 5.1 provides an explanation for this behavior since water contents above 20% are between points L and M where the void ratio and water content of the clay binder are shown to be constant.

On the basis of the above comparisons, it is concluded that the variation of both strength and compressibility with water content is consistent with the volumetric concepts embodied in Fig. 5.1.

5.3 Initial Negative Pore Water Pressure as a Function of Water Content

The variation of the initial negative pore water pressure with water content was shown in Fig. 4.32. A sharp increase in negative pore pressure occurred as the water content was reduced below 18% to 20%. The negative pore pressures were measured to be from -10 psi to -20 psi in this water content range.

One of the purposes for measuring the negative pore pressure was

to permit an estimation of the water content of the clay binder. The basis for the estimate was the assumption that the negative pore pressure in the loess was due to capillary stresses in the water in the clay-size voids. To provide an independent measurement of these capillary stresses, the relation between negative pore pressure and the water content of the clay-size particles was measured in a separate series of tests and presented in Fig. 4.35.

Equations 4.5.1 and 4.6.1 express the measured relation between pore pressure and water content for the loess and clay fraction respectively:

$$u\ (psi) = -\left(\frac{32.5}{w\%}\right)^{5} \qquad 4.5.1$$

$$u\ (psi) = -\left(\frac{100}{w_c\%}\right)^{5} \qquad 4.6.1$$

If these equations are assumed to result from the same phenomenon, the pore pressures may be equated thus relating the water contents:

$$w_c = 3.1\ w$$

However, it is evident from the following that this relation cannot hold. Since the clay content of the loess is 19%, the ratio w_c/w is 100/19 or 5.2 if all the water is in the clay voids. Therefore, for values of w_c/w less than 5.2, there must be water in the macro-voids; that is, the clay voids are not large enough to hold all of the water. This being the case, the pore pressures in the loess are due to water in the macro-voids are not related to the pressures given by Equation 4.6.1.

The volumetric relations in Fig. 5.1 provide another, more consistent, explanation of the variation of pore pressure with water content. In the region between points L and M, the clay binder is saturated and is exposed to the volume of water in the macro-voids. This volume is indicated by the difference between lines LM and LB. The measured pore pressures in the loess for water contents above point L, or 18%, are therefore due to capillary pressures in the silt-size macro-pores. It was noted above that the negative pore pressures at this water content are from -10 psi to -20 psi. These pressures are reasonable for the capillary effect in a silt-size material. A reduction in water content below point L is accompanied by the shrinkage of the clay binder and by increased negative pressures in the pore water which is present only in the clay-size voids below point L. This accounts for the sharp increase in negative pore pressure which occurs as the water content falls below 18% to 20%.

5.4 Properties at Natural Water Contents

In view of the variation in properties that occurs with water content, it is of interest to consider the range in natural water content which was measured at the field site and to estimate the upper and lower limits of strength and compressibility of the soil in situ.

The range in natural water contents for the twelve-month period ending in September 1967 is shown in Fig. 3.12. Between depths of 2 ft and 4 ft the natural water content varied from a minimum of 15% to a

maximum of 28%; from the 6 ft to the 12 ft depth, the range was from 25% to 32%. Values of p_o', C_c', ϕ_u and c_u for these water contents have been estimated on the basis of the curves in Figs. 4.4, 4.5, 4.26, and 4.27 respectively, and the results are listed in Table 5.1.

It is evident from Table 5.1 that there is no significant variation in properties below the 6 ft depth. This is true because the range in natural water contents is not great and, more significantly, because the properties are not sensitive to water content changes within this range. The underlying reason for this behavior, as demonstrated in Fig. 5.1, is that the volume of the clay binder, and hence its water content and strength, is constant between the water contents of 25% and 32%.

For the depths below 4 ft, however, there is an important variation in properties. The value of p_o' and the strength parameters are significantly higher for the minimum water content of 15% than for the maximum water content. Again, Fig. 5.1 demonstrates the reason for this. The lower water content falls between points K and L which define the region where the clay binder is shrinking, and therefore increasing in strength, due to desiccation.

If a field plate load test were conducted at a shallow depth during the period when the natural water content were near 15%, it is evident that the results would reflect a temporary high strength and low compressibility and would, therefore, be misleading. However, the water content profiles shown in Figs. 3.8 through 3.11 indicate that water contents

below 20% are exceptional at this site. Because of this, it may be concluded that this loess deposit is sufficiently moist to be stable, in that its properties do not change with normal water content variations. In a more arid region, where lower water contents prevail, an otherwise identical loess would be sensitive to variations in water content.

CHAPTER 6

SUMMARY AND CONCLUSIONS

6.1 Summary

The primary purpose of this study of undisturbed loess was to explore the relation between the water content of the whole soil and that of the binder and to develop thereby a new basis for interpreting the mechanical behavior. To this end, a single loess deposit was used as a source of undisturbed samples to eliminate as much as practical variables other than water content.

The undisturbed samples at their natural water contents, and at water contents modified in the laboratory to provide a range from 8% to 32%, were subjected to unconsolidated-undrained triaxial compression tests, to consolidation tests in which no water was added to the unsaturated samples, and to initial negative pore water pressure tests. The results of these tests were summarized in Tables 4.1, 4.2, and 4.3 respectively.

One of the original hypotheses was that the initial negative pore water pressure in the loess was the result of the capillary effects in the clay binder. It follows that equal capillary pressures in the loess, and in a specimen composed of the clay-size material only, would imply that the water content of the clay binder in the loess was the same as that in the clay sample. To investigate this, the clay-size fraction was separated from remainder of the loess and remolded specimens at various water contents were subjected to the initial negative pore pressure test. These

results were summarized in Table 4.4. The void ratio-pressure relations for the remolded clay fraction were also determined in one-dimensional and triaxial consolidation tests.

The water content in the field was obtained at regular intervals to provide an example of the range in properties that would be encountered at this site. These measurements were summarized in Fig. 3.12.

Finally the index properties of the loess and of the separated clay fraction were determined. These have been presented in Table 2.1.

6.2 Conclusions

The conclusions that follow are based on the test results and interpretations given in Chapter 4 and 5 respectively. At this point it should be noted that, by design, a single loess deposit was used as a source of samples. This choice permitted a detailed study with one significant variable, i.e. water content. While the conclusions provide a basis for comparing and explaining the properties of other loessial soils, they have been drawn from tests on only one soil and generalizations must be made with caution until other loessial soils are studied.

1. The water content of loess is a significant factor determining its behavior. There is a water content, or narrow range of water contents, above which the clay binder is volumetrically stable but below which the clay binder shrinks due to desiccation. This water content or range is referred to here as the critical water content.

2. The properties of the loess are not altered significantly by changes in water content above the critical value.

3. When the water content decreases below the critical value, the loess undergoes a sharp change in behavior. This is manifested by an increase in the quasi-preload p_o' and the undrained cohesion intercept c_u.

4. The relation between the initial negative pore pressure and the water content also changes abruptly at the critical water content. The negative pore pressures at water contents above the critical value are small and may be attributed to capillary water in the silt-size voids. On the other hand, the sharp increase in negative pore pressure that occurs when the water content falls below the critical value is attributed to capillary water in the clay-size voids.

5. The volumetric relations in Fig. 5.1 are useful in describing the basis for behavior. When the location of the line JKLM is established for a particular loess, the critical water content is given by point L.

6. The concept of critical water content is important for natural soils. If the natural water content is below the critical value, significant changes in properties will occur with small changes in water content. On the other hand, if the natural water content remains above the critical value, the properties of the loess will not vary significantly.

7. The concept of macro-void ratio, defined as the ratio of the volume of silt-size voids to the volume of solids plus clay-size voids, indicated that the structure of loess may be a medium to dense packing of low density

particles, that is, particles consisting of a silt grains coated with a binder of clay-size particles and clay-size voids. A study of the mechanical behavior of an idealized structure of this type would be instructive.

8. For the Hawkeye Loess, the critical water content is in the range from 15% to 20%. Since the clay-size particles make up 19% of the loess, the corresponding water contents of the clay binder are 78% and 104%. All the water assumed to be in the clay-voids when the loess is at its critical water content.

9. When the Hawkeye loess was above the critical water content, the quasi-preload p_o' was 1.7 tons per square foot and the undrained cohesion intercept c_u was in the range from 5 psi to 15 psi. At a water content of 8%, which is below the critical water content, these values increased to p_o' = 10 to 20 tsf and c_u = 48 psi.

APPENDIX I. - REFERENCES

ASTM, (1964), "Procedures for Testing Soils," American Society for Testing Materials, Philadelphia.

Clevenger, W. A., (1958), "Experiences with Loess as Foundation Material," Transactions, ASCE, Vol. 123, pp. 151-180.

Davidson, D. T. and Sheeler, J. B., (1952), "Studies of the Clay Fraction in Engineering Soils: III. Influence of Amount of Clay on Engineering Properties," Proceedings, Highway Research Board, Vol. 31, pp. 558-563.

Gibbs, H. J. and Coffey, C. T., (1963), "Measurement of Initial Negative Pore Pressure of Unsaturated Soil, Progress Report on Shear and Pore Pressure Research, Earth Research Program," Laboratory Report No. EM-665, U. S. Bureau of Reclamation, Denver, Colorado.

Gibbs, H. J., Hilf, J. W., Holtz, W. G., and Walker, F. C., (1960), "Shear Strength of Cohesive Soils," ASCE Research Conference on Shear Strength of Cohesive Soils, Boulder, Colorado, pp. 33-162.

Gibbs, H. J. and Holland, W. Y., (1960), "Petrographic and Engineering Properties of Loess," Engineering Monograph No. 28, U. S. Bureau of Reclamation, Denver, Colorado.

Handy, R. L., Lyon, C. A., and Davidson, D. T., (1955), "Comparison of Petrographic and Engineering Properties of Loess in Southwest, East-Central and Northeast Iowa," Iowa Academy of Science Proceedings, Vol. 62, pp. 279-297. (Reprinted in Bulletin No. 21, Iowa Highway Research Board, December 1960, pp. 65-87).

Holtz, W. G. and Gibbs, H. J., (1951), "Consolidation and Related Properties of Loessial Soils," Symposium on Consolidation Testing of Soils - 1951, American Society for Testing Materials, Special Technical Publication No. 126, pp. 9-26.

Larionov, A. K., (1965), "Structural Characteristics of Loess Soils for Evaluating Their Constructional Properties," Proceedings, 6th International Conference on Soil Mechanics and Foundation Engineering, Vol. 1, Montreal, pp. 64-68.

Leonards, G. A. and Ramiah, B. K., (1959), "Time Effects in the Consolidation of Clays," Papers on Soils - 1959 Meetings, American Society for Testing Materials, Special Technical Publication No. 254, pp. 116-130.

Lyon, C. A., Handy, R. L., and Davidson, D. T., (1954), "Property Variations in the Wisconsin Loess of East-Central Iowa," Iowa Academy of Science Proceedings, Vol. 61, pp. 291-312. (Reprinted in Bulletin No. 20, Iowa Highway Research Board, December 1960, pp. 44-64).

Olson, R. E. and Langfelder, L. J., (1965), "Pore Water Pressures in Unsaturated Soils," Journal of the Soil Mechanics and Foundations Division, ASCE, Vol. 91, No. SM4, Proceeding Paper, 4409, pp. 127-150.

Peck, R. B. and Ireland, H. O., (1958), Discussion on: Clevenger, W. A., "Experiences with Loess as a Foundation Material," Transactions, ASCE, Vol. 123, pp. 171-179.

Seed, H. B., Woodward, R. J. and Lundgren, R., (1964), "Fundamental Aspects of the Atterberg Limits," Journal of the Soil Mechanics and Foundation Division, ASCE, Vol. 90, No. SM6, pp. 75-105.

Sheeler, J. B. and Davidson, D. T., (1957), "Further Correlation of Consistency Limits of Iowa Loess with Clay Content," Proceedings, Iowa Academy of Science, Vol. 64, pp. 407-412. (Reprinted in Bulletin No. 21, Iowa Highway Research Board, December, 1960, pp. 221-226.

Skempton, A. W., (1953), "The Colloidal Activity of Clays," Proceedings, 3rd International Conference on Soil Mechanics and Foundation Engineering, Zurich.

Terzaghi, K., (1951), Discussion on: Holtz, W. G. and Gibbs, H. J., "Consolidation and Related Properties of Loessial Soils," Symposium on Consolidation Testing of Soils - 1951, American Socity for Testing Materials, Special Technical Publication No. 126, pp. 30-32.

Terzaghi, K. and Peck, R. B., (1967), Soil Mechanics in Engineering Practice, 2nd ed., Wiley, New York.

APPENDIX II - NOTATION

The following symbols have been used in this report:

a = intercept on modified Mohr-Coulomb diagram, psi;

A = activity, $\frac{\text{change in plasticity index}}{\text{corresponding change in clay content}}$;

c_u = apparent cohesion in undrained shear, psi;

C_c' = slope, $\Delta e/\log\left(\frac{p + \Delta p}{p}\right)$, of the steepest portion of the consolidation curve;

E_s = secant modulus at half the failure stress, psi;

E_i = initial tangent modulus, psi;

e = void ratio, V_v/V_s;

e_i = initial void ratio;

e_m = macro-void ratio, $V_{vm}/(V_{sm} + V_{sc} + V_{vc})$;

e_c = clay-void ratio, V_{vc}/V_{sc};

p_o' = pressure at the intersection on the void ratio-log pressure diagrams of the steepest slope of the consolidation curve and e_i, tsf;

S_{ri} = initial degree of saturation, %;

S_{rc} = degree of saturation after undrained compression due to cell pressure, %;

u = pore water pressure, psi;

V_v = volume of voids, cc;

V_s = volume of solids, cc;

V_w = volume of water, cc;

V_{sc} = volume of clay-size paritcles, cc;

V_{sm} = volume of silt-size particles, cc;

V_{vc} = volume of clay-voids, cc;

V_{vm} = volume of macro-voids, cc;

w = water content, %;

w_i = initial water content, %;

w_c = water content of clay fraction, %;

ϵ_f = axial strain at failure, %;

ϵ_s = axial strain at half the failure stress, %;

σ_3 = cell pressure, psi;

$(\sigma_1 - \sigma_3)_{f/2}$ = half the stress difference $(\sigma_1 - \sigma_3)$ at failure, psi;

ψ = slope of modified Mohr-Colomb diagram;

ϕ_u = angle of shearing resistance in undrained shear.

TABLE 2.1

SOIL INDEX PROPERTIES

Property (1)	No. of Tests (2)	Range (3)	Average (4)
(a) Loess H			
Liquid Limit	5	32-37	35
Plastic Limit	5	23-24	24
Plasticity Index			11
Specific Gravity	4	2.72-2.74	2.73
Percentage of Clay:			
less than 0.005 mm	4	24-28	26
less than 0.002 mm	4	17-21	19
Activity			1.10
Natural dry density, pcf	13	85.0-89.3	87
Natural water content, %	13	23.2-27.0	25
(b) Clay Fraction Less Than 0.002 mm			
Liquid Limit	2	146	146
Plastic Limit	2	43-48	46
Plasticity Index			100
Shrinkage Limit	2	14-17	15
Specific Gravity	1		2.72
Percentage of Clay:			
less than 0.002 mm			100

TABLE 3.1

TOTAL MONTHLY PRECIPITATION IN INCHES

Month (1)	Measured at Site Oct. 1966 to Sept. 1967 (2)	From Records of Iowa City Cooperative Observer Weather Station Oct. 1966 to Sept. 1967 (3)	10 year average 1951-1960 (4)	70 year average 1897-1966 (5)
October	I. R.	2.61	2.81	2.48
November	1.48	1.46	1.93	1.98
December	0.90	0.83	1.31	1.40
January	0.78	0.63	1.05	1.34
February	0.70	0.56	1.35	1.25
March	2.80	2.58	2.45	2.28
April	I. R.	4.52	3.37	3.12
May	I. R.	1.15	4.69	4.14
June	6.01	7.49	3.78	4.57
July	I. R.	2.80	4.01	4.05
August	I. R.	4.57	3.10	3.54
September	4.93	4.62	2.27	3.75
	TOTALS	33.82	32.12	33.90

I. R. = Incomplete Record

TABLE 4.1

SUMMARY OF CONSOLIDATION TESTS

Specimen No. (1)	w_i % (2)	e_i (3)	S_{ri} % (4)	p_o' tsf (5)	C_c' (6)
(a) Nominal Water Content = 8%					
1	9.6	0.895	29.3	9.4-20	-
2	8.4	0.895	25.4	10.8-20	-
(b) Nominal Water Content = 14%					
3	16.3	0.938	47.2	4.6	0.469
4	15.6	0.895	47.6	7.5	0.486
5	13.9	0.849	44.5	11.0	0.483
(c) Nominal Water Content = 20%					
6	19.2	0.998	52.5	1.6	0.406
7	22.4	0.987	62.0	2.1	0.435
8	21.2	0.958	60.4	2.4	0.399
9	20.5	0.978	57.2	2.4	0.466
10	20.0	0.952	57.4	2.1	0.402
(d) Nominal Water Content = 26%					
11	26.5	0.957	75.7	1.6	0.372
12	23.2	0.971	65.0	1.9	0.389
13	26.4	0.952	76.0	2.1	0.379
14	24.6	0.987	67.7	1.4	0.332
(e) Nominal Water Content = 32%					
15	29.2	0.987	80.6	1.5	0.359
16	31.3	0.957	89.4	1.7	0.362
17	32.6	1.018	87.3	1.4	0.432
18	32.6	1.002	89.0	1.5	0.402
19	32.2	0.972	90.3	1.9	0.372
20	32.4	0.987	89.5	1.7	0.386
21	30.5	0.962	86.3	1.8	0.395
22	32.5	0.962	92.0	1.4	0.346

TABLE 4.2

SUMMARY OF TRIAXIAL TESTS

Specimen No.	w	e_i	S_{ri}	σ_3	S_{rc}	$\frac{(\sigma_1-\sigma_3)_f}{2}$	ϵ_f	ϵ_s	ϵ_f/ϵ_s	E_s	E_i
	%		%	psi	%	psi	%	%		psi	psi
(1)	(2)	(3)	(4)	(5)	(6)	(7)	(8)	(9)	(10)	(11)	(12)
(a) Nominal water content = 8%											
1	8.3	0.903	25.3	0	25.3	76	1.58	0.50	3.2	15,000	15,000
2	9.2	0.875	28.8	20	30.9	74	1.76	0.56	3.1	13,000	17,000
3	8.3	0.882	25.7	60	27.6	107	4.59	0.68	6.8	16,000	23,000
4	7.7	0.882	23.9	100	25.1	148	7.28	0.87	8.4	17,000	21,000
5	8.0	0.860	25.4	140	27.0	180	20.0	1.10	18.2	16,400	35,000
6	7.4	0.907	22.3	140	23.0	162	20.0	1.35	14.8	12,000	23,000

TABLE 4.2 (Continued)

SUMMARY OF TRIAXIAL TESTS

Specimen No.	w	e_i	S_{ri}	σ_3	S_{rc}	$\frac{(\sigma_1-\sigma_3)_f}{2}$	ϵ_f	ϵ_s	ϵ_f/ϵ_s	E_s	E_i
	%		%	psi	%	psi	%	%		psi	psi
(1)	(2)	(3)	(4)	(5)	(6)	(7)	(8)	(9)	(10)	(11)	(12)
(b) Nominal water content = 14%											
7	14.6	0.935	42.7	0	42.7	20	1.52	0.32	4.8	6,300	6,400
8	14.1	0.869	44.5	20	46.3	49	3.53	0.58	6.1	8,400	8,400
9	14.8	0.947	41.8	40	45.0	40	20.00	1.02	19.6	3,900	5,700
10	15.7	0.963	44.7	60	47.9	48	20.00	2.50	8.0	1,900	4,600
11	15.0	0.882	46.5	80	50.8	69	20.00	2.00	10.0	3,450	10,500
12	16.3	0.966	46.2	100	56.3	68	20.00	4.45	4.5	1,530	11,000
13	15.1	0.892	46.2	120	52.1	87	20.00	4.19	4.8	2,080	8,500
14	15.3	0.881	47.4	140	53.9	85	18.31	3.77	4.9	2,260	11,000

TABLE 4.2 (Continued)

SUMMARY OF TRIAXIAL TESTS

Specimen No.	w	e_i	S_{ri}	σ_3	S_{rc}	$\frac{(\sigma_1-\sigma_3)_f}{2}$	ϵ_f	ϵ_s	ϵ_f/ϵ_s	E_s	E_i
	%		%	psi	%	psi	%	%		psi	psi
(1)	(2)	(3)	(4)	(5)	(6)	(7)	(8)	(9)	(10)	(11)	(12)
(c) Nominal water content = 20%											
15	20.0	0.932	58.4	0	58.4	15	1.24	0.44	2.8	3,400	3,400
16	20.3	0.963	57.5	20	-	16	12.05	0.42	28.7	3,800	5,600
17	20.2	0.960	57.4	40	61.3	24	16.15	1.29	12.5	1,900	4,500
18	20.3	0.948	58.6	60	66.8	32	20.00	2.86	7.0	1,120	3,800
19	18.9	0.977	52.9	80	66.8	44	20.00	3.26	6.1	1,350	8,400
20	22.0	0.917	65.0	100	85.2	31	8.08	1.43	5.7	2,200	5,800
21	20.2	0.900	61.5	120	78.8	48	11.75	2.12	5.5	2,300	6,700
22	20.5	0.948	59.2	140	87.3	50	12.93	1.83	7.1	2,700	10,300

TABLE 4.2 (Continued)

SUMMARY OF TRIAXIAL TESTS

Specimen No.	w	e_i	S_{ri}	σ_3	S_{rc}	$\frac{(\sigma_1 - \sigma_3)_f}{2}$	ϵ_f	ϵ_s	ϵ_f / ϵ_s	E_s	E_i
	%		%	psi	%	psi	%	%		psi	psi
(1)	(2)	(3)	(4)	(5)	(6)	(7)	(8)	(9)	(10)	(11)	(12)
(d) Nominal water content = 26%											
23	26.1	0.907	78.6	0	78.6	12	0.91	0.32	2.8	3,800	3,700
24	26.8	0.952	73.9	20	84.3	12	1.18	0.18	6.6	6,700	7,200
25	26.5	0.928	77.8	40	87.5	15	4.70	0.22	2.1	6,800	8,500
26	25,3	0.933	74.0	60	84.9	18	7.93	1.18	6.7	1,500	6,000
27	25.2	0.926	74.3	80	92.0	17	5.00	0.53	9.4	3,200	7,600
28	25,5	0.932	74.8	100	-	20	3.75	0.64	5.9	3,100	4,000
29	25.2	0.963	71.4	120	93.7	23	3.43	0.53	6.5	4,300	7,100
30	25.8	0.976	72.2	140	98.8	16	2.43	0.37	6.6	4,300	4,300
31	27.0	0.974	75.8	140	-	15	2.41	0.35	6.9	4,300	4,300

TABLE 4.2 (Continued)

SUMMARY OF TRIAXIAL TESTS

Specimen No.	w	e_i	S_{ri}	σ_3	S_{rc}	$\frac{(\sigma_1-\sigma_3)_f}{2}$	ϵ_f	ϵ_s	ϵ_f/ϵ_s	E_s	E_i
	%		%	psi	%	psi	%	%		psi	psi
(1)	(2)	(3)	(4)	(5)	(6)	(7)	(8)	(9)	(10)	(11)	(12)
(e) Nominal water content = 32%											
32	32.6	1.001	88.9	0	88.9	4	0.74	0.35	2.1	1,100	1,100
33	31.5	0.975	88.0	20	93.3	9	0.74	0.18	4.1	5,000	5,000
34	30.9	0.952	88.6	40	95.3	10	1.76	0.23	7.7	4,300	5,200
35	31.2	0.982	86.8	60	96.4	7	1.32	0.14	9.4	5,000	5,000
36	31.0	0.964	87.5	80	98.4	8	1.18	0.13	9.1	6,200	6,200
37	30.6	0.983	84.9	100	99.3	8	1.32	0.12	11.0	6,600	6,600
38	31.2	0.979	87.1	120	99.3	9	1.18	0.12	9.8	7,500	7,500
39	30.3	0.947	87.3	140	100.0	10	1.03	0.13	7.9	7,700	7,700

TABLE 4.3

SUMMARY OF INITIAL NEGATIVE PORE WATER PRESSURE TESTS

Test No.	Triaxial Specimen No.	w %	Degree of Saturation %	u psi	Time Lag for Equilibrium hr.-min.	End-plate Air Entry Value psi
(1)	(2)	(3)	(4)	(5)	(6)	(7)
(a) Nominal Water Content = 14%						
1	7	14.6	42.7	-49.5	22-0	210
2	9	14.8	41.8	-55.0	5-0	80
3	11	15.0	46.5	-55.6	2-0	80
4	12	16.4	46.2	-27.5	27-0	40
(b) Nominal Water Content = 20%						
5	15	20.0	58.4	-13.0	0-40	40
6A	17	20.2	57.4	-8.6	0-30	40
6B		20.2	57.4	-9.9	0-20	40
7	18	20.3	58.8	-9.6	0-15	40
8	19	18.9	52.9	-12.0	1-30	40
9	21	20.2	61.5	-13.3	1-10	40
10	22	20.5	59.2	-12.6	0-10	40
11		20.9	60.5	-13.1	0-30	40
12		21.5		-12.6	5-0	80
13		18.0		-12.4	5-0	80
14		17.9	51.3	-18.5	10-0	80
15		20.9		-11.0	0-15	80
16		20.5	57.5	-11.4	0-20	40
(c) Nominal Water Content = 26%						
17	23	26.1	78.6	-5.8	0-15	40
18	25	26.6	77.8	-4.7	0-30	80
19	26	25.3	74.0	-5.9	0-10	40
20	27	25.2	74.3	-5.4	0-40	80
(d) Nominal Water Content = 32%						
21	33	31.5	88.0	-1.1	0-10	40
22	34	30.9	88.6	-1.2	0-05	40
23	35	31.2	86.8	-0.8	0-10	40
24	36	31.0	87.5	-1.0	0-10	40
25	37	30.6	84.9	-1.1	0-05	40
26	38	31.3	87.1	-1.1	0-10	40
27	39	30.4	87.3	-1.4	0-05	40

TABLE 4.4

INITIAL NEGATIVE PORE WATER PRESSURE TESTS

ON CLAY FRACTION

Test No. (1)	w % (2)	u psi (3)	Time lag for Equilibrium hr.-min. (4)	End-plate Air Entry Value psi (5)
1	112.2	-0.7	0 - 15	40
2	103.5	-0.7	1 - 15	40
3	83.8	-2.0	0 - 10	40
4	78.5	-3.6	1 - 15	40
5	62.9	-10.9	5 - 40	40
6	58.0	-10.5	26 - 00	40
7	54.3	-27.0	8 - 00	80
8	52.5	-16.0	26 - 00	80
9	46.9	-40.0	19 - 30	80
10	35.0	>80	>4 - 00	80

TABLE 5.1

PROPERTIES AT NATURAL WATER CONTENTS

Depth ft	Natural water content	p_o' tsf	C_c'	ϕ_u degrees	c_u psi
(1)	(2)	(3)	(4)	(5)	(6)
2 to 4	15% min.	7.5	0.46	22	15
	28% max.	1.6	0.40	2	7
6 to 12	25% min.	1.7	0.41	4	9
	32% max.	1.6	0.39	1	6

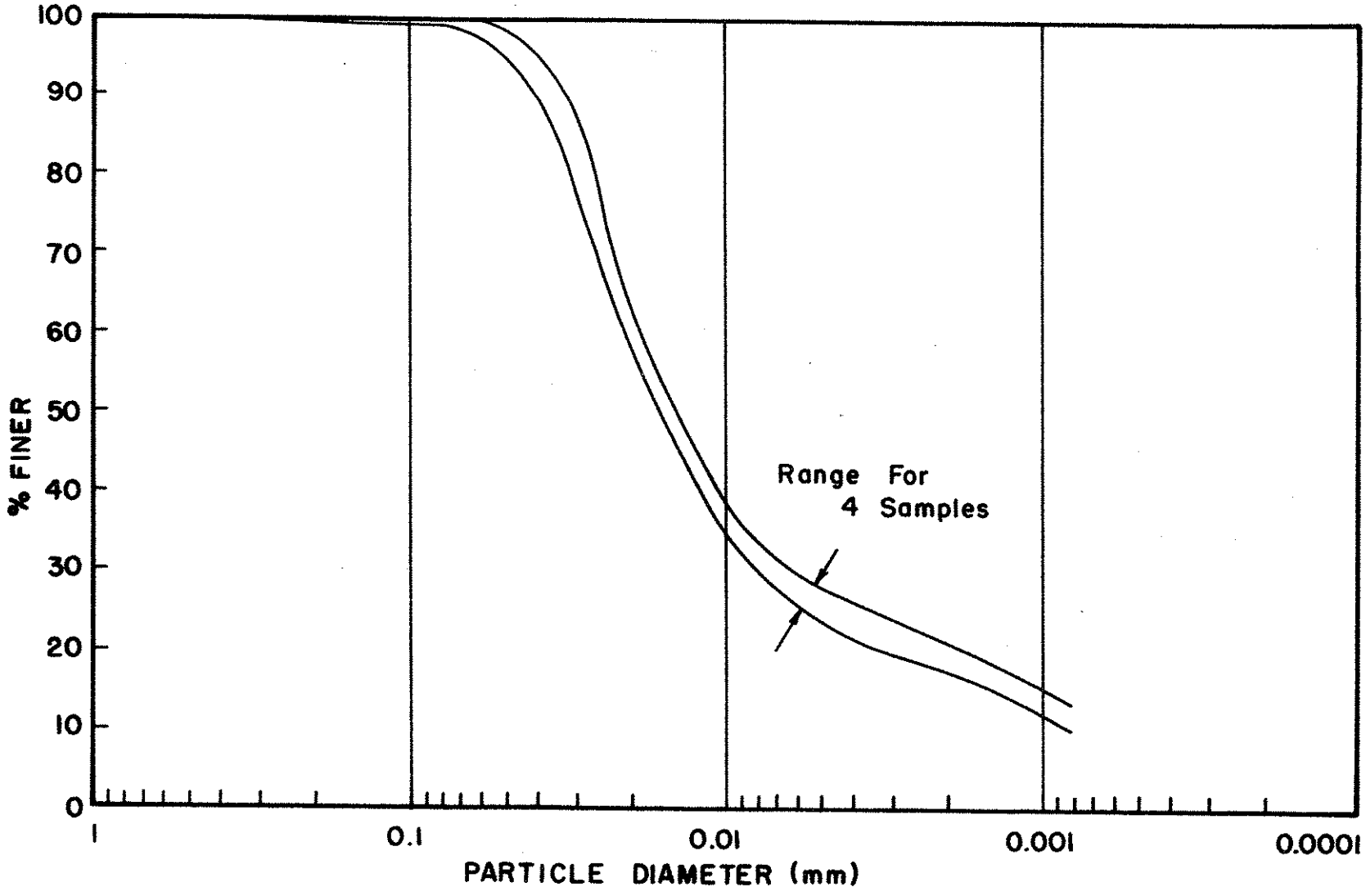

Fig. 2.1. Grain-Size Distribution for Loess H.

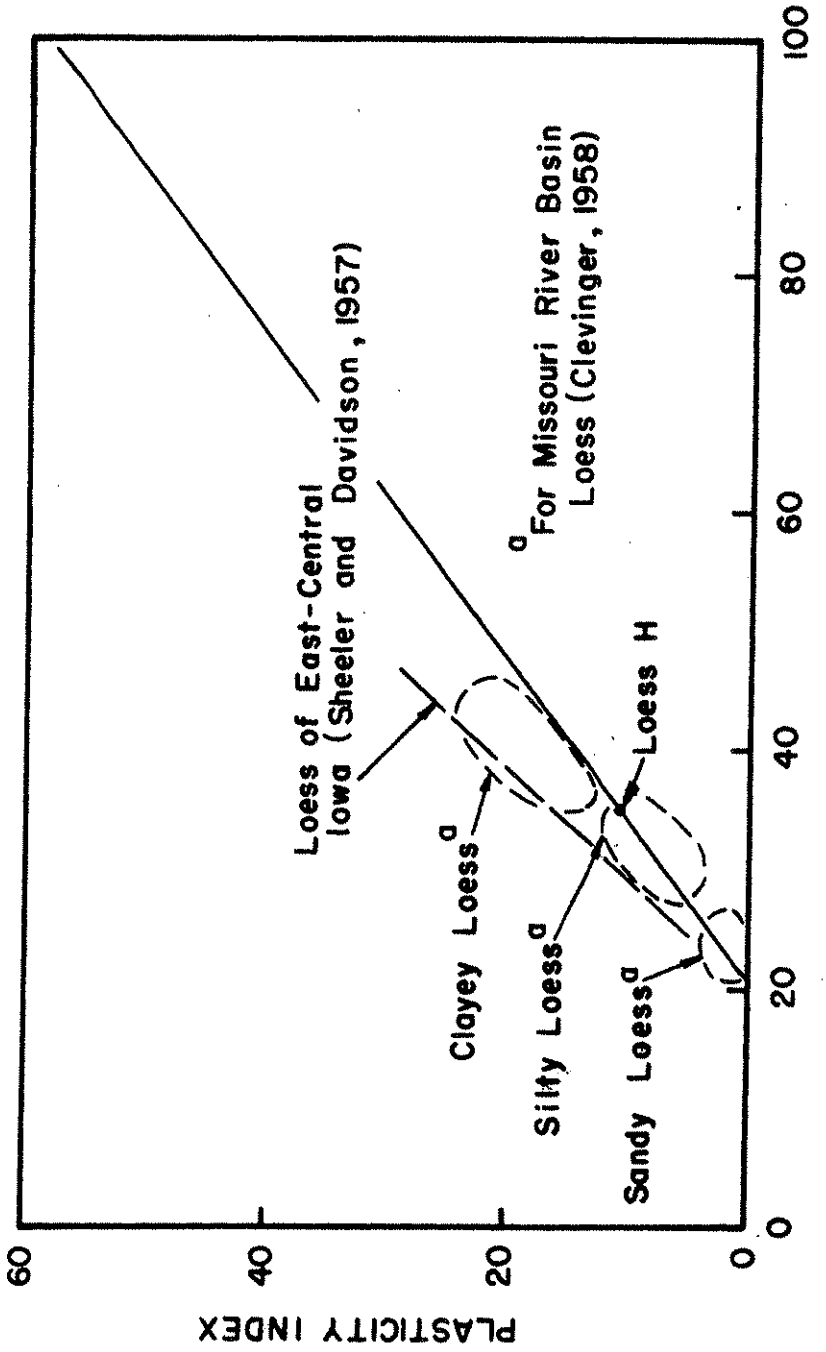

Fig. 2.2. Plasticity Chart Comparing Loessial Soils.

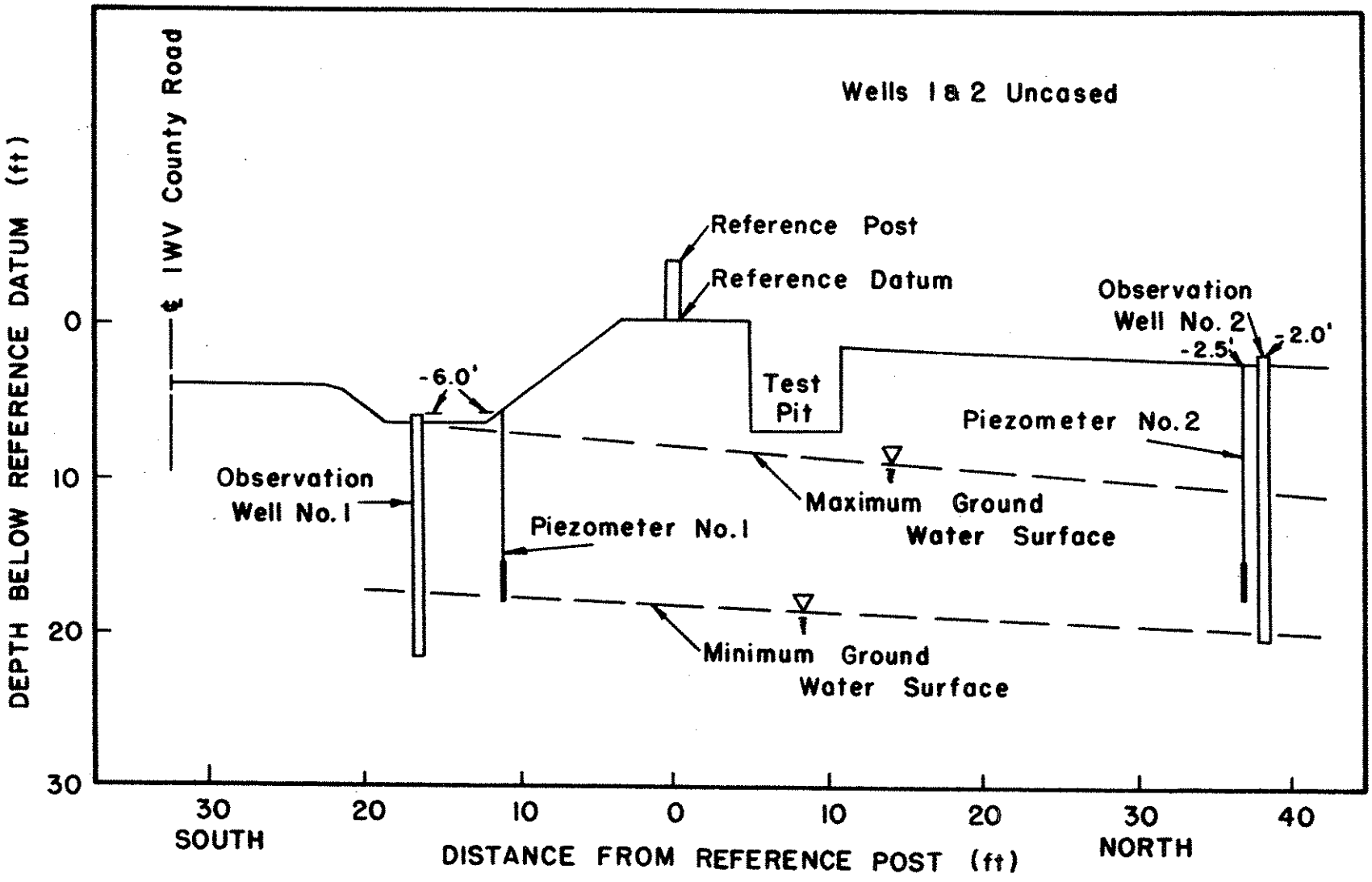

Fig. 3.1. Section Through Test Site.

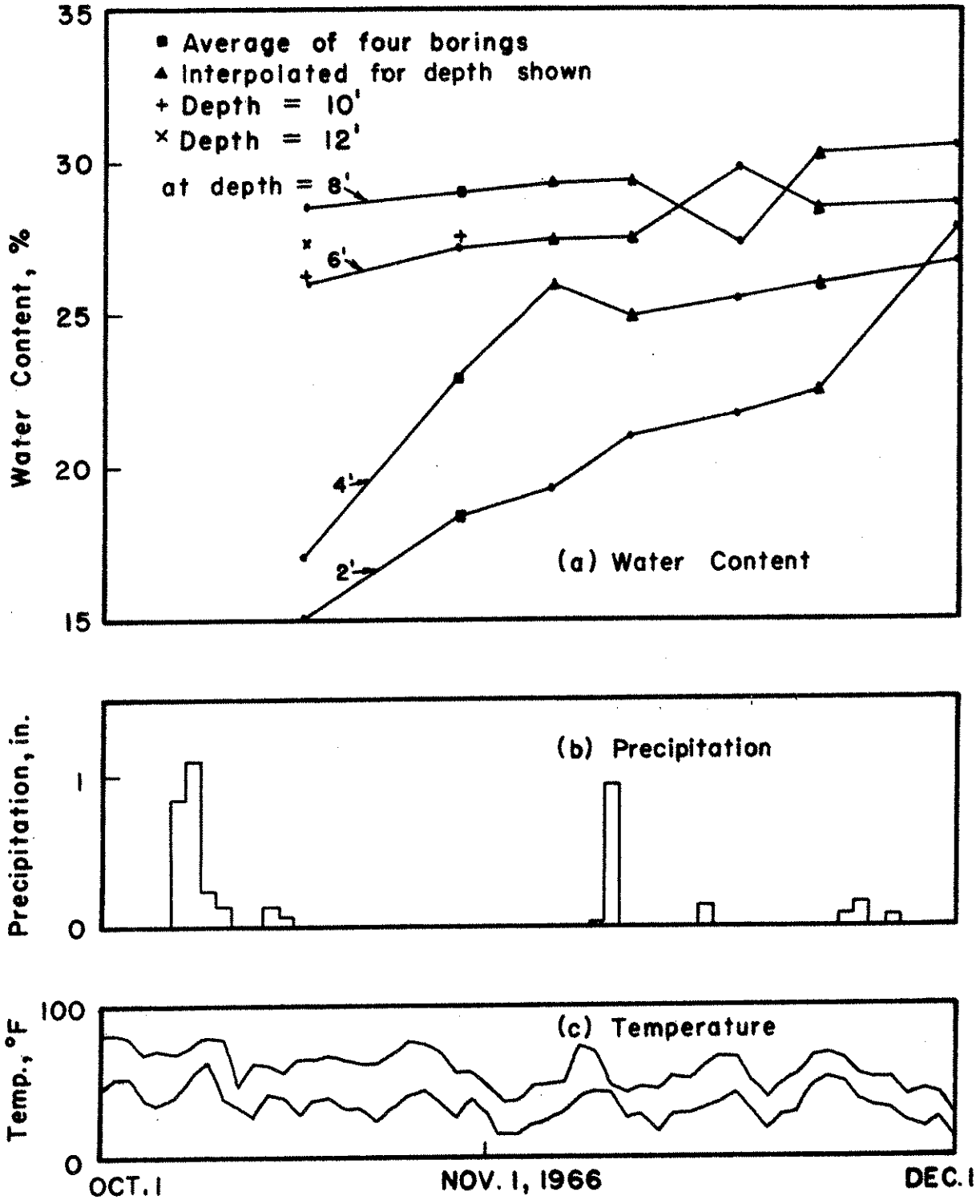

Fig. 3.2. Field Measurements, October and November 1966.

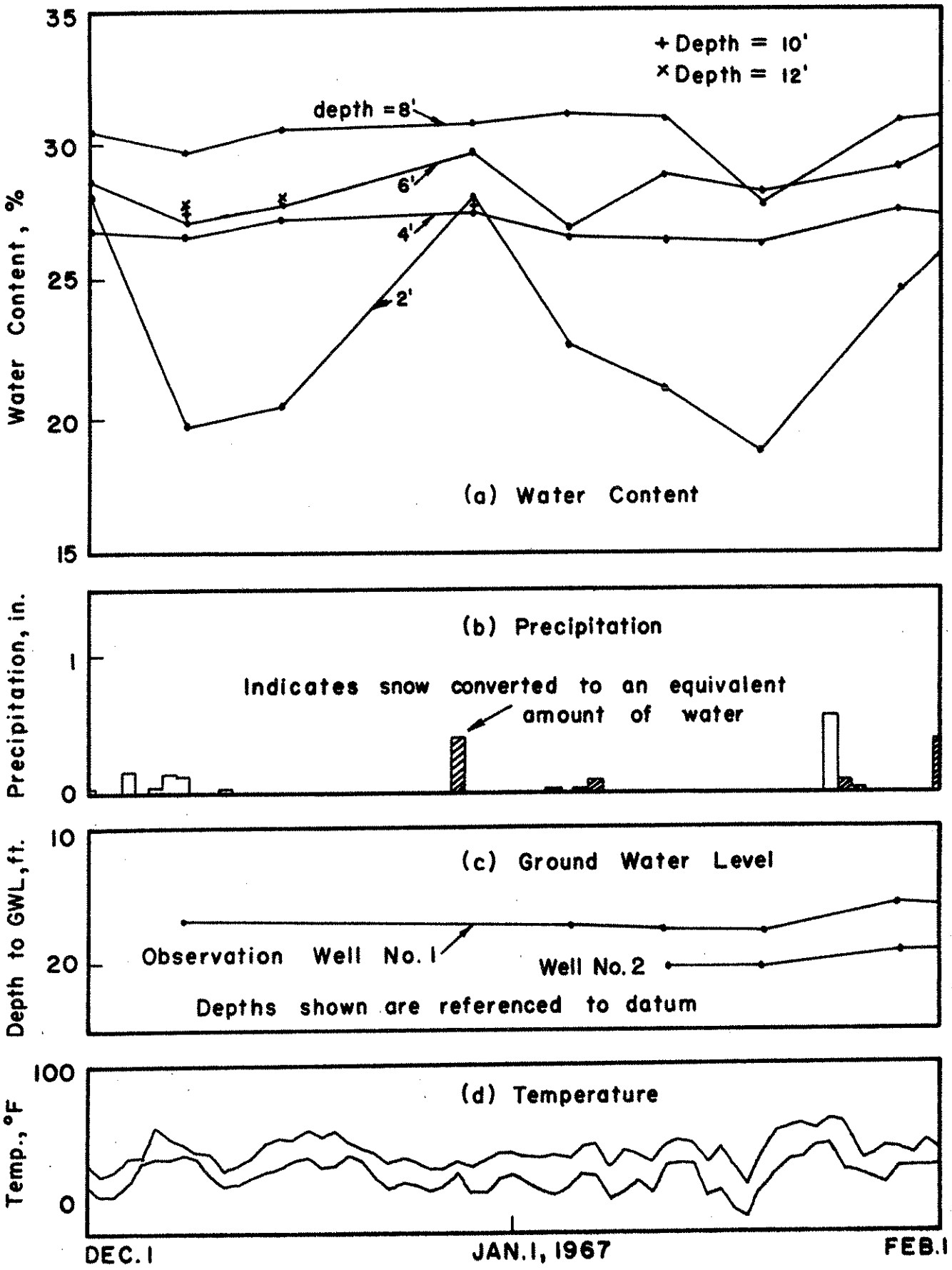

Fig. 3.3. Field Measurements, December 1966 and January 1967.

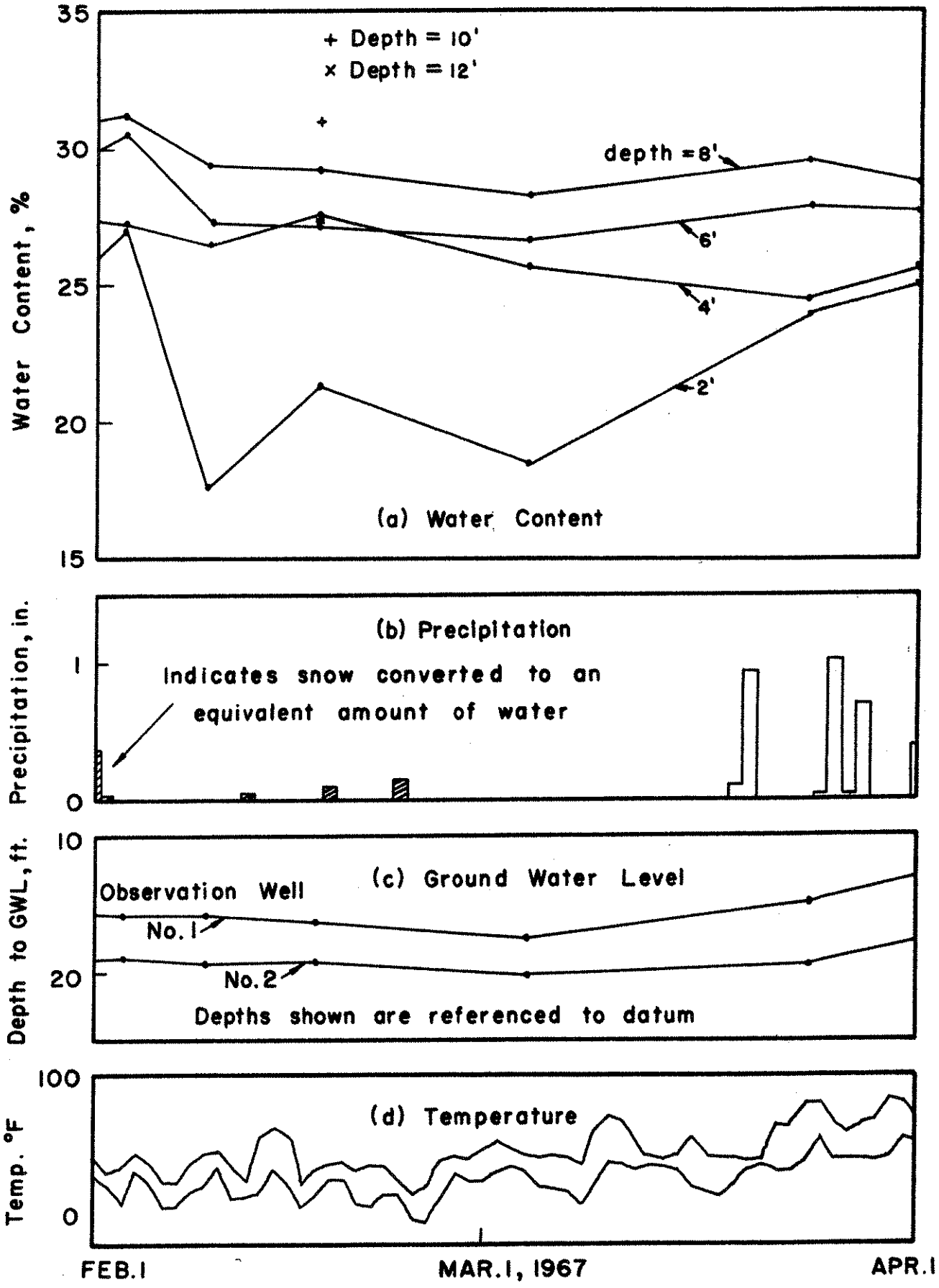

Fig. 3.4. Field Measurements, February and March 1967.

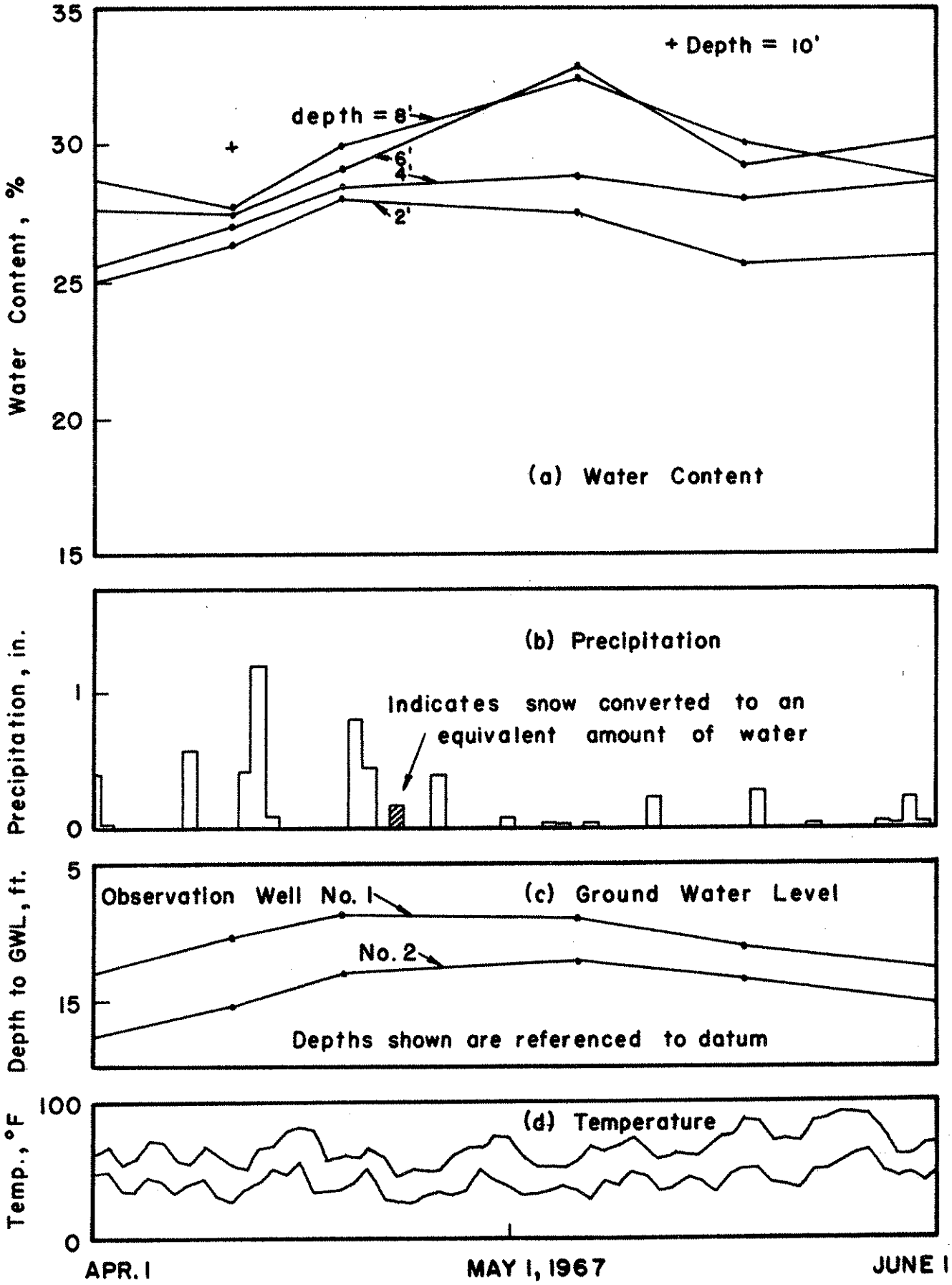

Fig. 3.5. Field Measurements, April and May 1967.

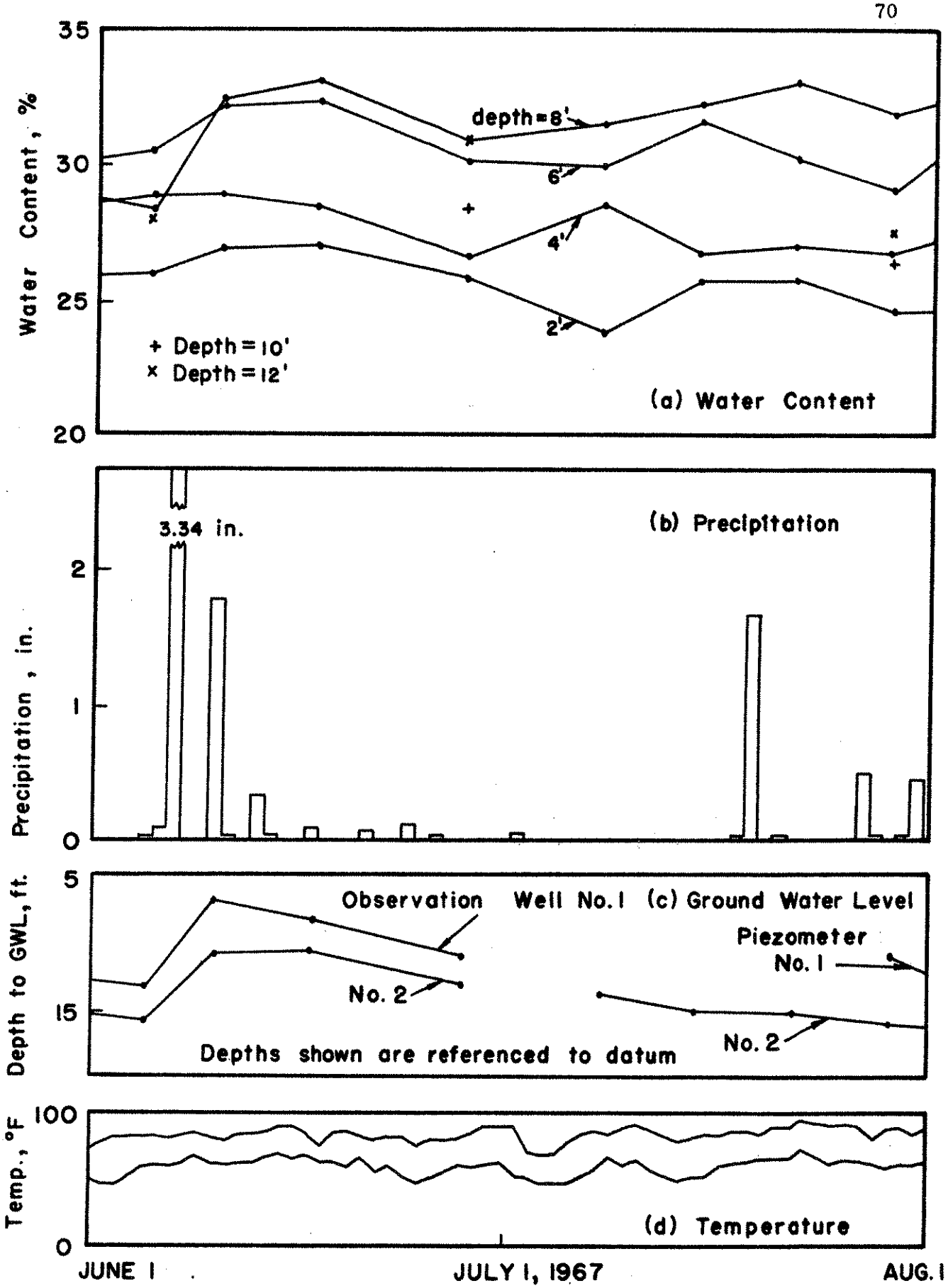

Fig. 3.6. Field Measurements, June and July 1967.

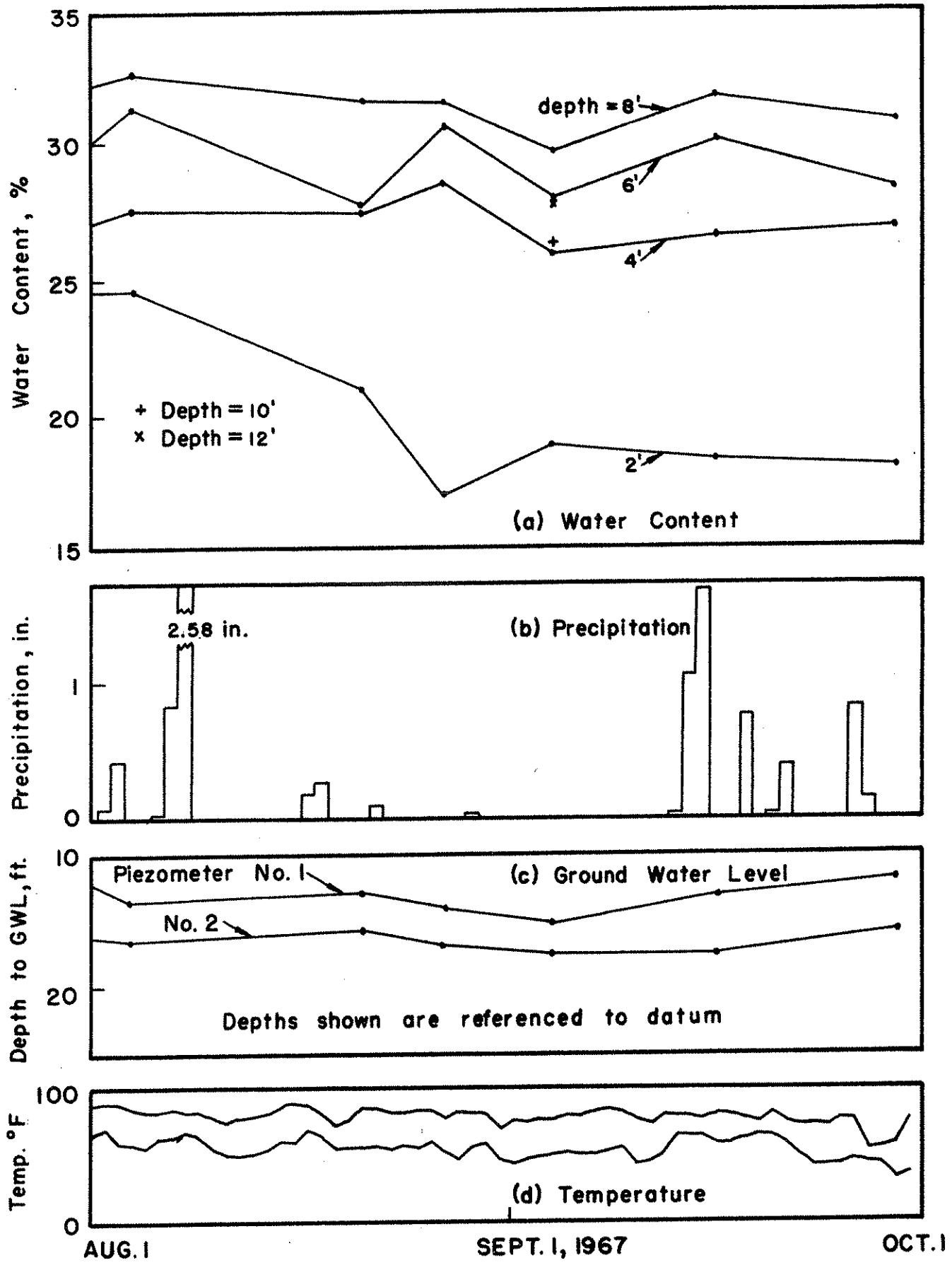

Fig. 3.7. Field Measurements, August and September 1967.

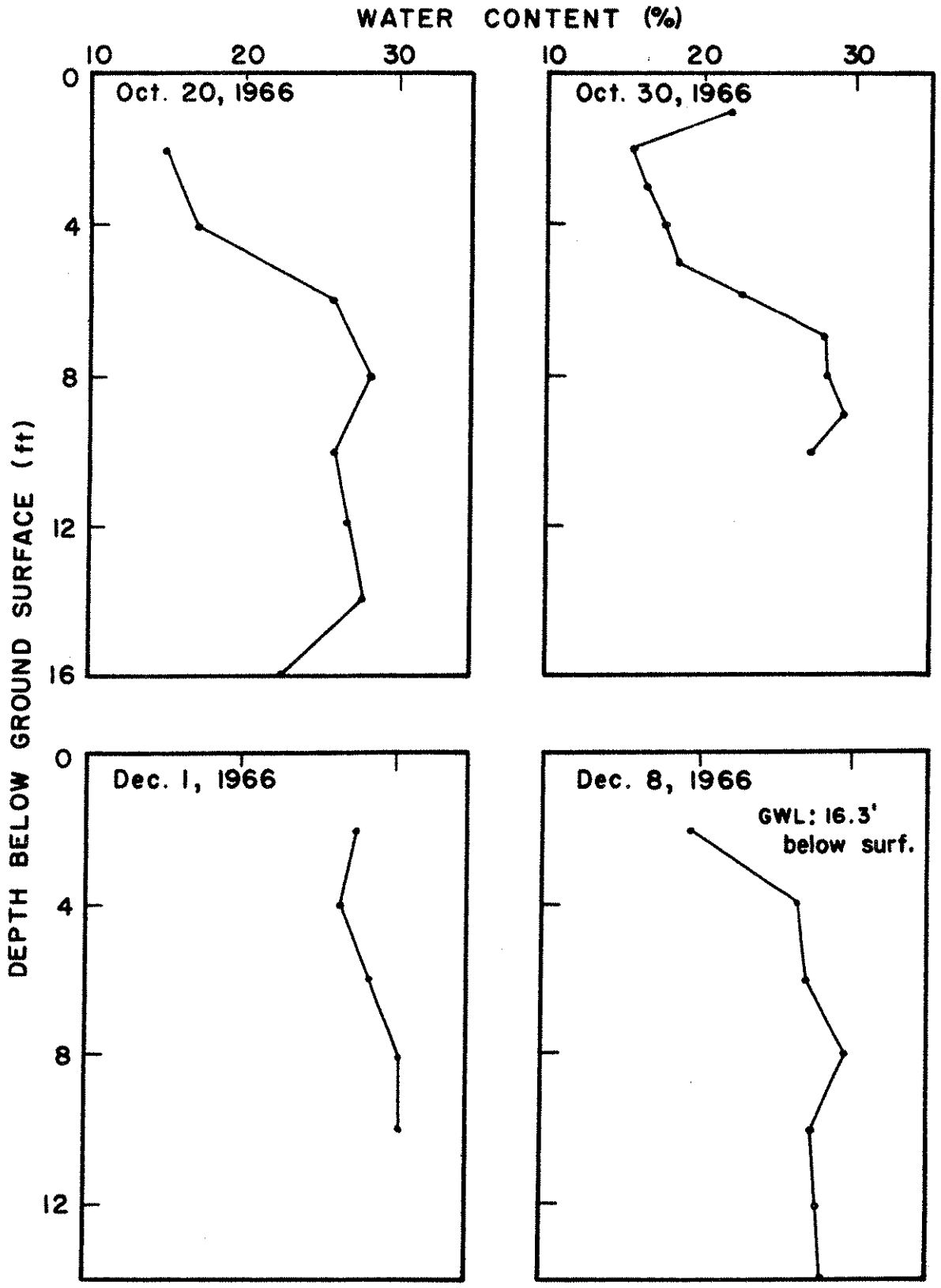

Fig. 3.8. Natural Water Content Profiles, October to December 1966.

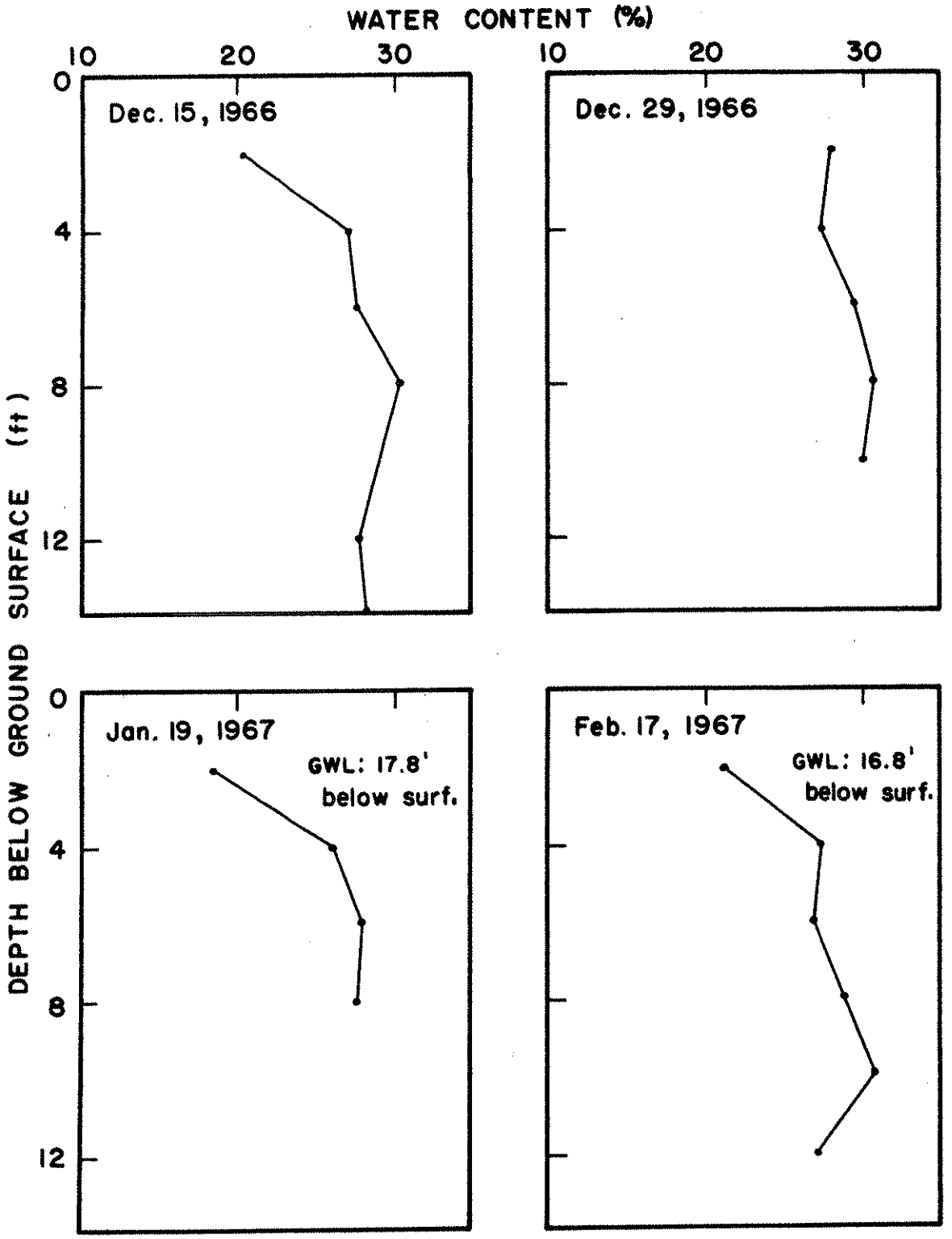

Fig. 3.9. Natural Water Content Profiles, December 1966 to February 1967.

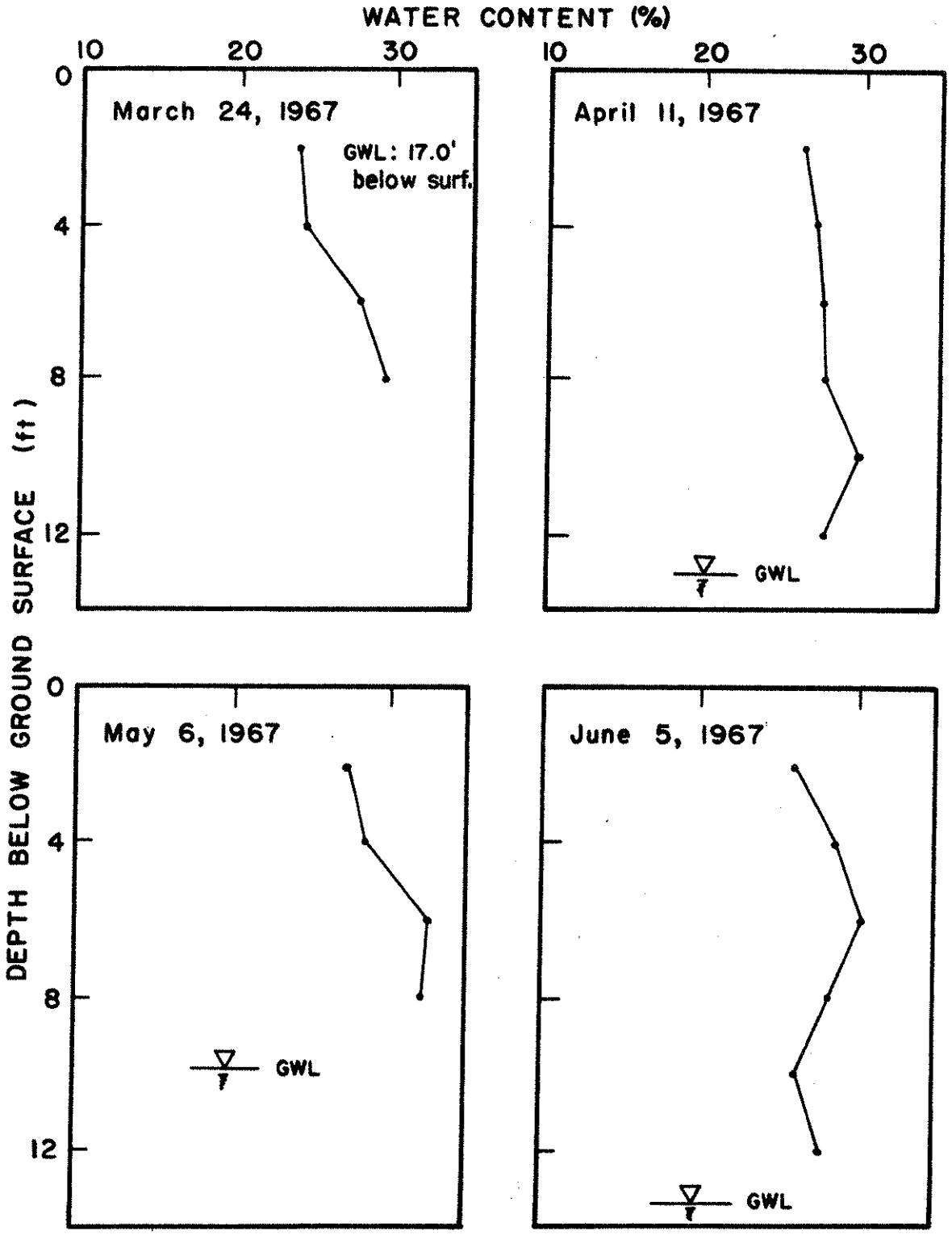

Fig. 3.10. Natural Water Content Profiles, March to June 1967.

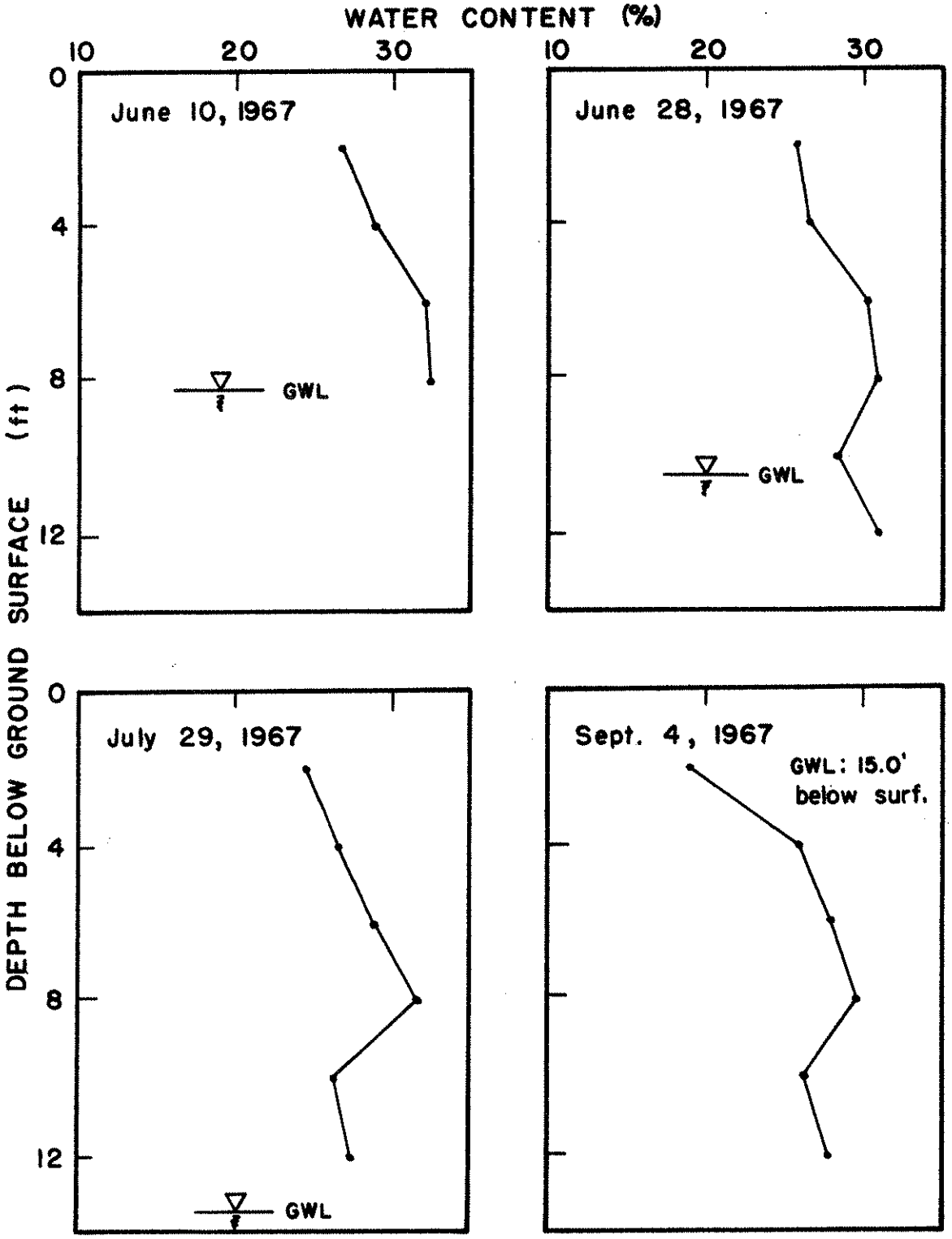

Fig. 3.11. Natural Water Content Profiles, June to September, 1967.

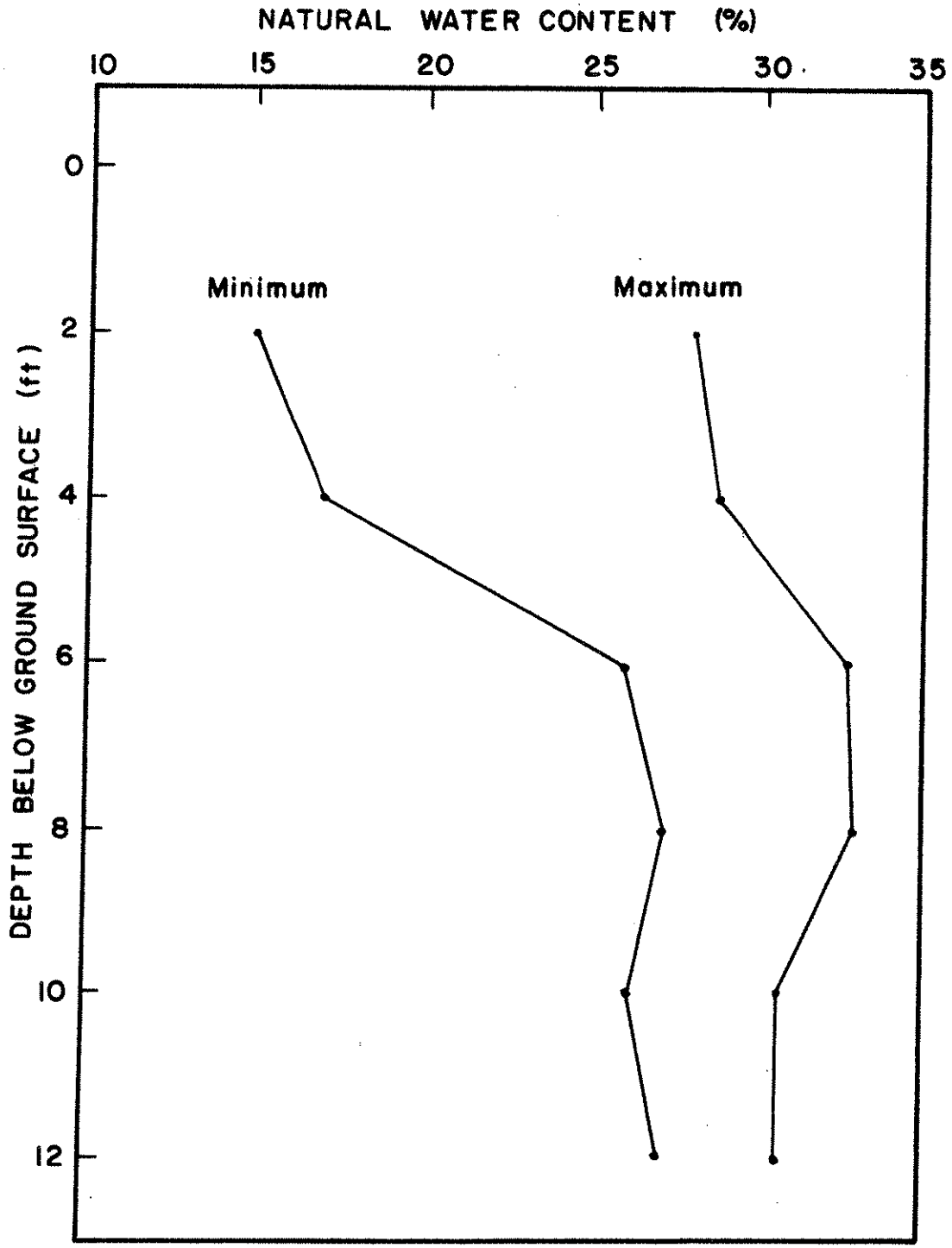

Fig. 3.12. Range in Natural Water Contents, October 1966 to September 1967.

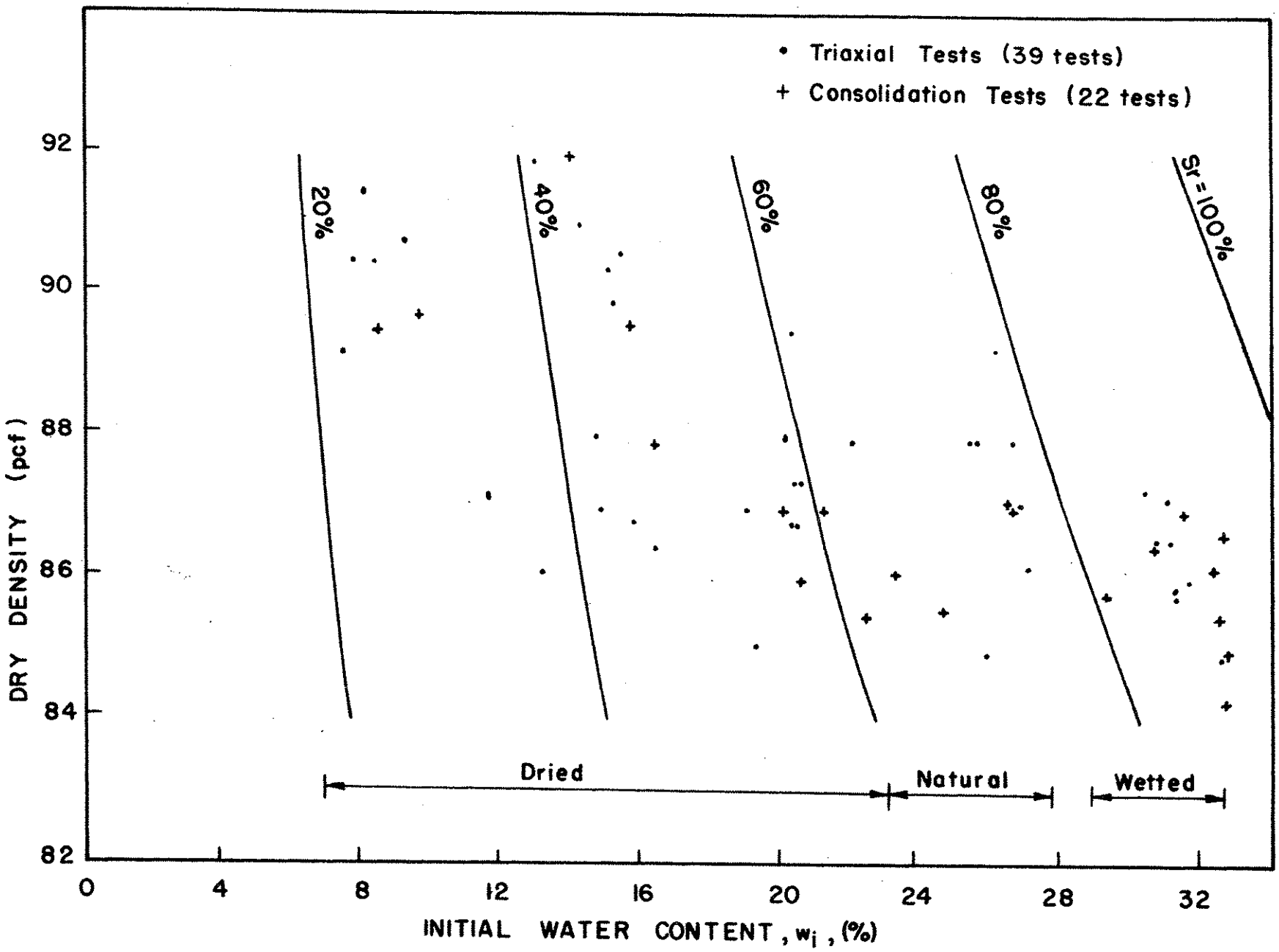

Fig. 4.1. Water Contents and Dry Densities of Test Specimens.

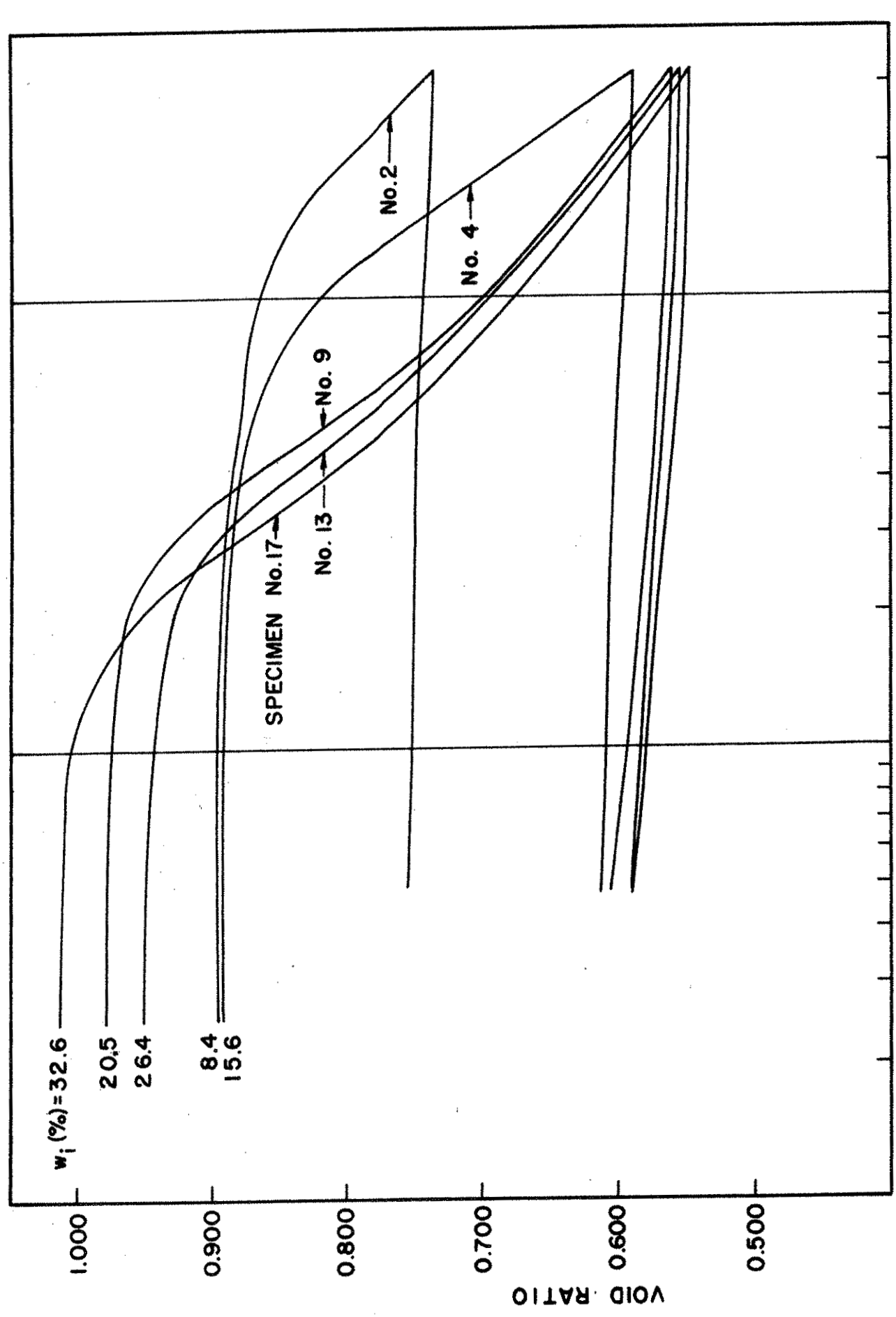

Fig. 4.2. Typical Void Ratio-Log Pressure Relationships.

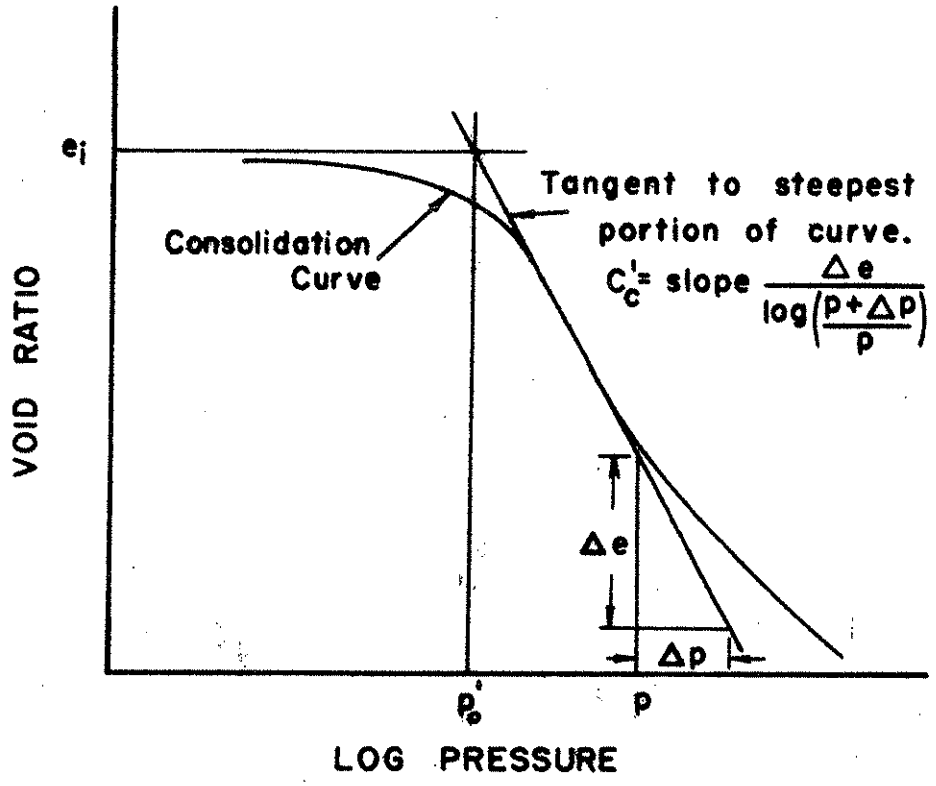

Fig. 4.3. Definitions of Parameters p_o' and C_c'.

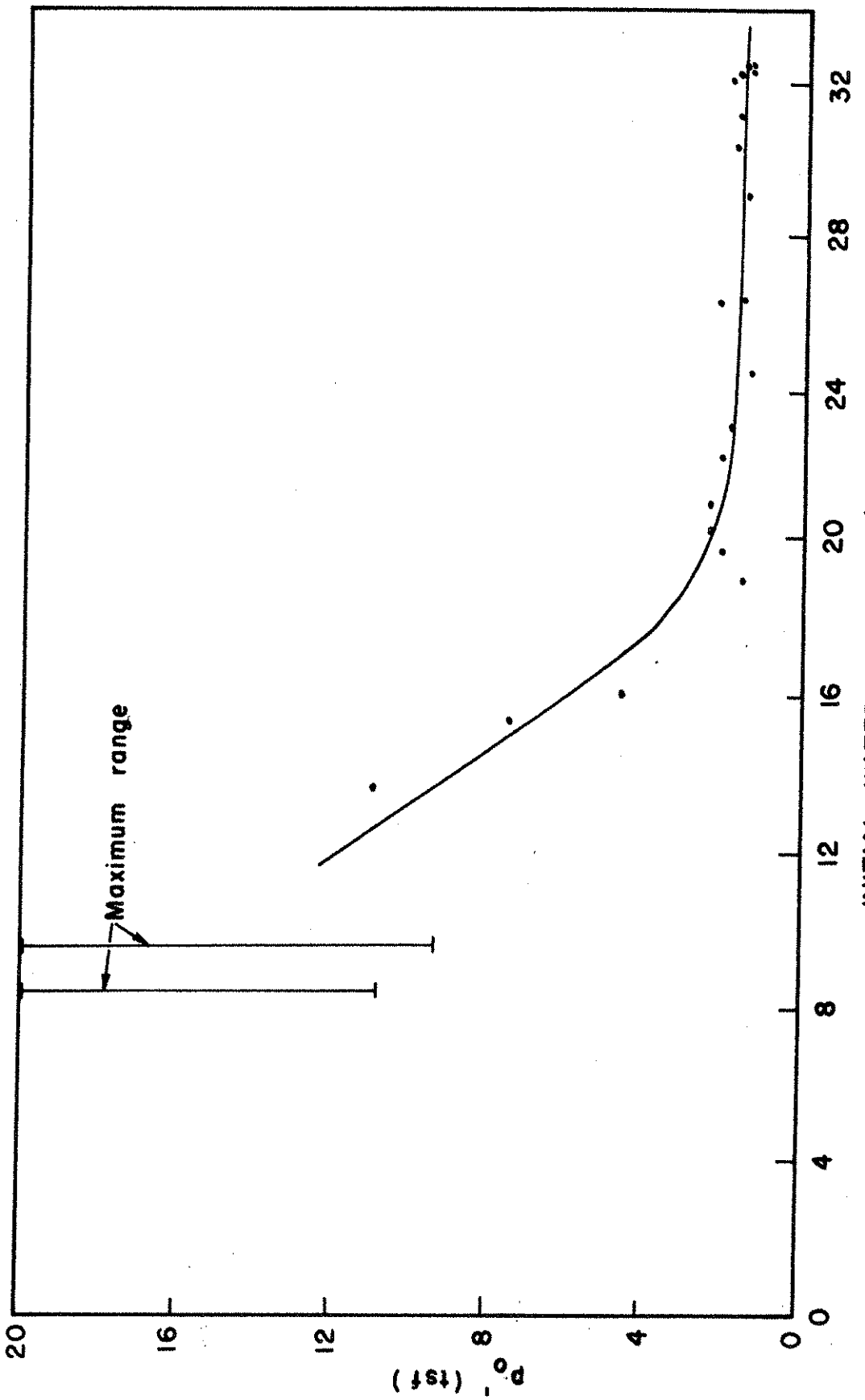

Fig. 4.4. Variation of p_o' With Initial Water Content.

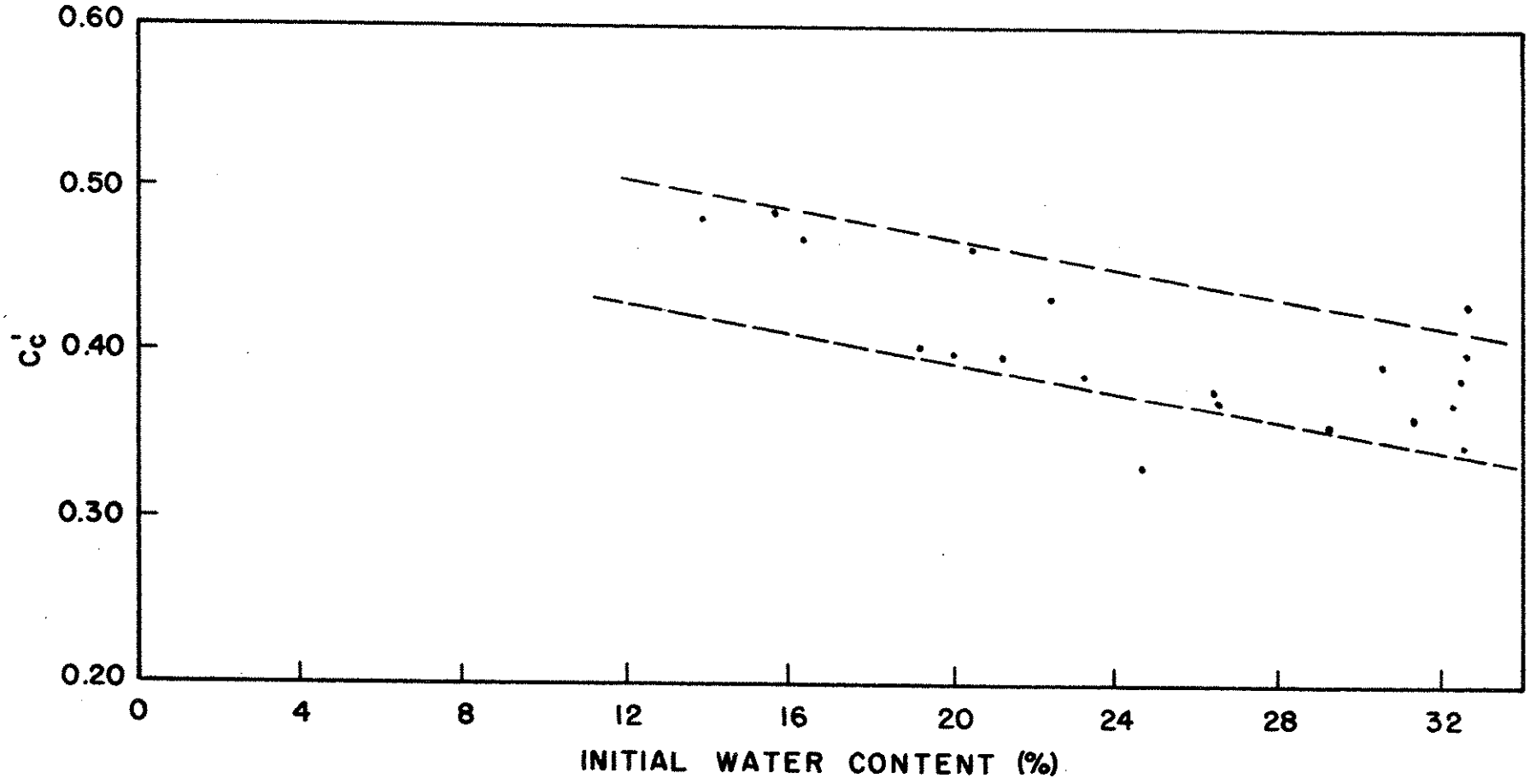

Fig. 4.5. Variation of C_c' With Initial Water Content.

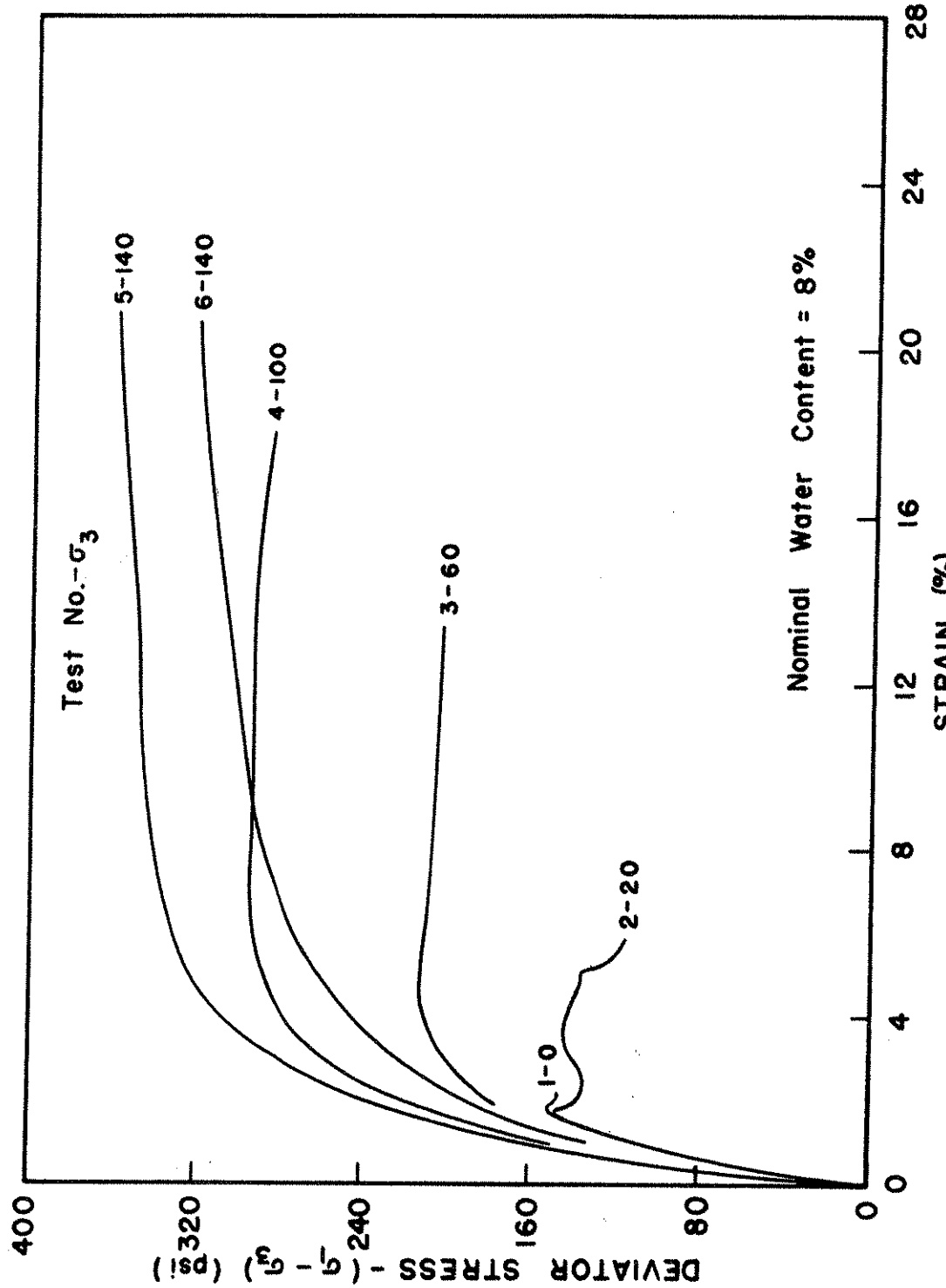

Fig. 4.6. Stress-Strain Curves, Specimens No. 1 to 6.

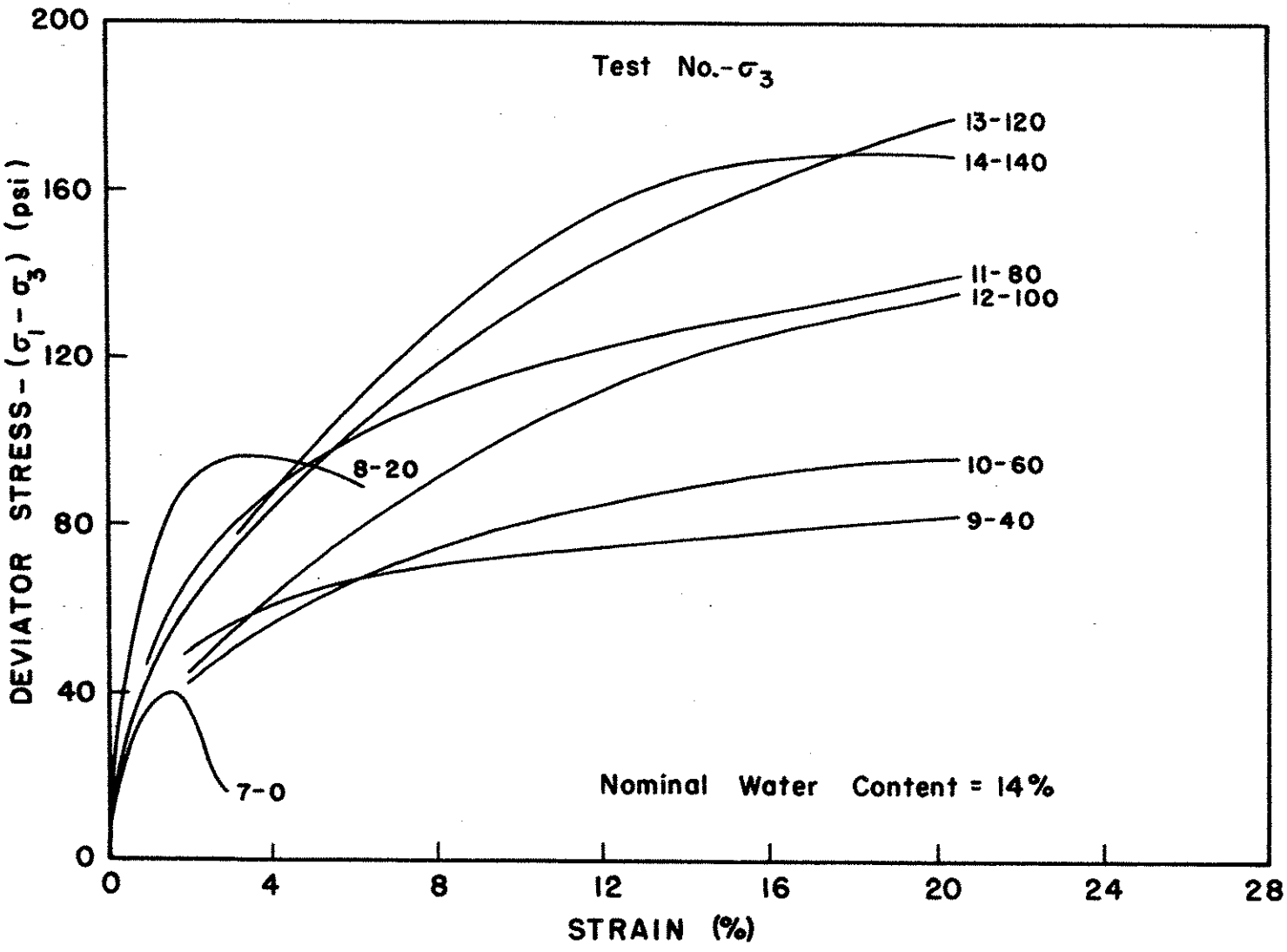

Fig. 4.7. Stress-Strain Curves, Specimens No. 7 to 14.

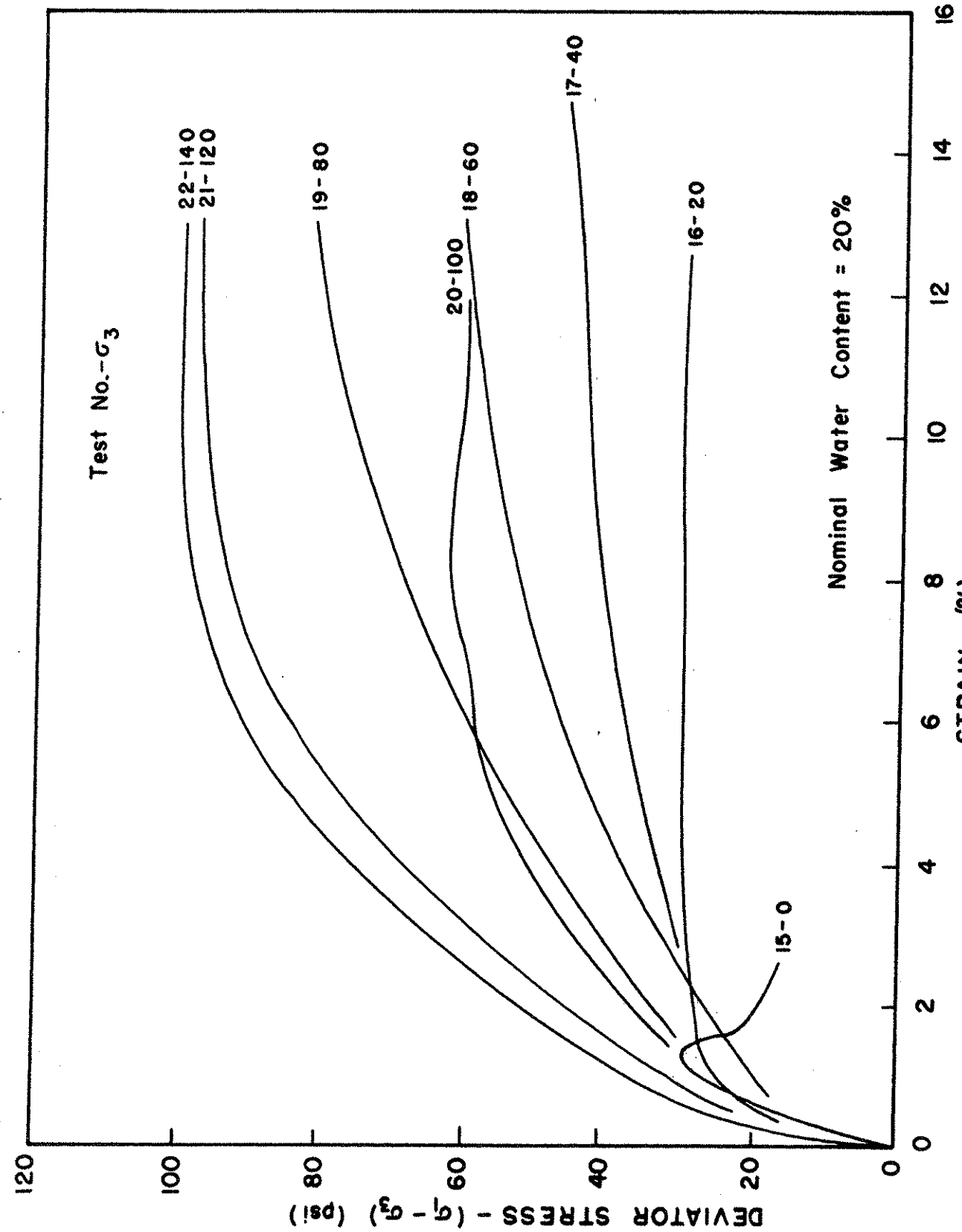

Fig. 4.8. Stress-Strain Curves, Specimens No. 15 to 22.

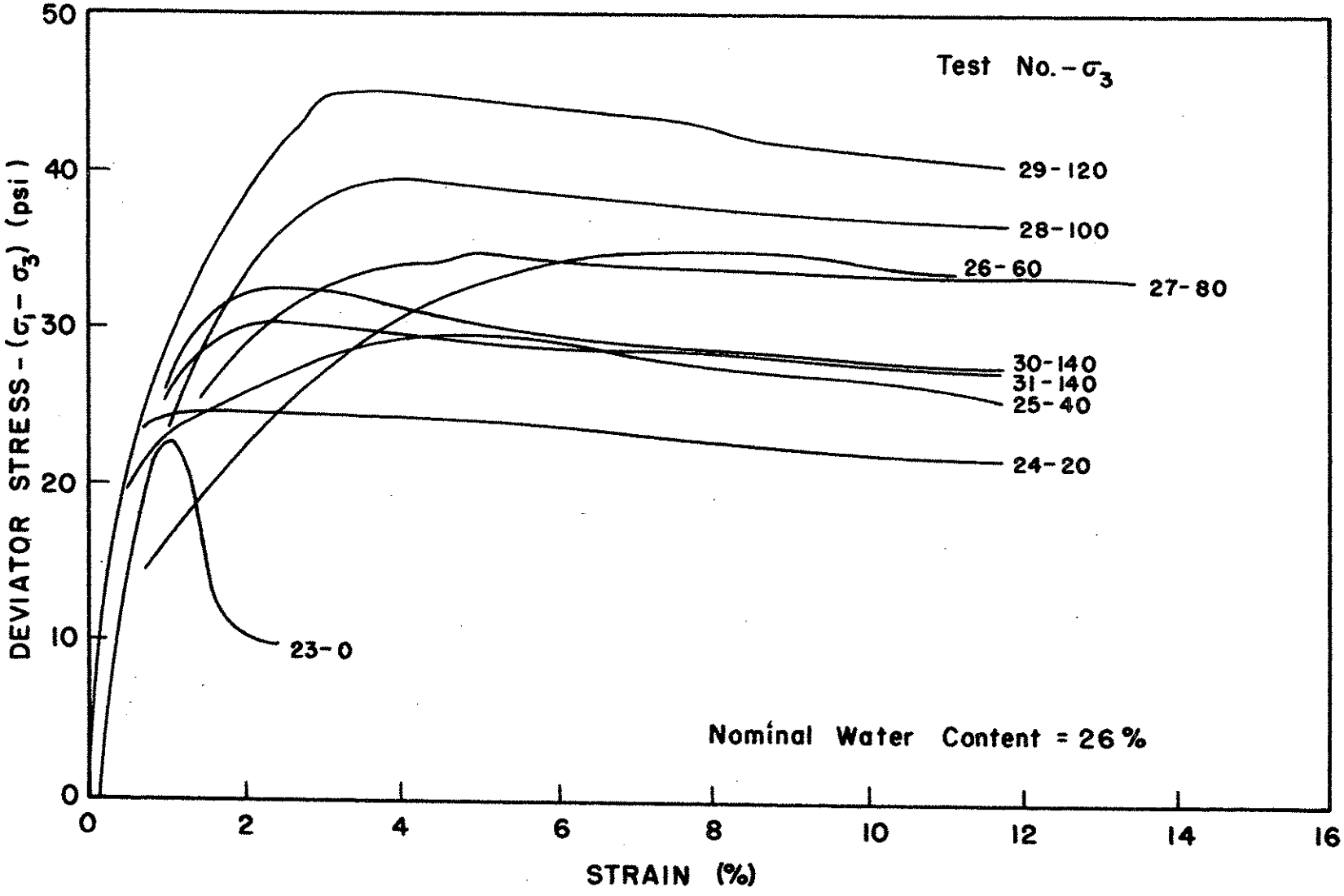

Fig. 4.9. Stress-Strain Curves, Specimens No. 23 to 31.

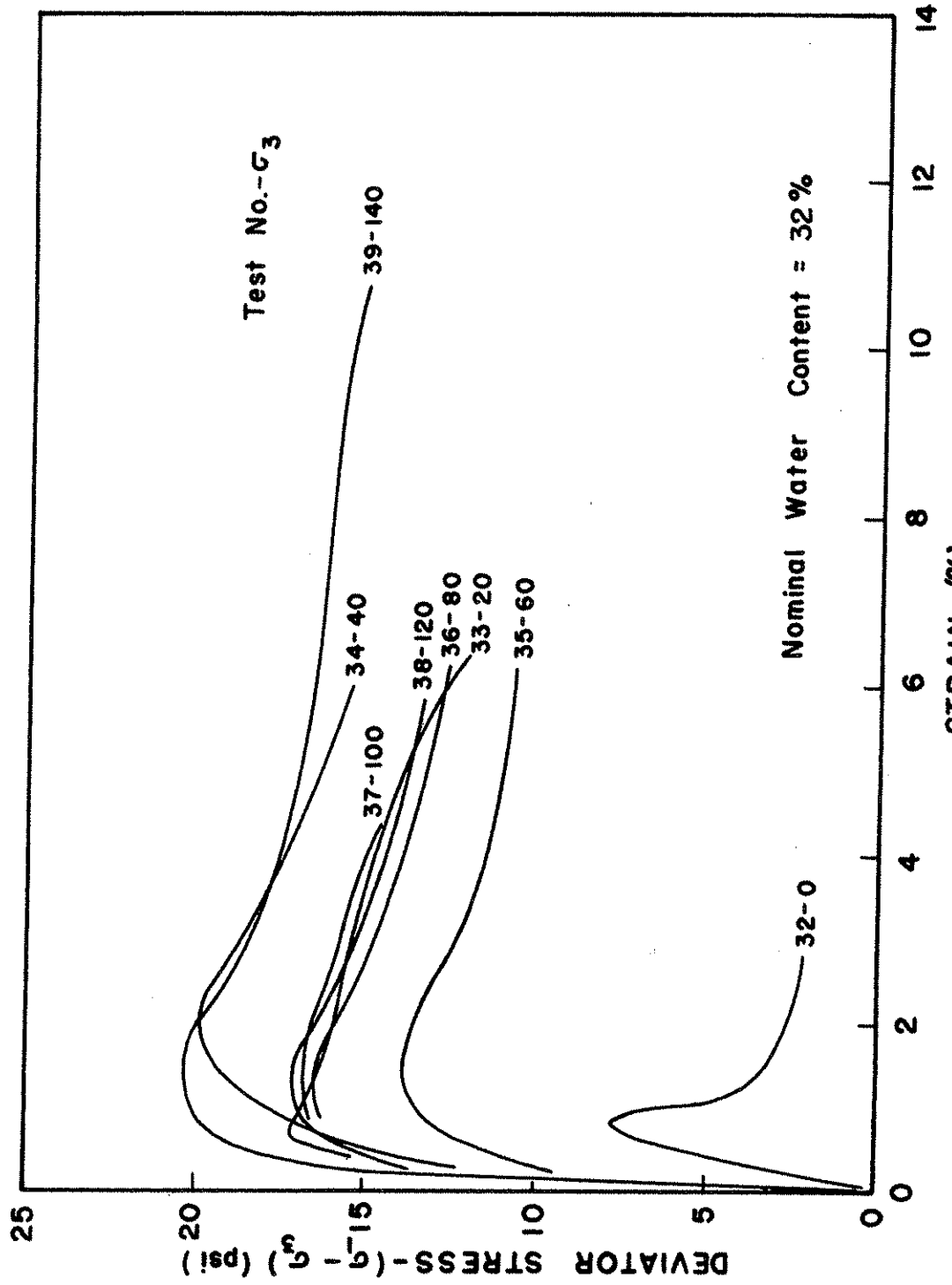

Fig. 4.10. Stress-Strain Curves, Specimens No. 32 to 39.

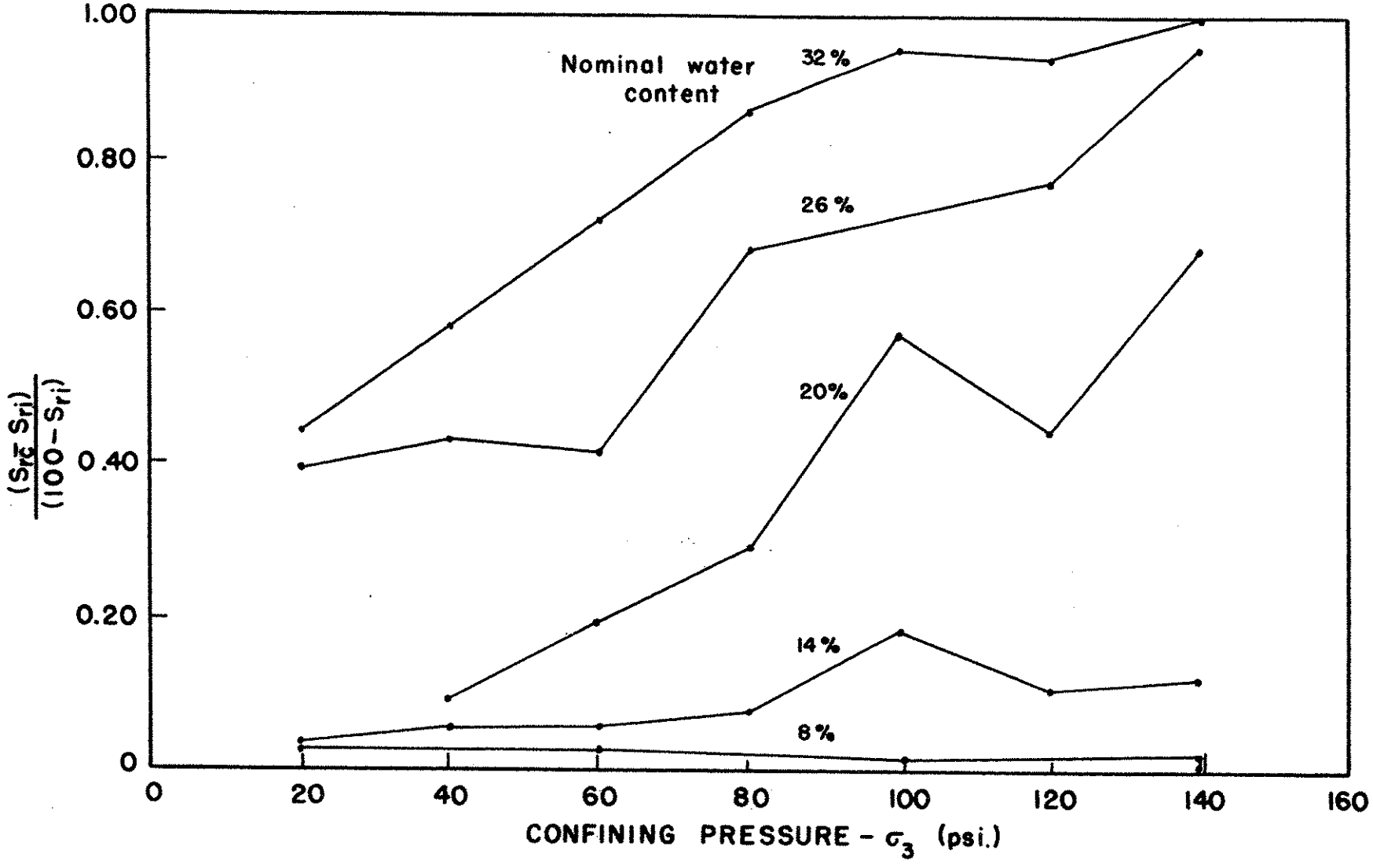

Fig. 4.11. Relative Increase in Degree of Saturation Due to Undrained Hydrostatic Compression.

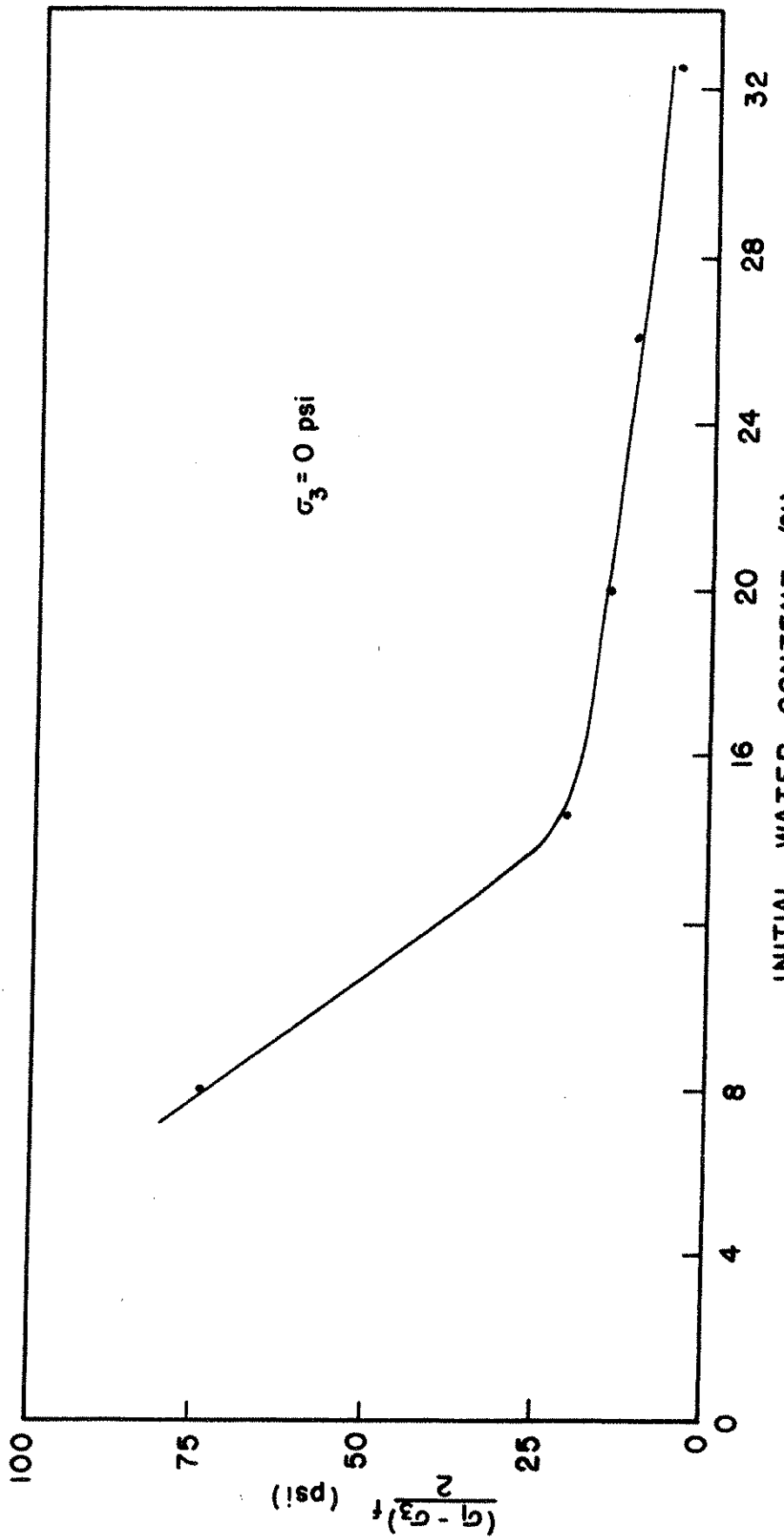

Fig. 4.12. Unconfined Shear Strength-Water Content Relations.

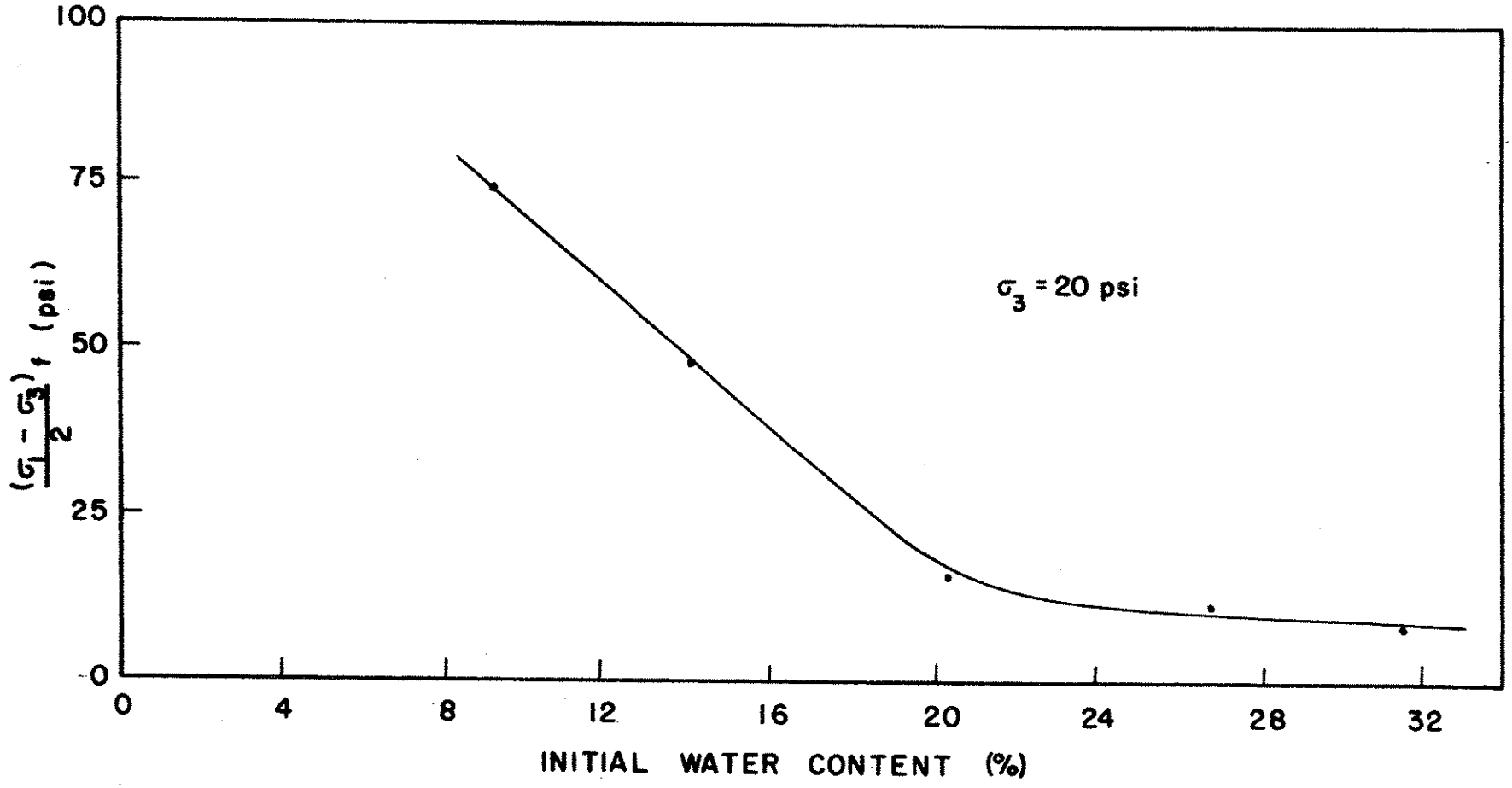

Fig. 4.13. Triaxial Shear Strength-Water Content Relations, σ_3 = 20 psi.

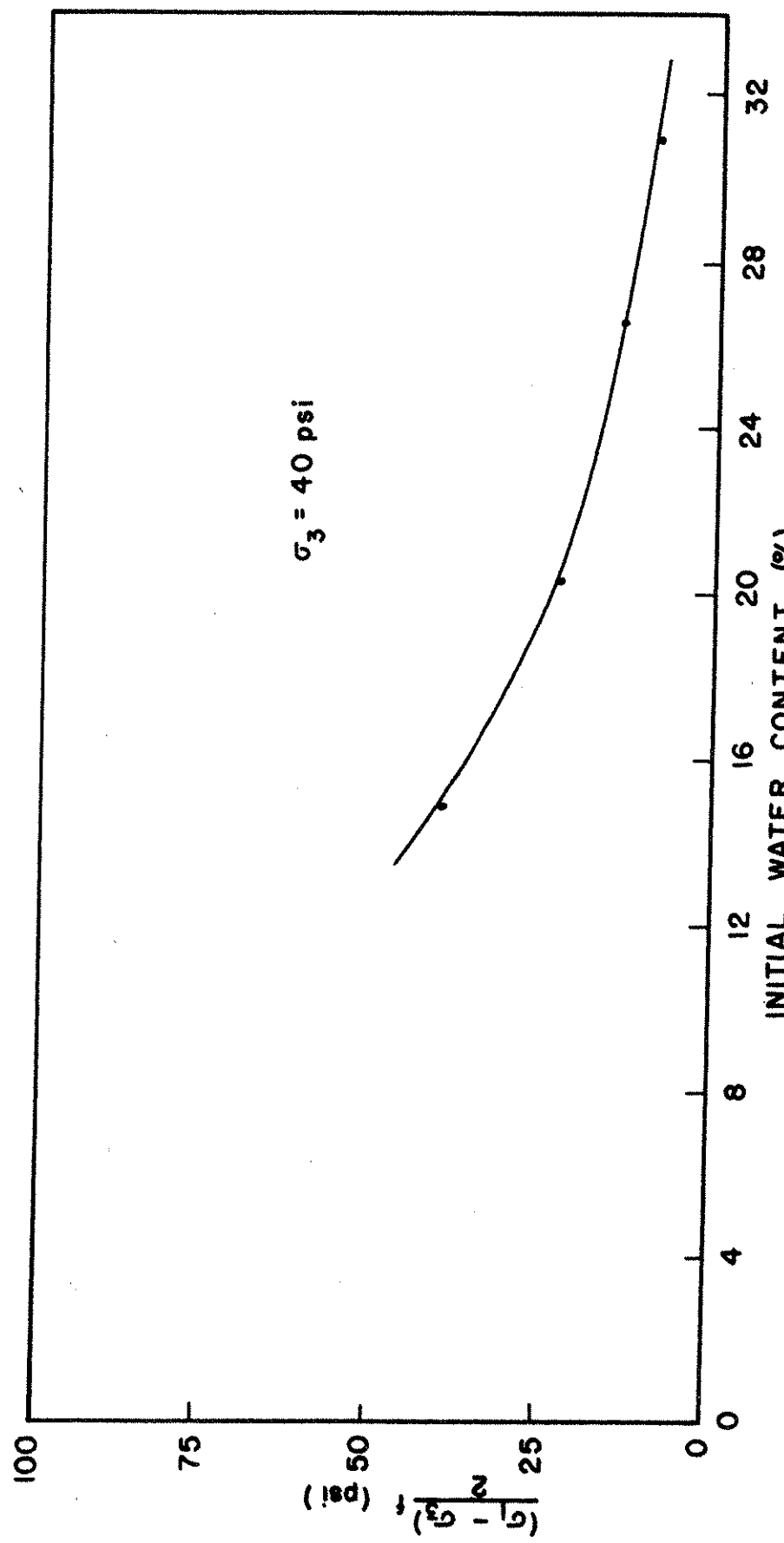

Fig. 4.14. Triaxial Shear Strength-Water Content Relations, σ_3 = 40 psi.

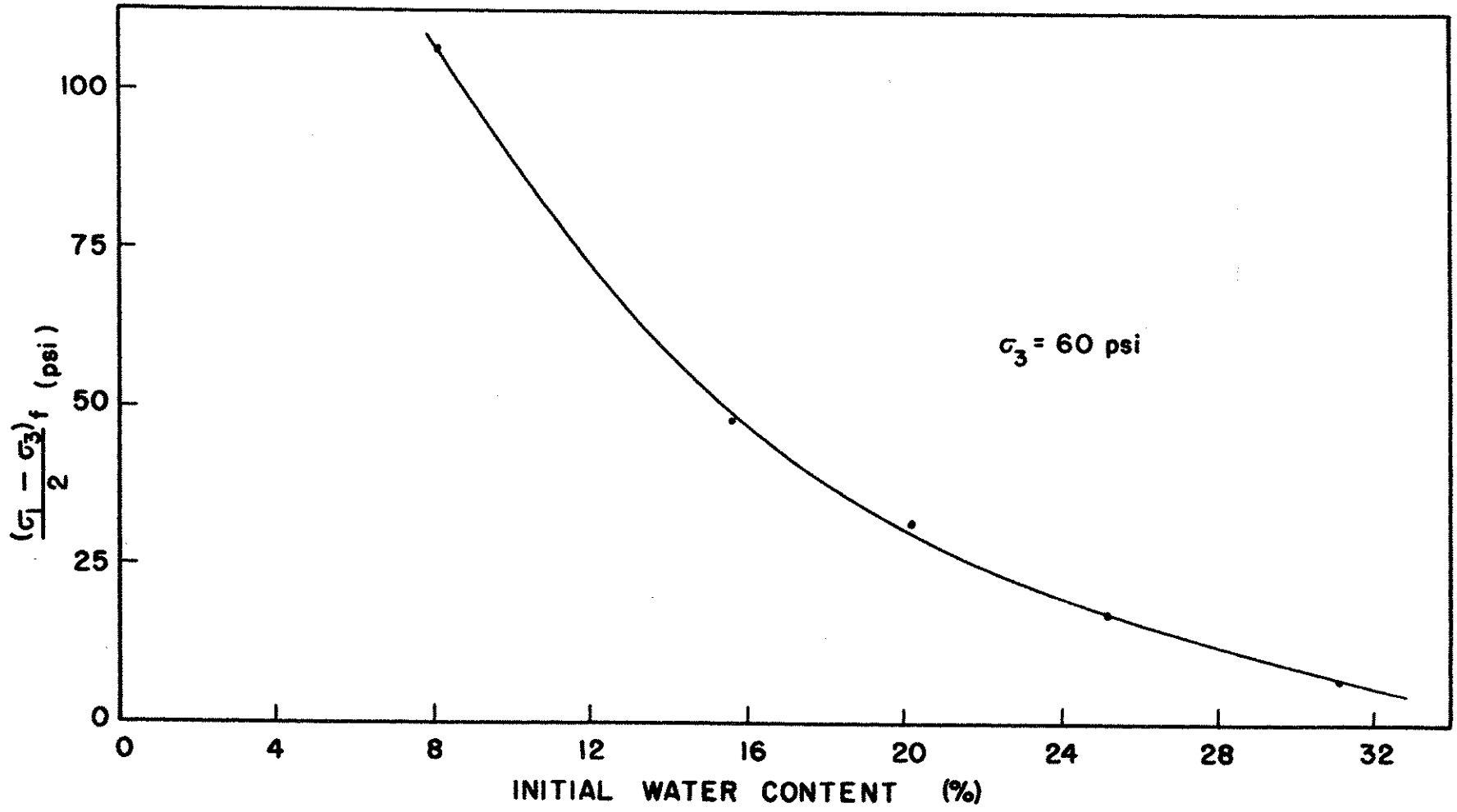

Fig. 4.15. Triaxial Shear Strength-Water Content Relations, σ_3 = 60 psi.

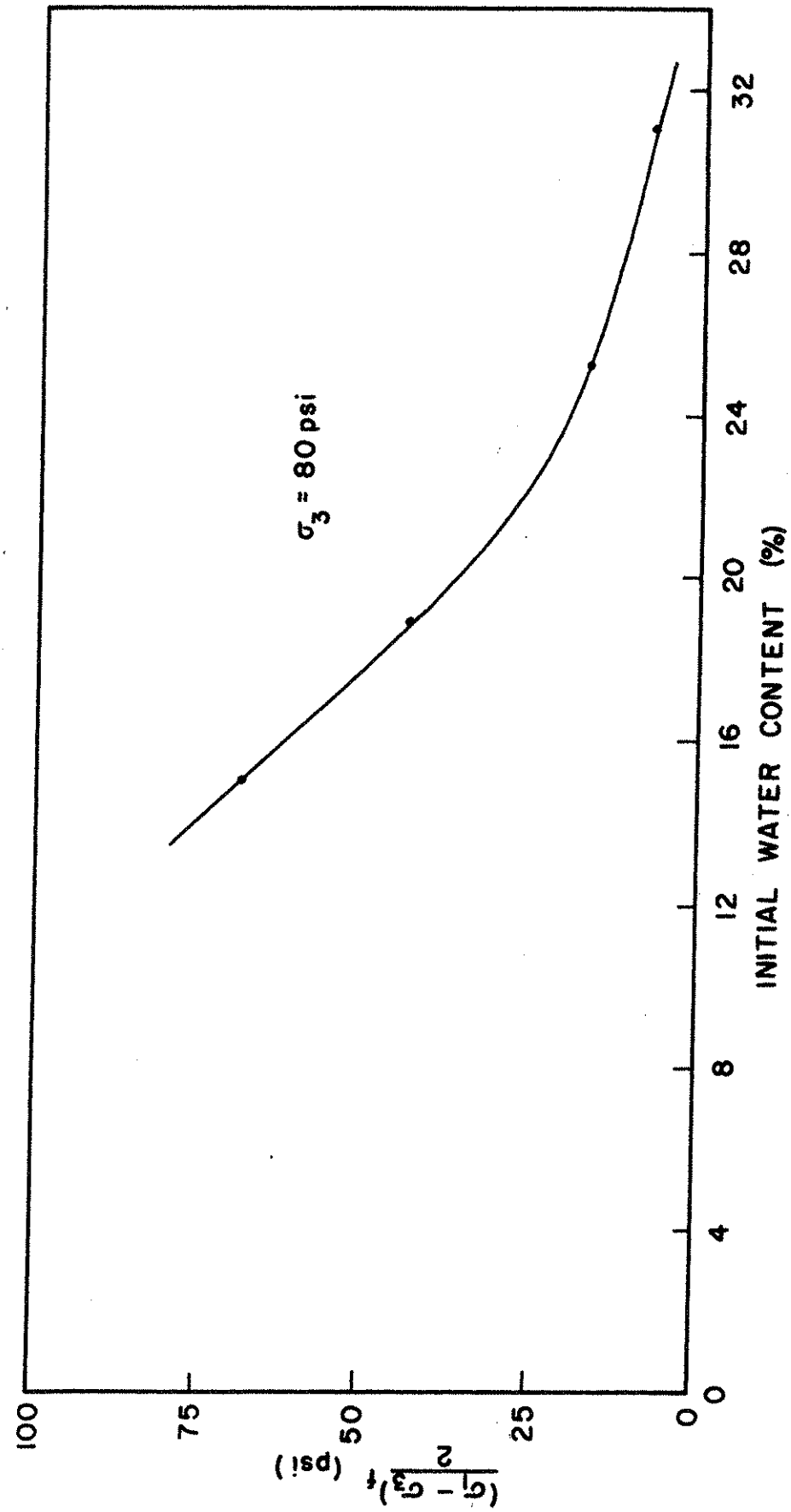

Fig. 4.16. Triaxial Shear Strength-Water Content Relations, σ_3 = 80 psi.

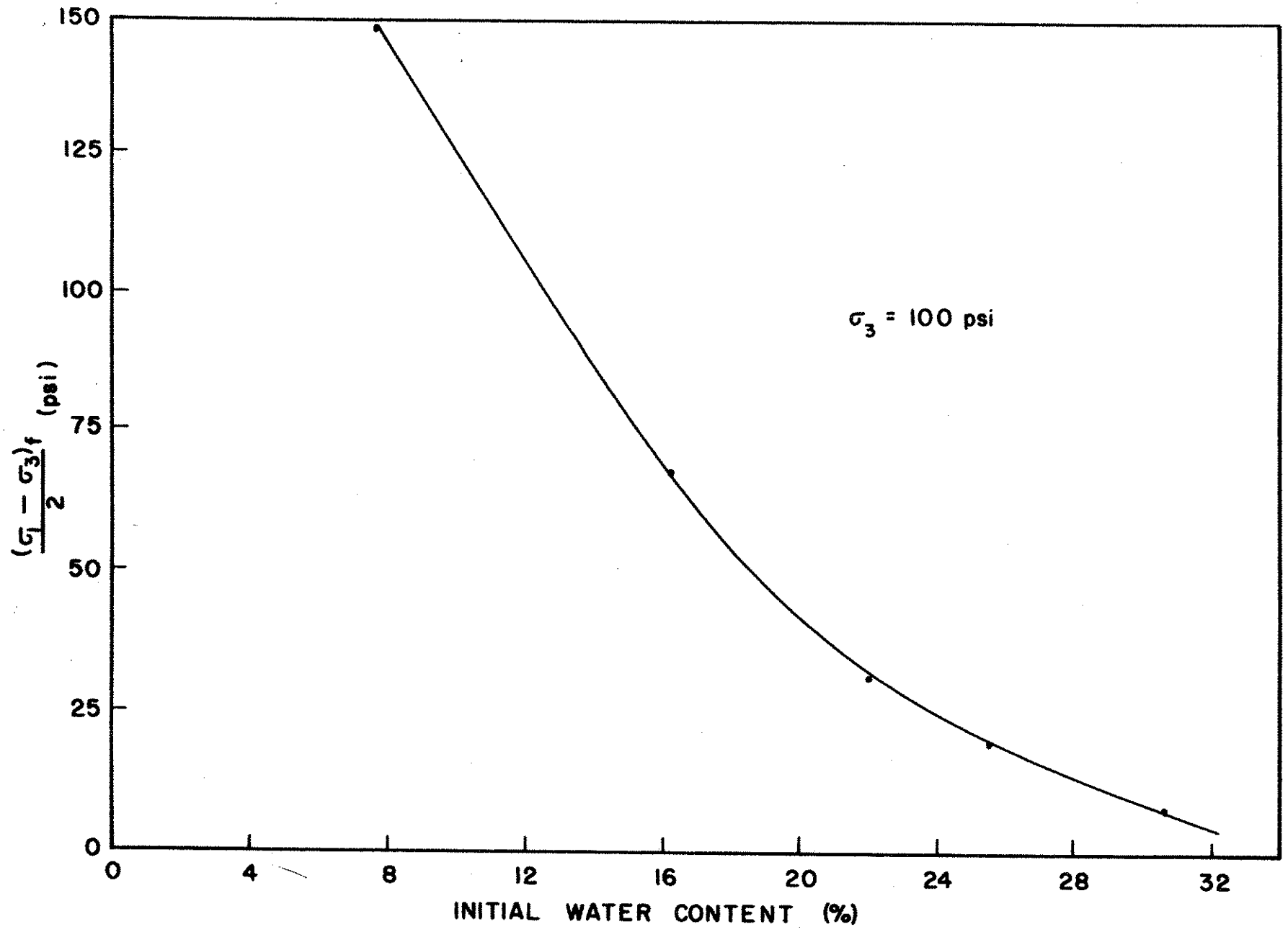

Fig. 4.17. Triaxial Shear Strength-Water Content Relations, σ_3 = 100 psi.

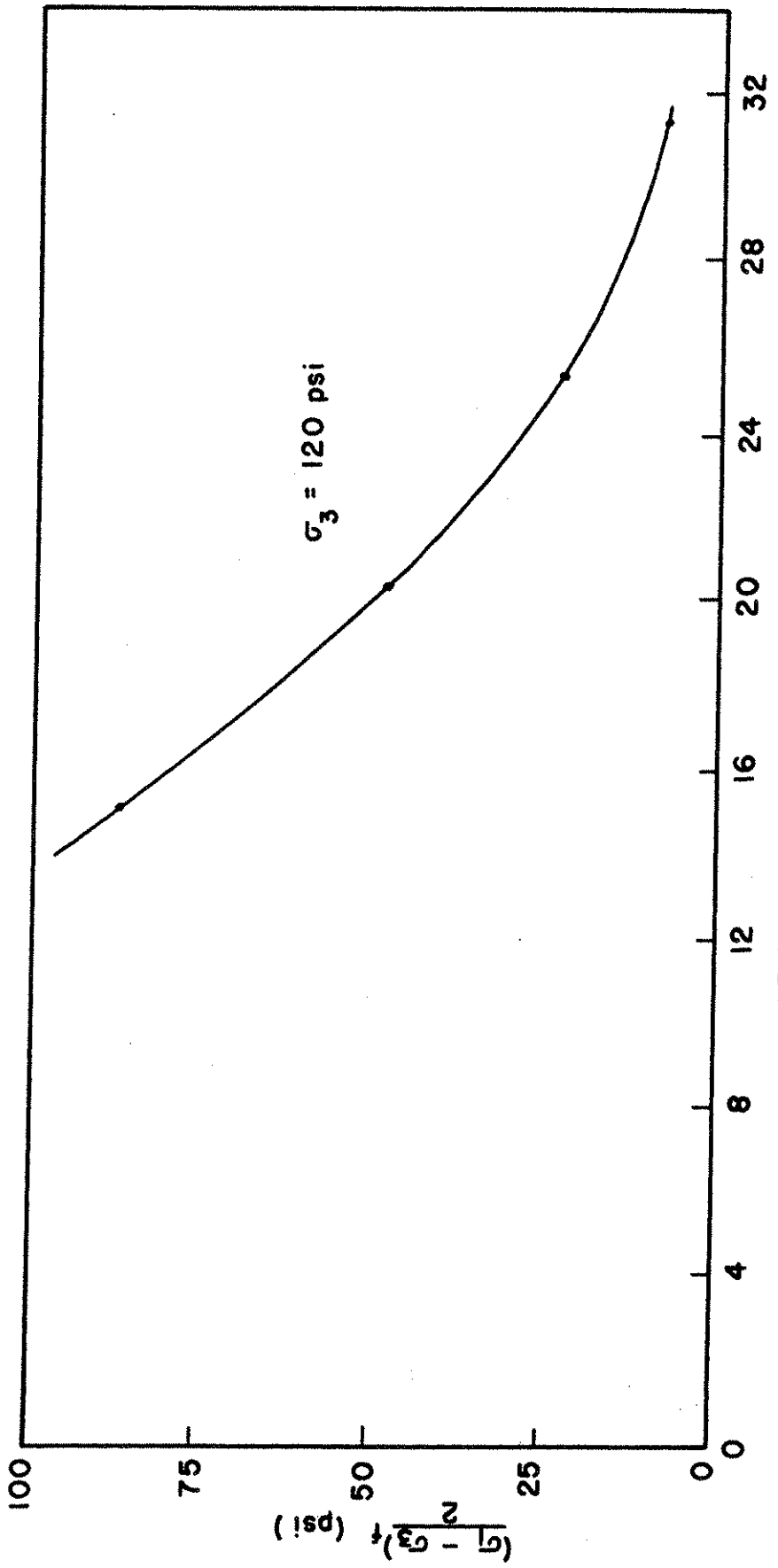

Fig. 4.18. Triaxial Shear Strength-Water Content Relations, σ_3 = 120 psi.

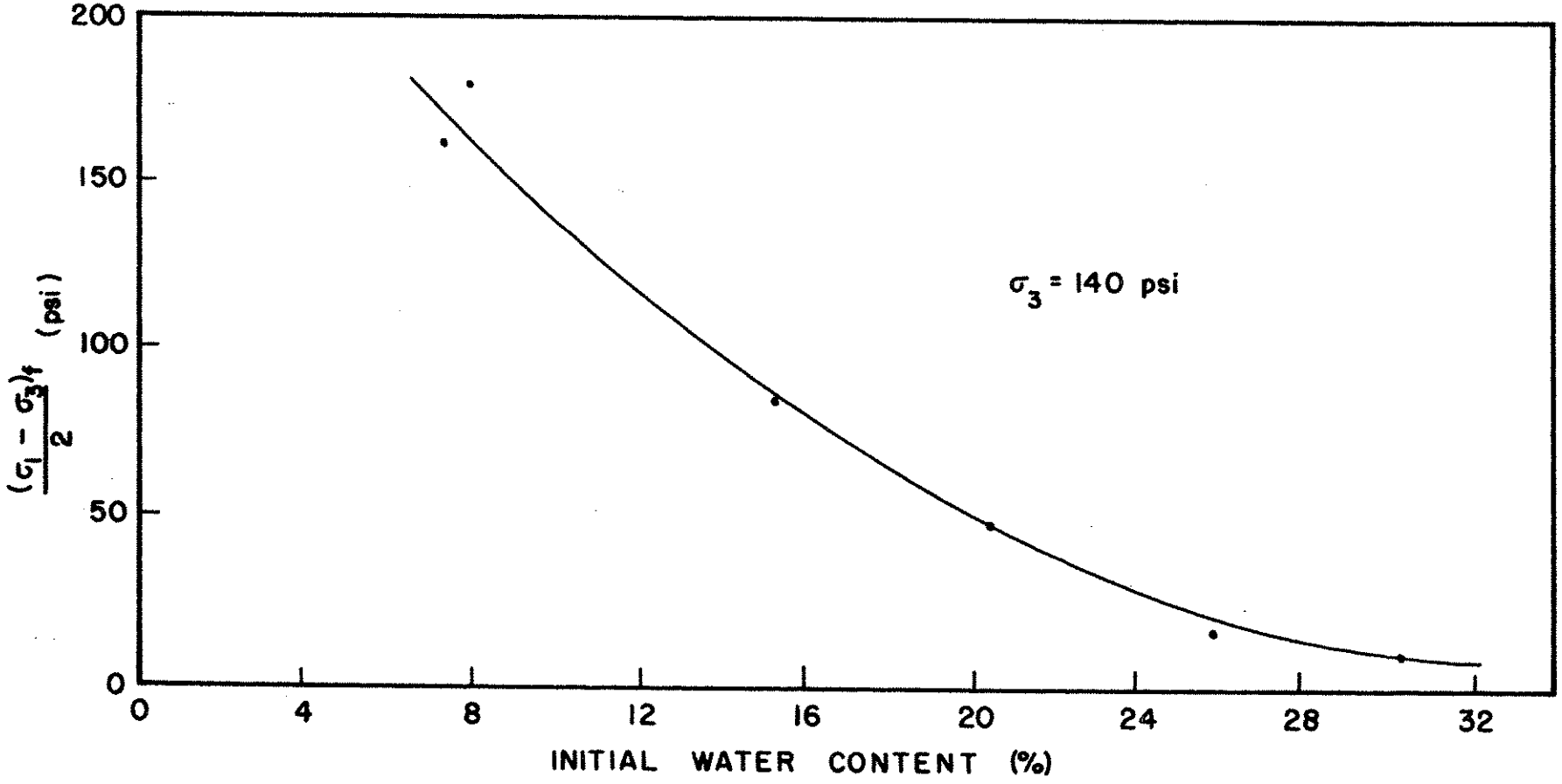

Fig. 4.19. Triaxial Shear Strength-Water Content Relations, σ_3 = 140 psi.

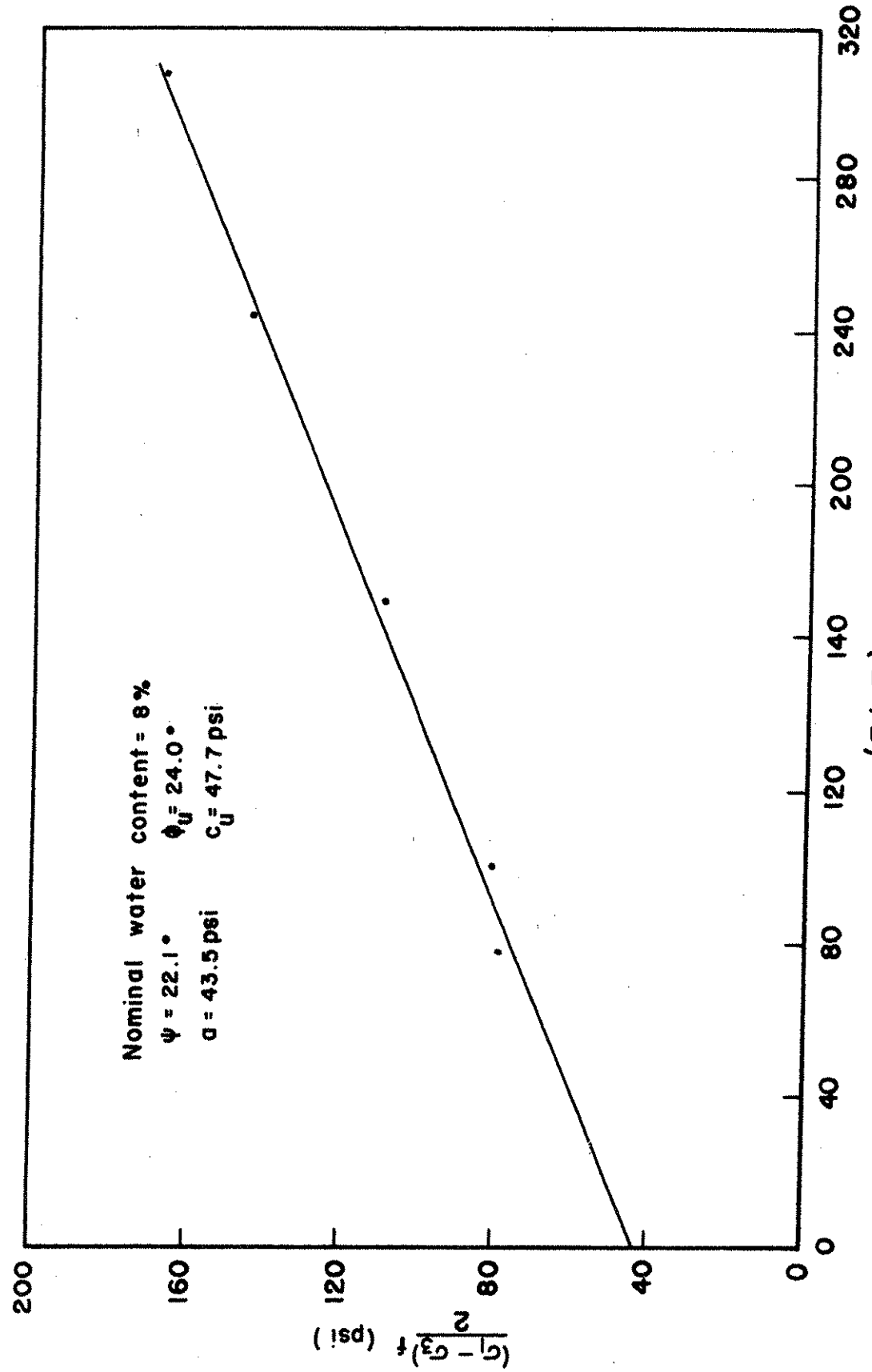

Fig. 4.20. Modified Mohr-Coulomb Diagram, w = 8%.

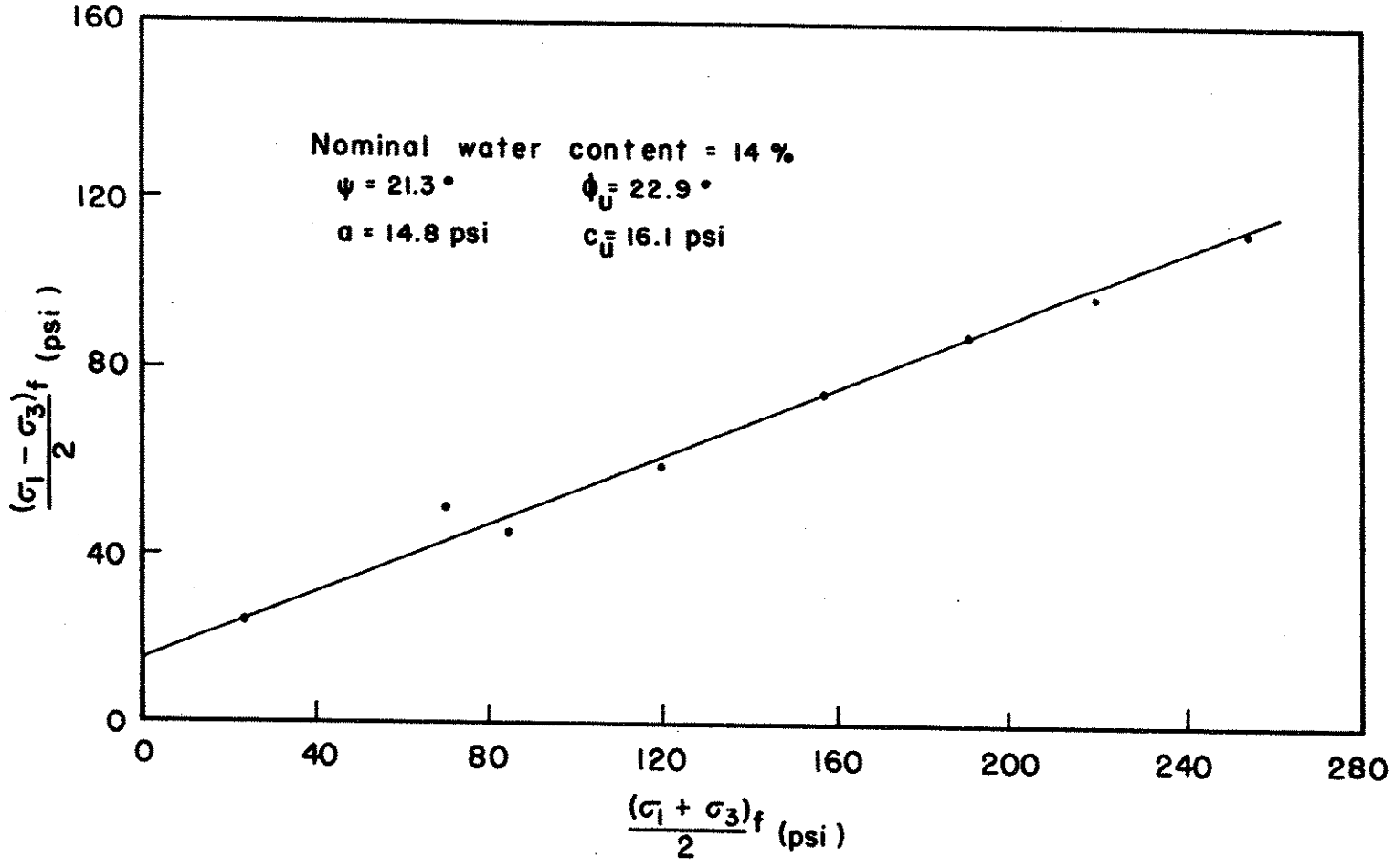

Fig. 4.21. Modified Mohr-Coulomb Diagram, w = 14%.

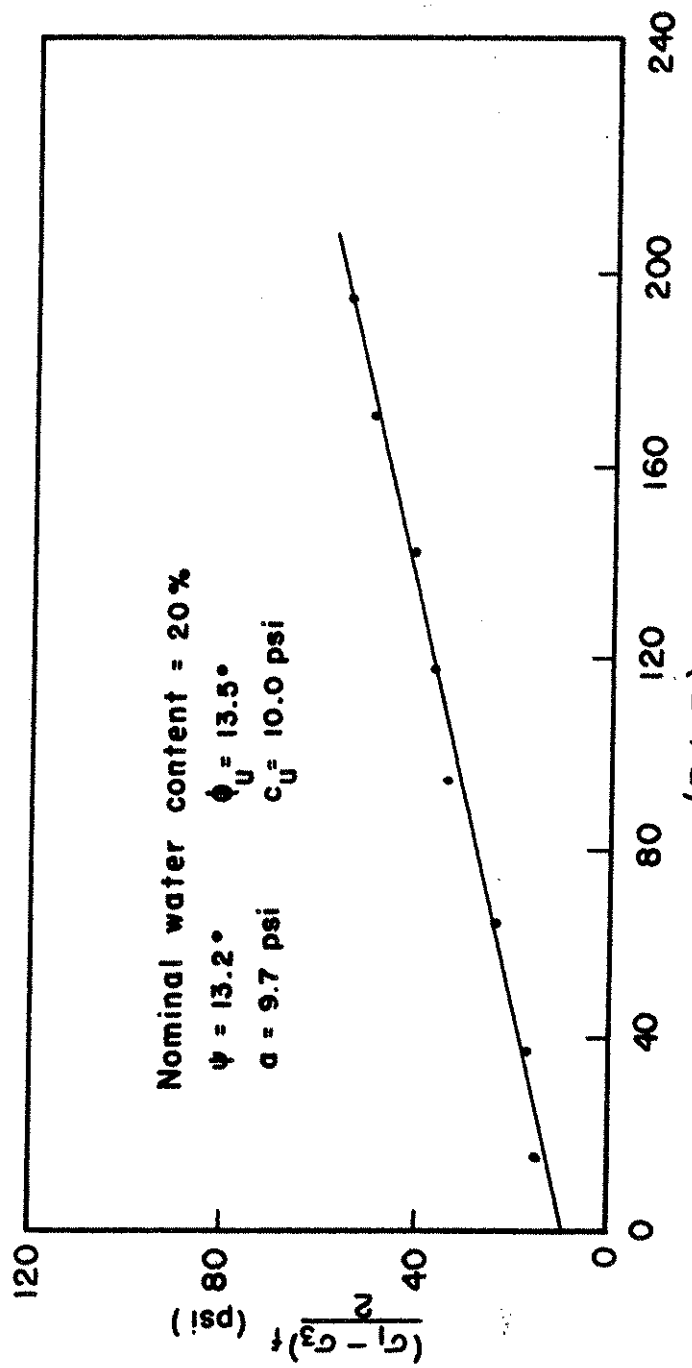

Fig. 4.22. Modified Mohr-Coulomb Diagram, w = 20%.

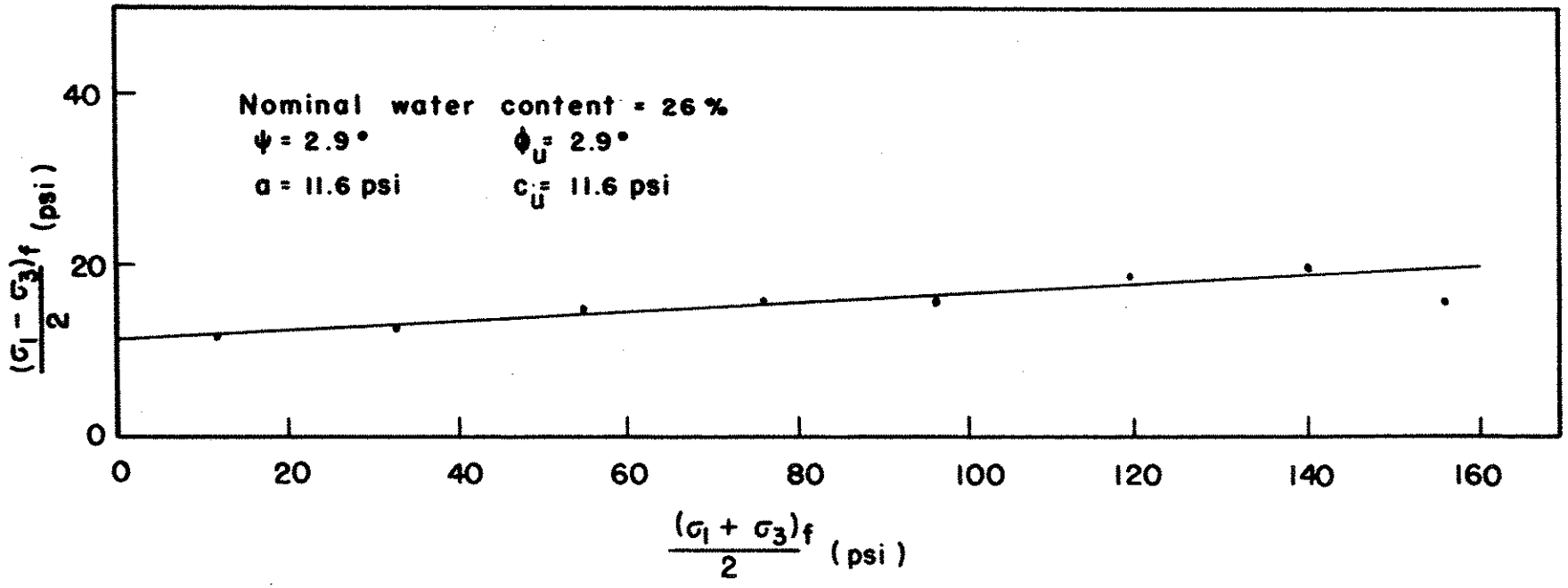

Fig. 4.23. Modified Mohr-Coulomb Diagram, w = 26%.

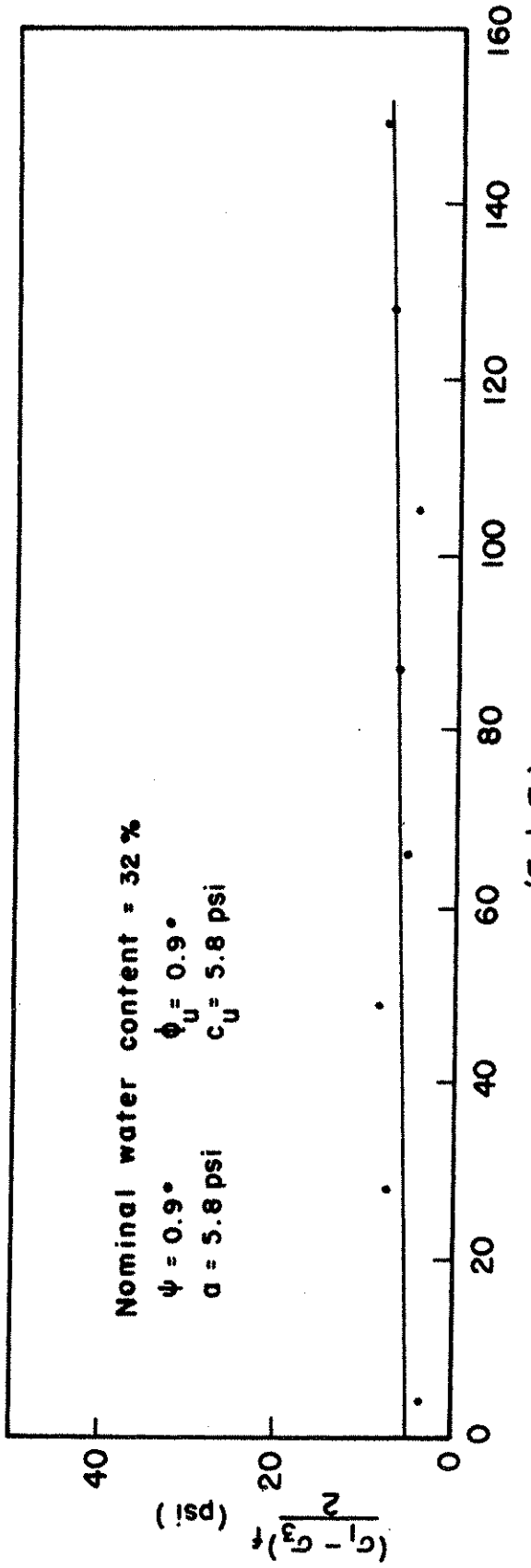

Fig. 4.24. Modified Mohr-Coulomb Diagram, w = 32%.

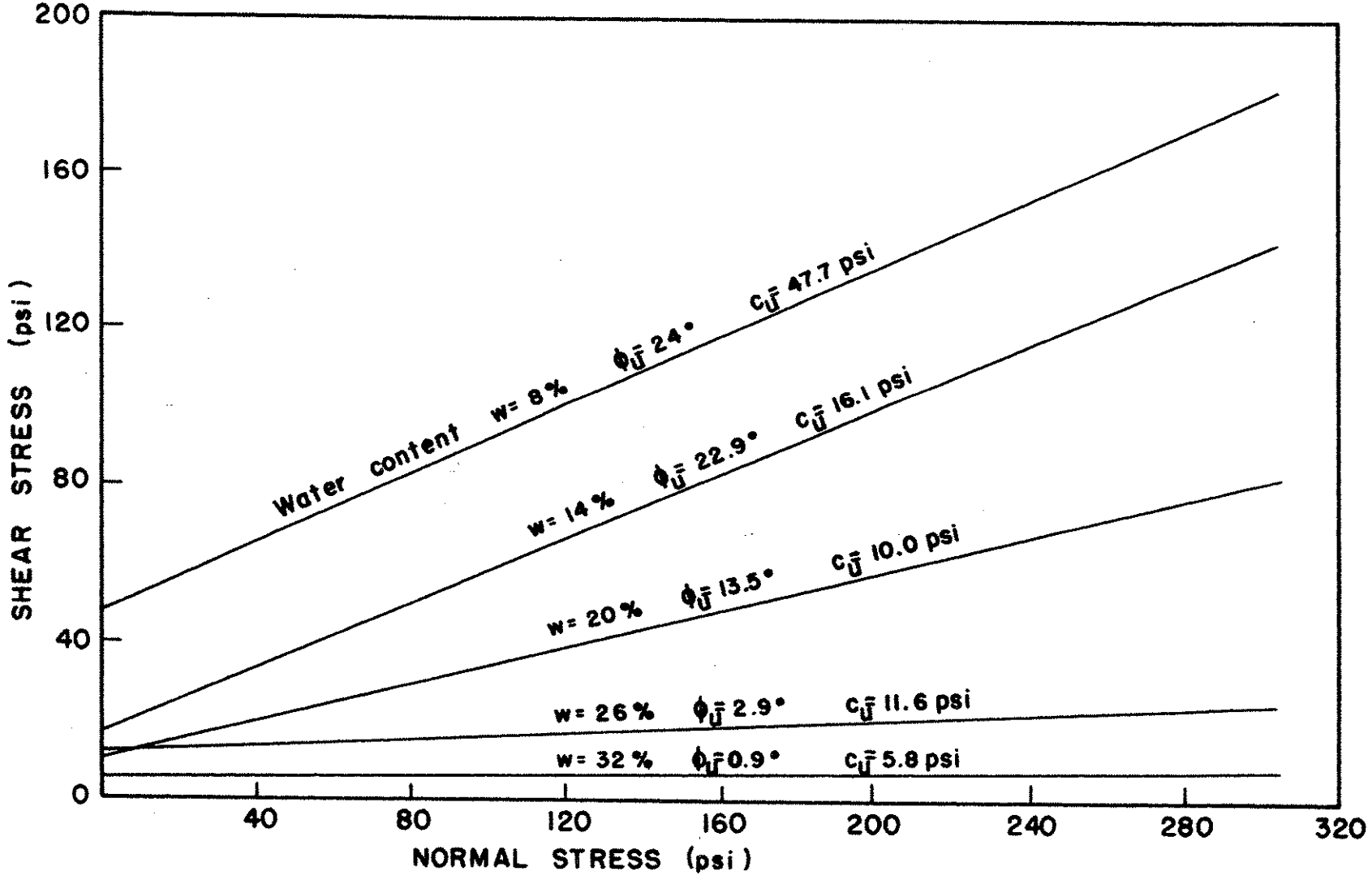

Fig. 4.25. Mohr-Coulomb Failure Envelopes for Undrained Triaxial Tests.

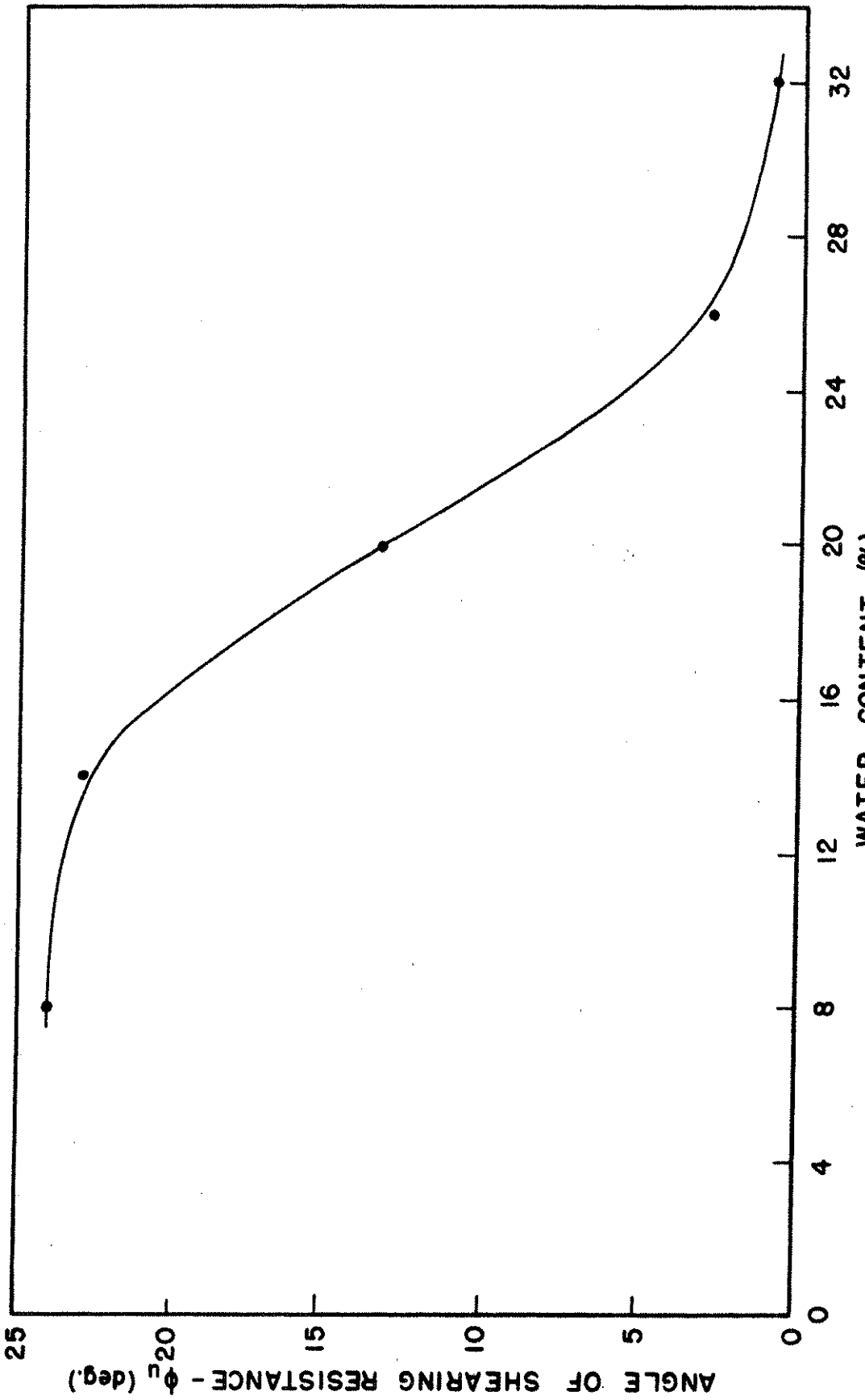

Fig. 4.26. Angle of Shearing Resistance-Water Content Relations.

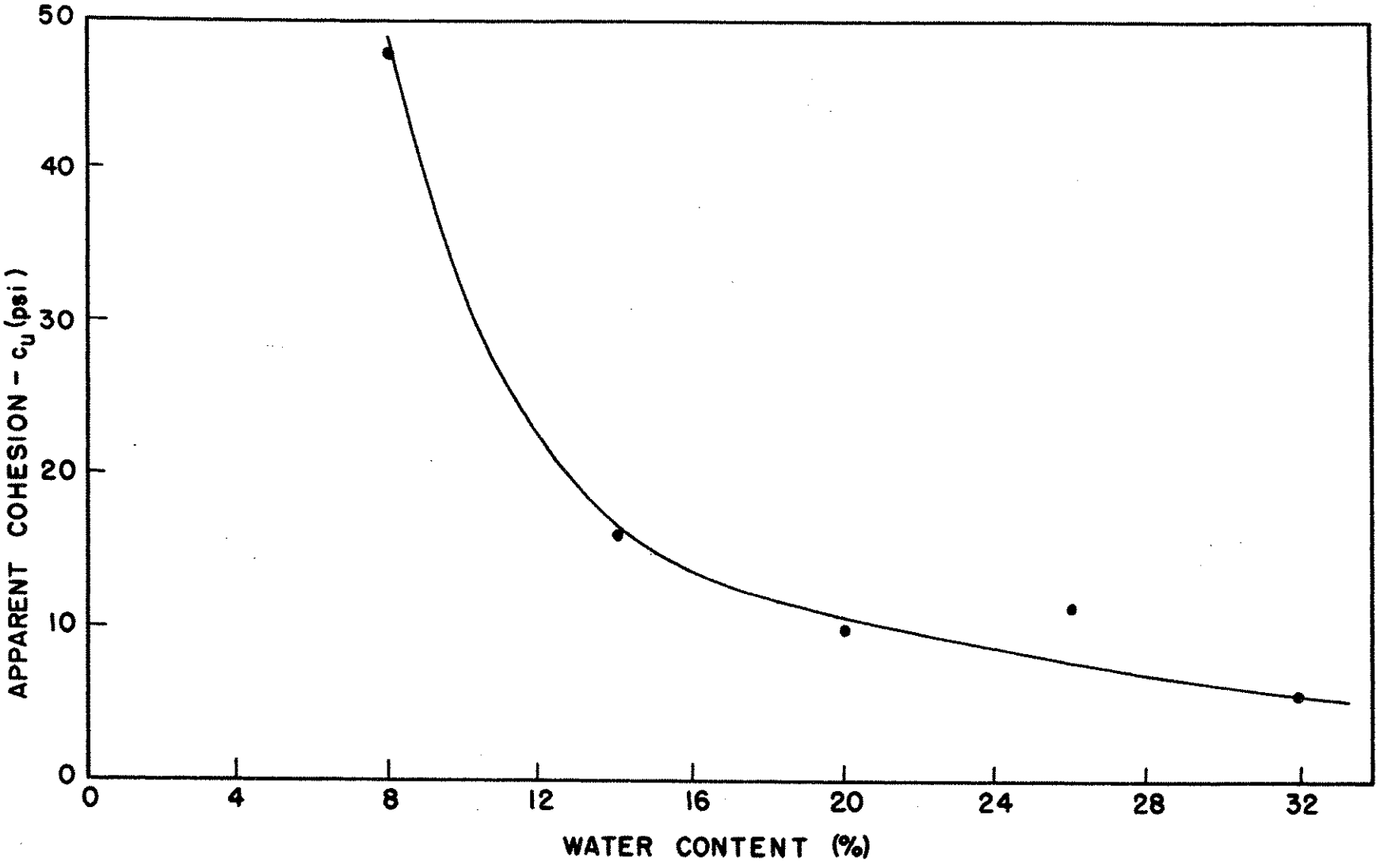

Fig. 4.27. Apparant Cohesion-Water Content Relations.

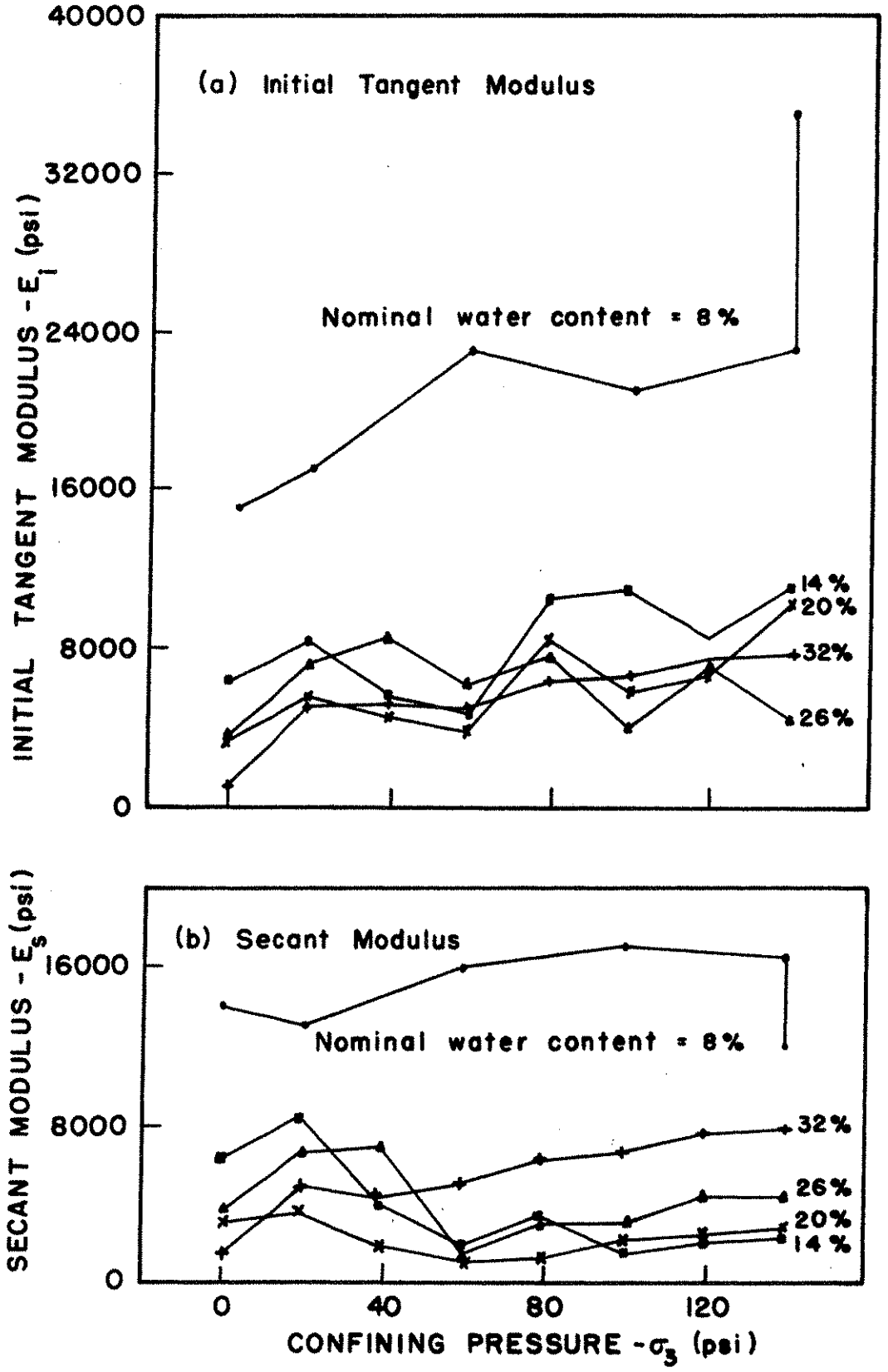

Fig. 4.28. Relationship of Moduli to Water Content and Confining Pressure.

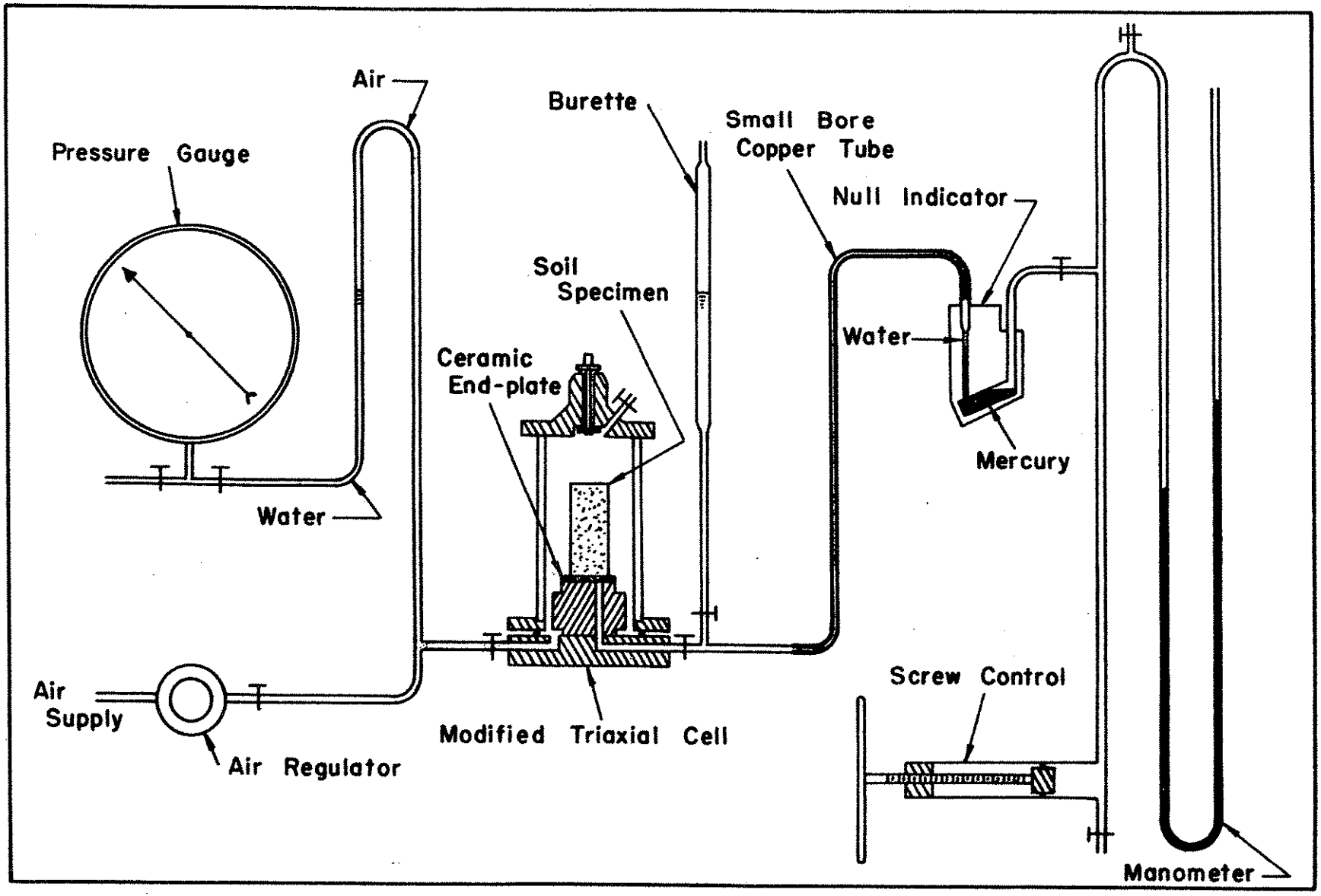

Fig. 4.29. Apparatus for Initial Negative Pore Water Pressure Tests.

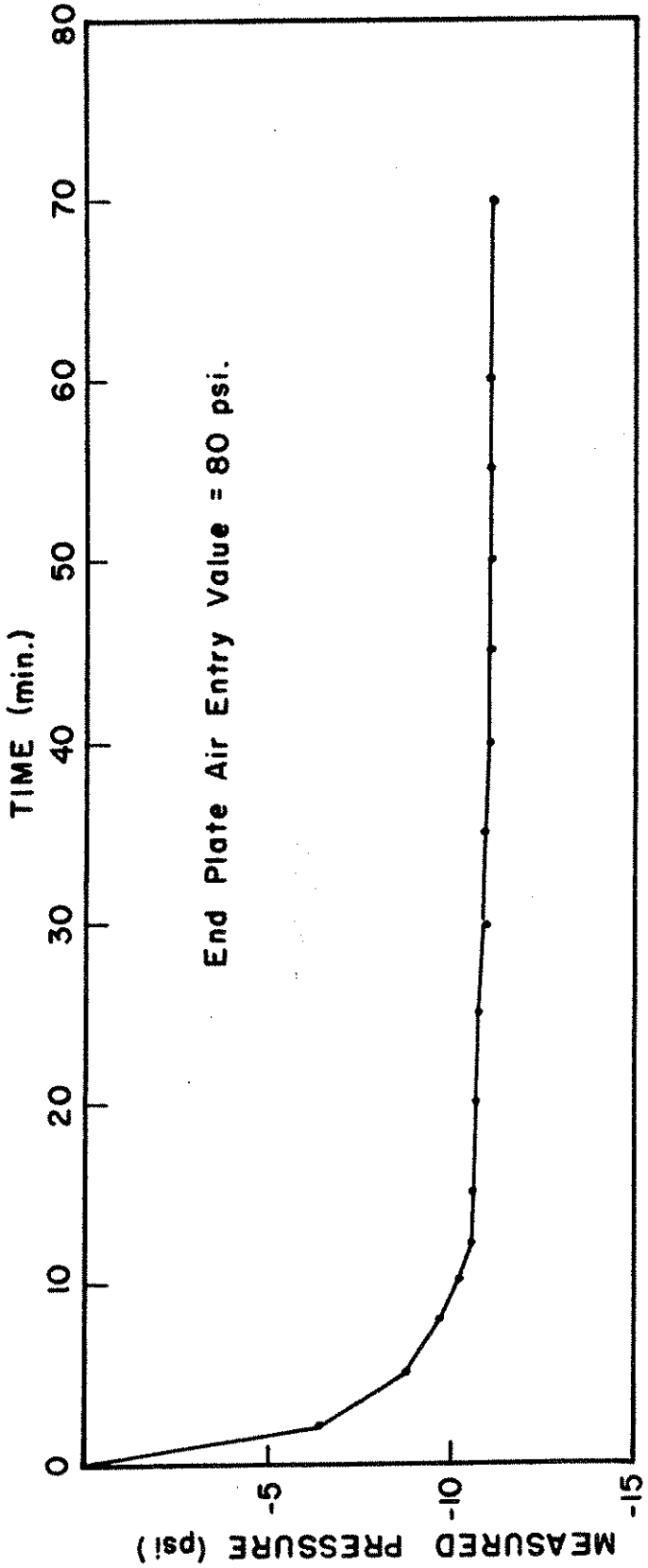

Fig. 4.30. Response Time for Negative Pore Water Pressure Test No. 15.

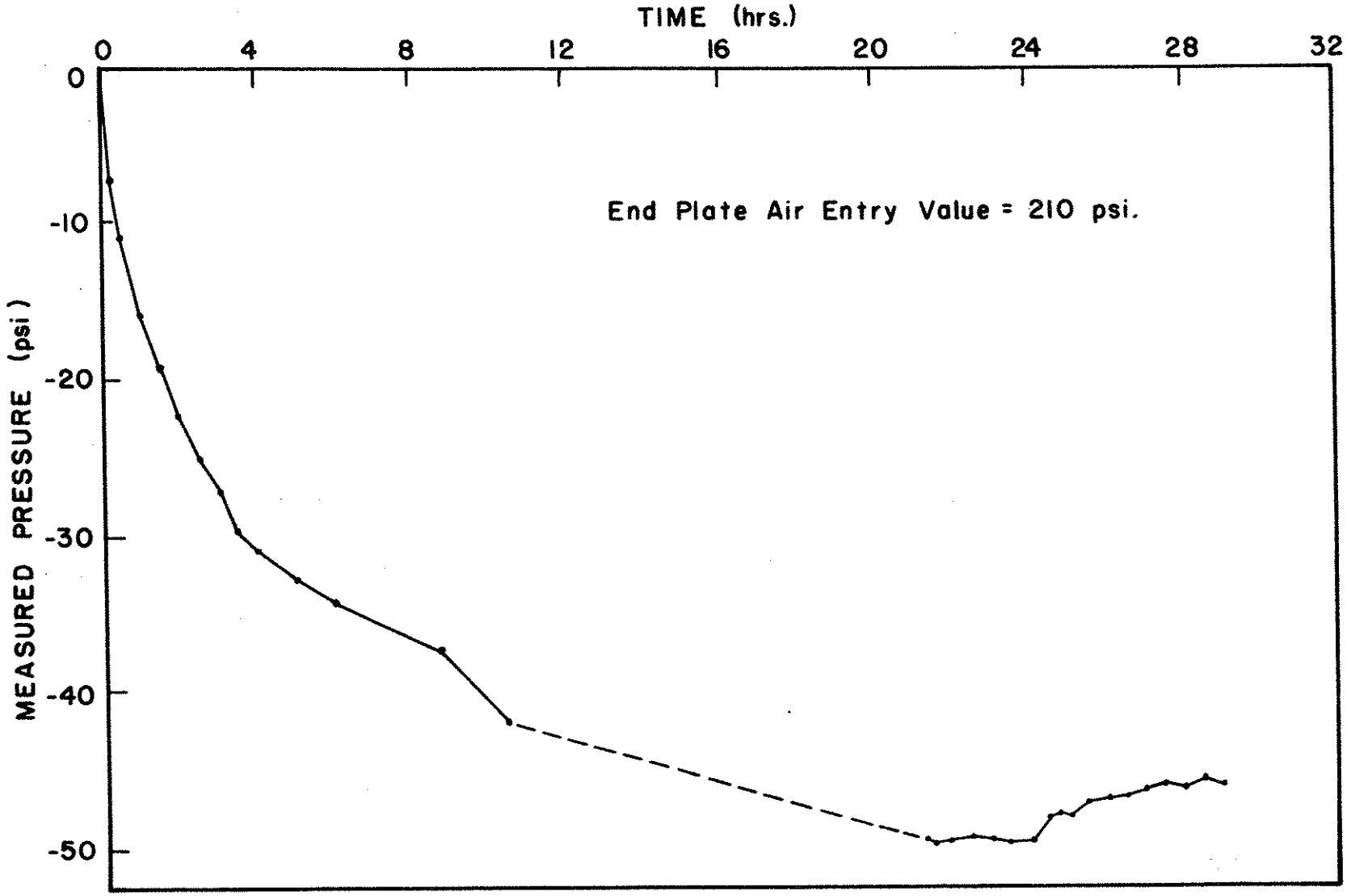

Fig. 4.31. Response Time for Negative Pore Water Pressure Test No. 1.

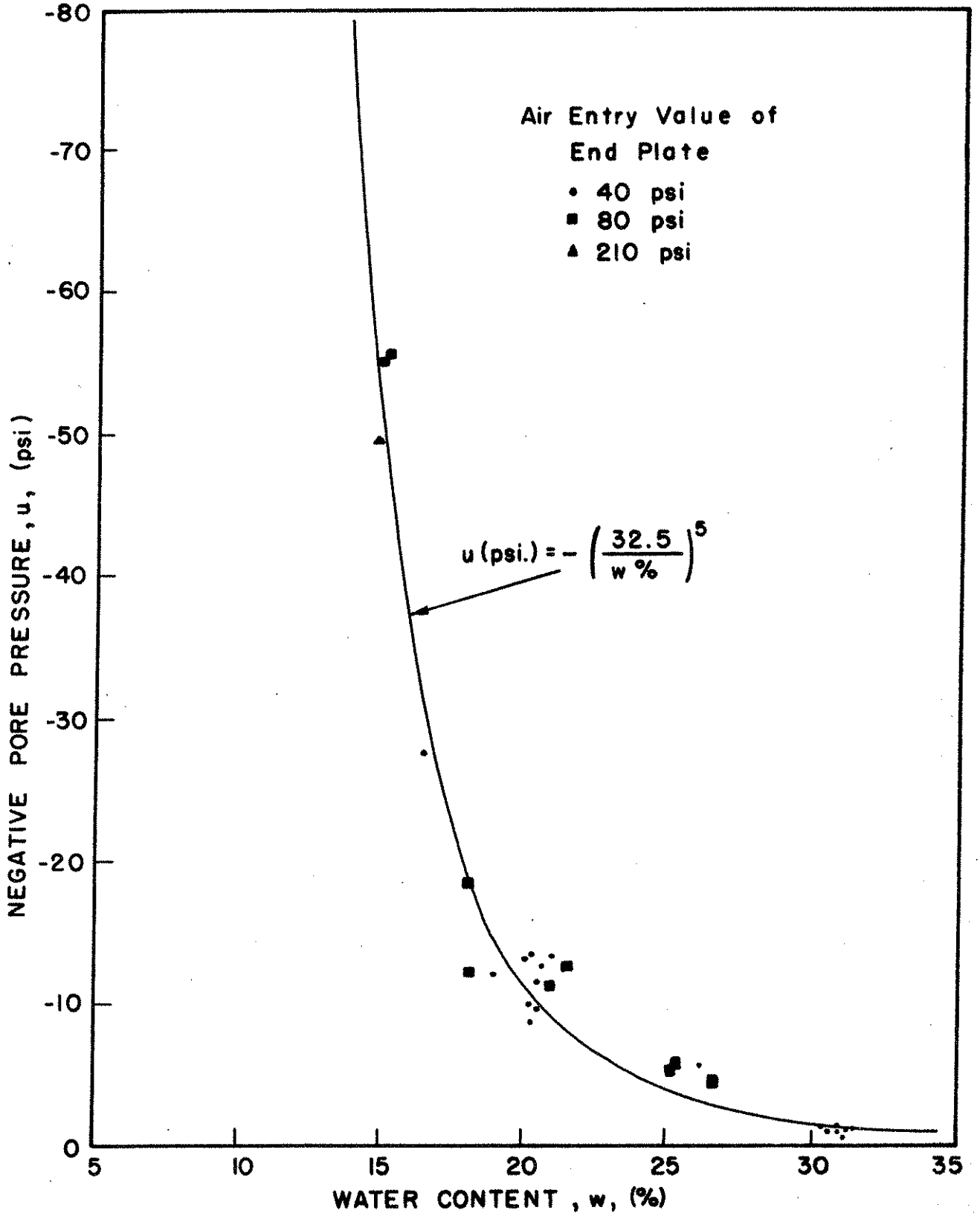

Fig. 4.32. Negative Pore Water Pressure-Water Content Relations for Loess H.

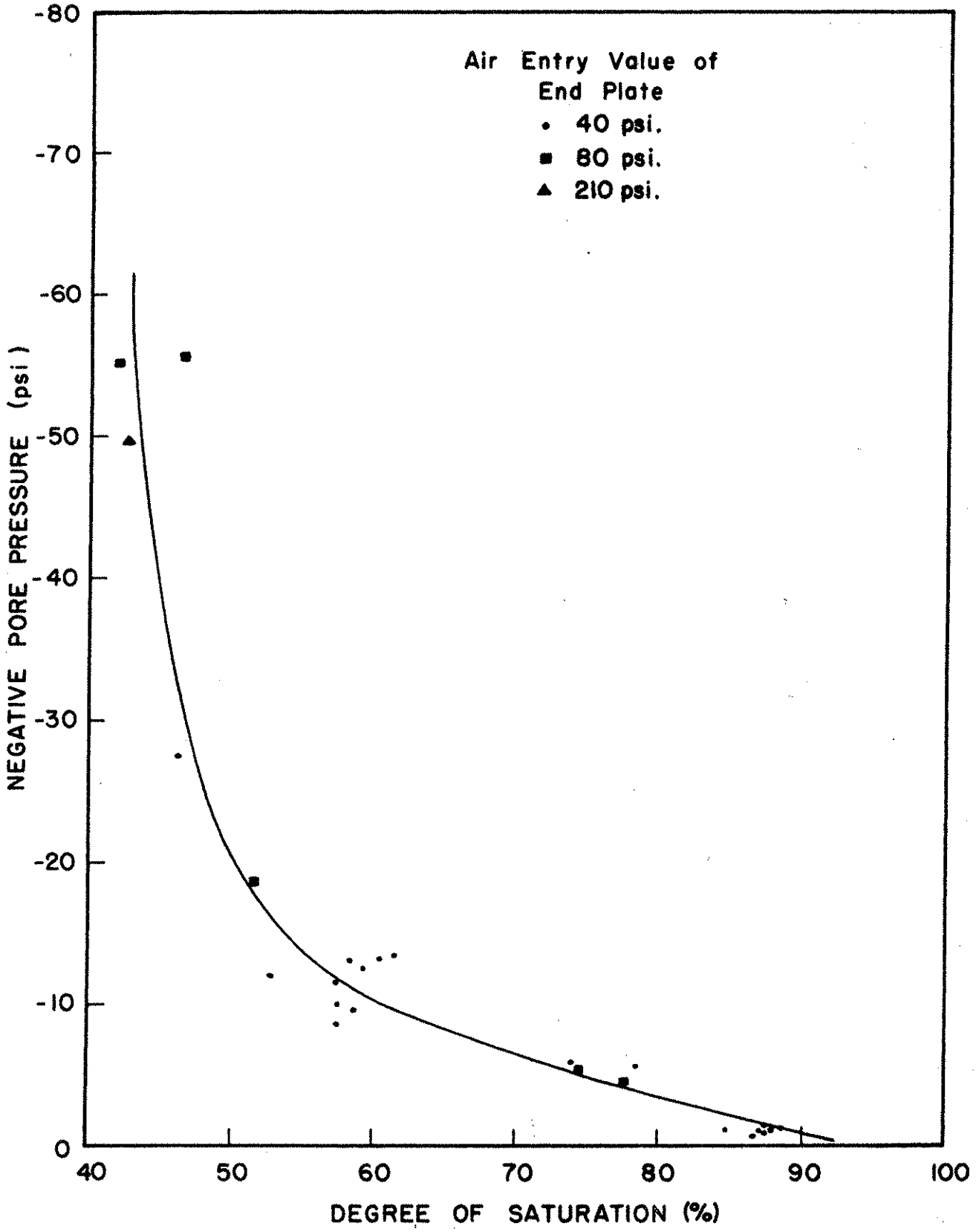

Fig. 4.33. Negative Pore Water Pressure-Degree of Saturation Relations for Loess H.

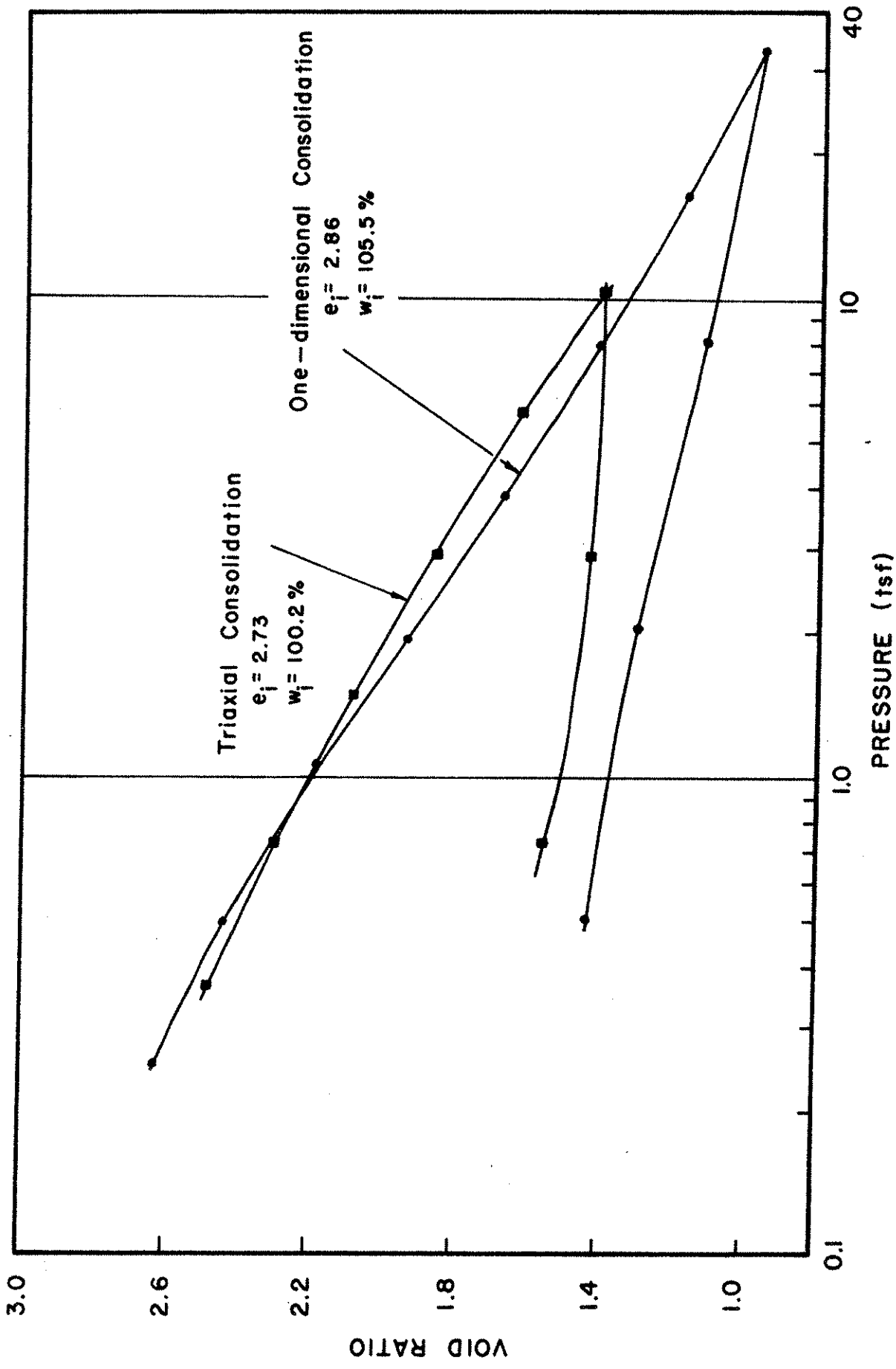

Fig. 4.34. Consolidation Tests on Clay Fraction.

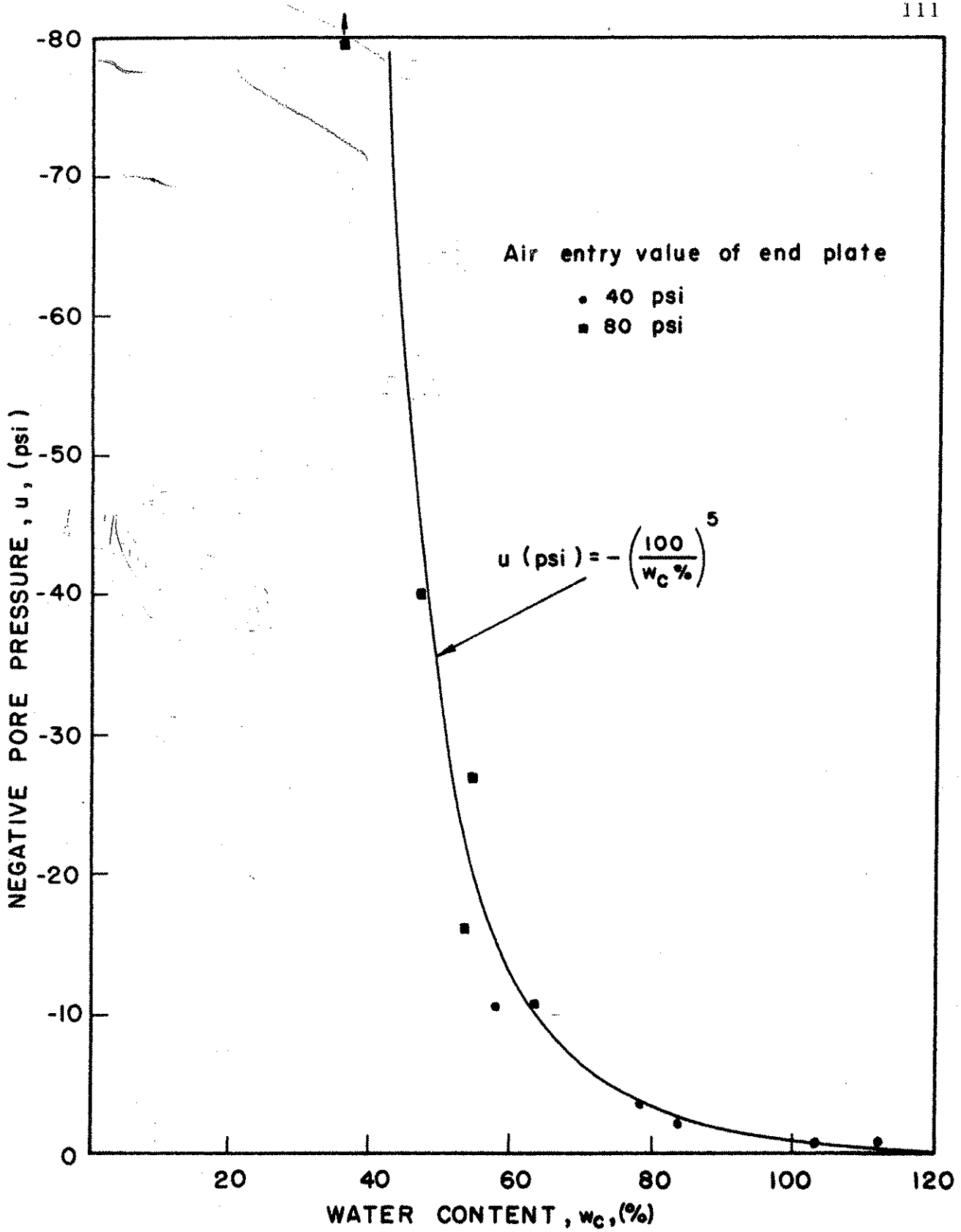

Fig. 4.35. Negative Pore Water Pressure-Water Content Relations for Clay Fraction.

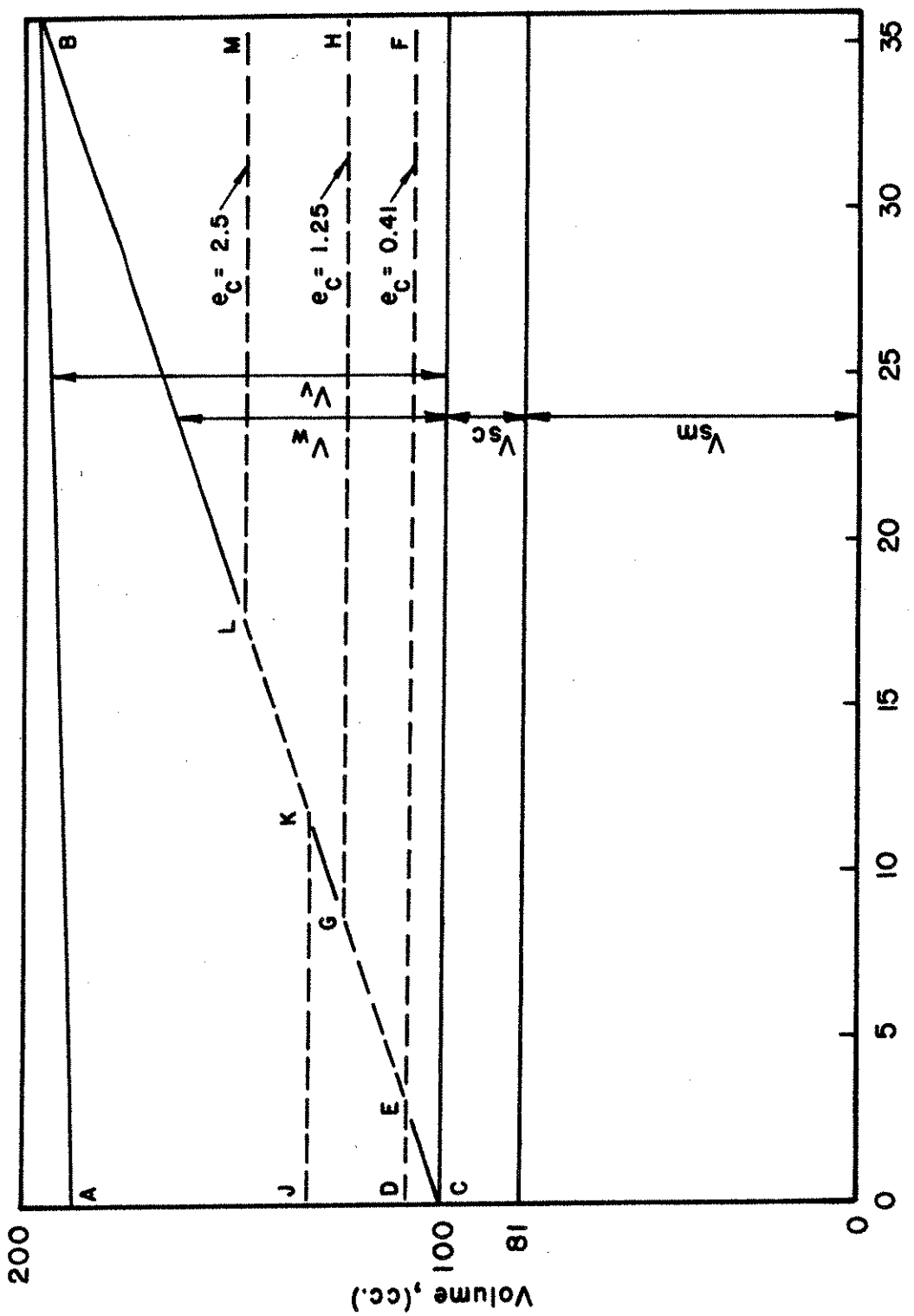

Fig. 5.1. Volumetric Relations for Loess H.

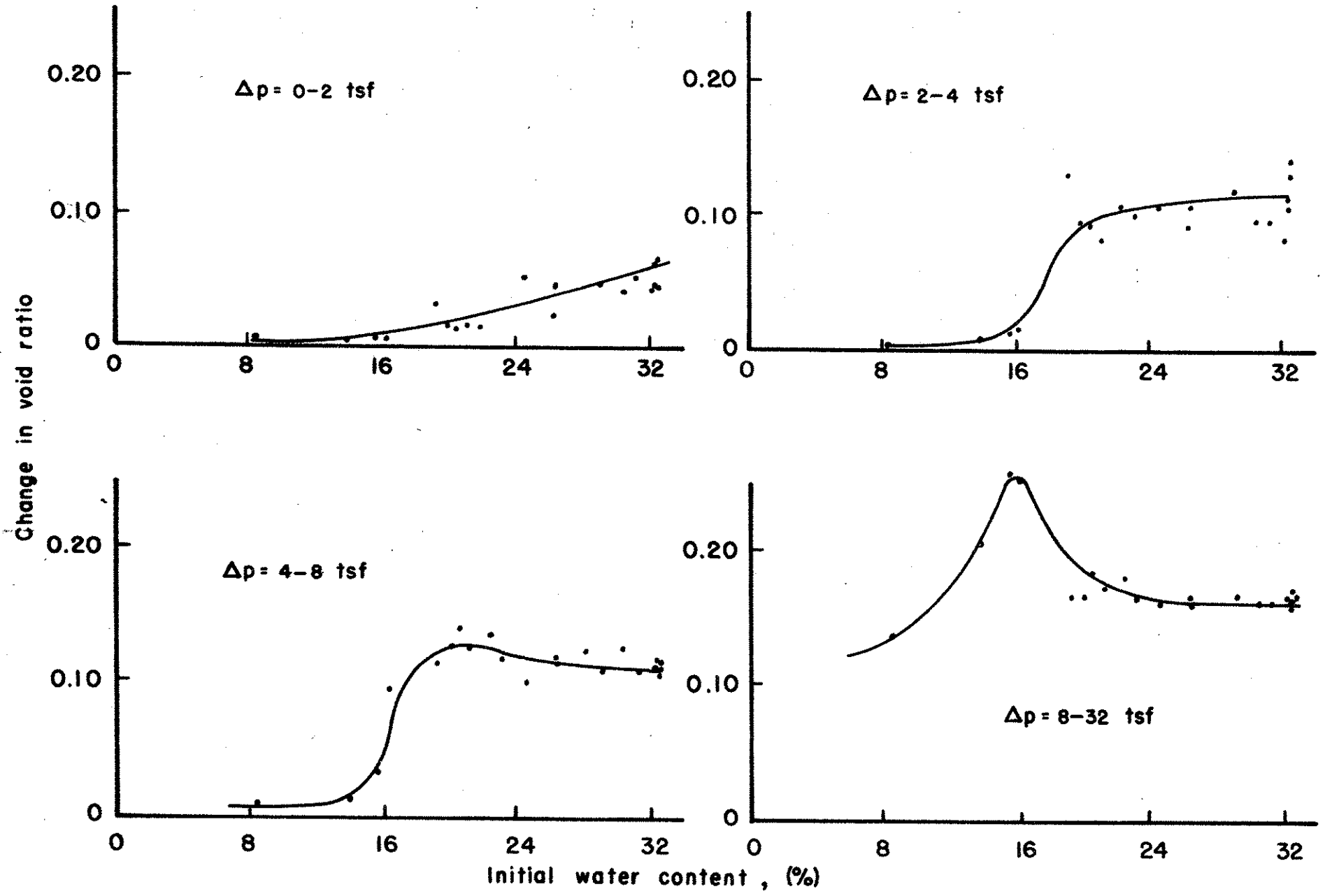

Fig. 5.2. Change in Void Ratio Due to Consolidation Pressure Increments.